Draft Final Report

Determining the Impact of Milltown Reservoir Drawdowns on the Adjacent Unconfined Aquifer: Remediation Stage 1 Observed and Stage 2 Forecasted

Prepared by

Antony Berthelote, Anthony Farinacci, Meryl Storb and William W. Woessner

Department of Geosciences

The University of Montana

Missoula, MT 59812

Prepared for

Keith Large MT DEQ

Russ Forba USEPA

DEQ Contract No. 406006

Federal Catalog No. 66.802

July 19, 2007

Executive Summary

The Department of Geosciences of the University of Montana entered into a contract with the Montana Department of Environment Quality to develop a tool to forecast the likely impact to groundwater levels and domestic well operation from remediation efforts related to the removal of Milltown Dam, western Montana. We were tasked to develop a water level monitoring program, collect limited data needed to fill identified data gaps, and to generate a calibrated three-dimensional groundwater model of the Milltown area and adjacent regions. This summary will briefly describe the well monitoring network, data sets collected to enhance knowledge of the hydrogeologic conditions, a description of the numerical model, and results of drawdown predictions.

The investigation centered on the Milltown Reservoir and the adjacent alluvial filled bedrock bounded aquifer (Figure 1ES, Figures are in Appendix A). The reservoir is filled with fine grain sediments the majority of which came from the Clark Fork River, a gravel-bedded river with a watershed that under went large scale mining and smelting in its headwaters over the last 100 years. As a result, metal and arsenic contaminated sediments collected behind the dam. Percolating reservoir water released metals and arsenic into the underlying sand, gravel and cobble unconfined aquifer forming a groundwater plume that leaves the reservoir, and currently underlies Milltown and an area west of the Blackfoot River arm of the reservoir. In 2004 remediation plans were finalized for reservoir and groundwater remediation, a process that would lower the water levels in the reservoir in three stages, Stage 1-about 10 ft, Stage 2-about 10 additional feet, and Stage 3 would lower the stage and river elevations about an additional 7 ft at which time the spillway would no longer be in place.

Characterization of the physical and hydrological setting relied on previous work, well log record interpretation, implementation of an extensive monitoring well network, and additional geophysical gravity surveys to delineate aquifer boundaries (Figure 2ES and 3ES). Generally, the unconsolidated material filling the valleys is saturated and a highly productive aquifer. Over 400 domestic wells tap this unconfined aquifer for water supply. The underlying bedrock is

irregular being at land surface on the valley edges and over 200 ft below land surface in some portions of the area (Figure 3ES).

To understand factors controlling water table behavior, a network of monitoring wells, river staff gauges, and stream-groundwater exchange sites were initiated in March of 2006. Water levels were collected from a network of 74 wells at 56 locations and 20 staff gauges (Figure 4ES).

Generally, groundwater flows from the east to the west (Figure 5ES). Field instrumentation of river channels and the adjacent aquifer showed river reaches in the Clark Fork River above the reservoir were both gaining flow from groundwater discharge and losing river flow to the underlying and adjacent groundwater. The reservoir and the Blackfoot arm of the reservoir both lose flow to the groundwater system. The Clark Fork River from below the dam to Hellgate Canyon leaks water into the aquifer except for a short reach below the dam (Figure 1ES and Figure 6ES).

Numerous authors have attempted to determine the magnitude and distribution of the coarse grained valley fill aquifer hydraulic transmission properties. Additional analyses of these parameters were completed in an attempt to refine estimates of the magnitude and spatial distribution of aquifer hydraulic properties including hydraulic conductivity.

Based on previous studies and new data sets a conceptual model of the study site was developed (Figure 7ES). A water balance was developed to allow for quantification of the multiple parameters of the conceptual model:

In = Out +/- Change in Storage

$GW_{inCFR} + GW_{inBRF} + GW_{inDC} + GW_{inMC} + BFR_{leak} + CFR_{leak} + Res_{leak} + GW_{inBR} = GW_{outCFR} + GW_{ConsP} + GSW_{out} +/- GW_S$

Where: GW_{inCFR} is lateral groundwater underflow into the model area at Turah Bridge, GW_{inBRF} is lateral groundwater underflow into the model area from the Blackfoot River valley, GW_{inDC} is lateral groundwater underflow into the model area from Deer Creek, GW_{inMC} is lateral groundwater underflow into the model area from Marshall Creek, BFR_{leak} is seepage (recharge) from the Blackfoot River channel into the valley aquifer, CFR_{leak} is seepage (recharge) from the Clark Fork River channel into the valley aquifer, Res_{leak} is seepage (recharge) from Milltown Reservoir into the underlying aquifer, GW_{inBR} is the seepage into the valley aquifer from a bedrock groundwater system, GW_{outCFR} is lateral groundwater underflow from the Clark Fork River Valley at Hellgate Canyon out of the model domain, GW_{ConsP} is consumed groundwater pumped from wells, GSW_{out} is groundwater seepage into the Clark Fork River within the model area, and +/- GW_S is the net change in groundwater storage (net annual water level changes).

Based on these data sets and interpretations, a three-dimensional numerical groundwater model was formulated using MODFLOW. The seven layer model consists of 53,192 active 150 by 150 ft cells. It was parameterized and calibrated using standard techniques to steady state conditions (March 31, 2006), transient conditions (March 31, 2006 to April 21, 2007), and history matched with October 8, 1992 steady state data and a second transient data set, 1992-1993 (Figure 8ES).

A calibrated steady state model for March 31, 2006 was then modified by inputting the anticipated river and reservoir stage after the Stage 2 drawdown was complete (a reduction in the pre remediation river stage and pool elevation in the vicinity of the reservoir of 19 ft). The results show groundwater levels are likely to respond by lowering approximately 7 - 8 feet in the northwestern area of Piltzville, 2 - 3 feet in the southwestern area of Piltzville, 12 - 14 feet in Milltown, and 10 - 11 feet in Bonner and the area of Stimson Lumber Company (Figure 9ES). Downstream of the reservoir, the impact is predicted to be a groundwater level reduction of 8-9 feet in West Riverside, 5-8 feet in the area near Pine Grove, 3 - 5 feet in Bandmann Flats, and 2 - 4 feet in East Missoula.

Predictions contain a degree of uncertainty. This research effort also identified limitations of the current model and suggests how uncertainty in model results can be reduced.

Table of Contents

List of Tables

List of Figures

List of Appendices

1.0 Introduction

In June, 2006, The Department of Geosciences of The University of Montana entered into a contract with the Montana Department of Environmental Quality who was administering resources provided by the USEPA to prepare by June 15, 2007 a draft preliminary estimate of the affect of planned river and reservoir drawdowns on the local groundwater levels associated with remediation of the Milltown Reservoir Super Fund Site. The purpose of this effort was to anticipate the locations and degree of impact of remediation efforts on existing domestic wells serving the adjacent population with drinking water. Study results will be used to identify the likely timing and areas of varying degrees of impact.

This work was anticipated to be completed in three phases or more, an initial year long study (this work) to develop monitoring networks, fill identifiable data gaps, and determine limitations of impact forecasts. The second year of work would refine forecasts by auditing initial predictions with field collected data, and performing additional model calibration. The third year would evaluate final remediation groundwater levels and likely additional consequences of stream restoration plans. Additional forecasts associated with river restoration are likely, though not refined at this time. This report represents the results of the first year of work.

The contract with the MTDEQ focused year one efforts on three tasks as stated in the contract:

Task No. 1. Review and develop steady state and transient data sets for conceptual and numerical model development and calibration. Data sets related to the groundwater investigation and analyses efforts from 1981 through 2006 will be reviewed, organized and assessed to develop an appropriate groundwater conceptual model for the study area. These will include geological, geophysical, hydrological, climatic and hydrogeological information. This evaluation will be used, along with Dr. Chris Brick's existing model, to frame the numerical model construction process including the setting of boundary conditions, vertical and horizontal discretization, parameter assignment and reservoir-river interactions. In addition, calibration data sets that can be used as steady state and transient history matching will be organized. Data gaps will be identified and additional limited field investigations (budget) including geophysical

surveys and aquifer characterization will be initiated as required. An extensive monitoring well network will be designed and maintained with guidance from the Missoula Water Quality District, DEQ and EPA.

Task No. 2. Construction of a calibrated three-dimensional transient numerical groundwater model of the Milltown area between Bandmann Flats, the mouth of the Blackfoot Canyon (about one and a half miles upstream of the Milltown Dam), and about 4 miles upstream of the dam on the Clark Fork River to Turah Bridge. It will be used to forecast the elevation of the water table as stages of drawdown occur at the reservoir site. MODFLOW will be used to simulate site conditions. The model will be calibrated to historical steady state and transient water level and flux data. As data sets are available, it will be calibrated to historical drawdown responses and the June 2006 drawdown of Milltown reservoir. The model will then be used to predict the response of wells to the November 2007 second phase of drawdown.

Task No. 3. Provide general assistance in assessing and communicating effects and predicted impacts of drawdowns. As requested by DEQ, the Contractor will meet with DEQ and EPA representatives and provide assistance in interpreting model results and predictions.

The contract listed the following specific deliverables:

Task No. 1: Contractor will provide the following as deliverables under Task No. 1:

1) Groundwater Conceptual Model and supporting information;
2) Water level monitoring data and interpretations;
3) Field collected geophysical data sets: and
4) History matching model calibration data sets.

Task No. 2: Contractor will provide the following as deliverables under Task No. 2:

1) Calibrated 3D MODFLOW model of the study site; and
2) Predictions of water level changes in response to Phase 2 reservoir drawdown.

This document presents text and figures describing the approach to the hydrogeological evaluation, methods used, data sets obtained and interpreted, and the conceptual and numerical

model development, forecasts of the consequences of remediation drawdowns on local groundwater levels, and limitations of the current predictions.

1.1 Site Conditions-Background

The 28 foot high Milltown Dam was built at the confluence of the Clark Fork River and Blackfoot River about 7 miles east of downtown Missoula, Montana in 1906-1907 to generate power. The pool behind the dam is referred to as the Milltown Reservoir. The Milltown area has a semi-arid climate. The mean annual temperature for nearby Missoula, Montana is 44.8^{o}F and the area receives a mean annual precipitation of 13.82 inches (http://www.ncdc.noaa.gov). The communities of Milltown, Bonner, West Riverside, Piltzville, Turah and East Missoula are located adjacent to or near the reservoir in a narrow sand, gravel, cobble and boulder filled river valley bounded by the bedrock of the Rattlesnake Hills and Garnet Range to the north and the Sapphire Range to the south (Figure 1) (All Figures are found in Appendix A).

The bedrock bordering and underlying the reservoir and bounding the adjacent valley is comprised of argillite, quartzite and limestone metasediments of the Precambrian Belt Series (Figure 2). The valley bedrock boundary has been estimated using gravity and other geophysical approaches (e.g. Nyquest, 2001). A diabase sill intrudes the metamorphosed sediments near the southern abutment of Milltown Dam. Structurally, the Clark Fork Shear Zone can be traced along the Clark Fork River valley. It is intersected in Milltown by the Blackfoot thrust that is coincident with the Blackfoot Valley (Nelson and Dobell, 1961). The valley sediments overlying the Precambrian Belt Series bedrock are fluvial sand, gravel, cobbles and boulders deposited by the ancestral Clark Fork River and Blackfoot River during glacial (Lake Missoula floods) and recent times.

In 1908, a 100+ year flood damaged the dam, shortly after that event it was repaired. During this 100+ year flood and over the last 100 years, contaminated upstream river sediments (mining and smelting operations) have been accumulating behind the dam and have filled up the reservoir. In 1981, the Montana Department of Health and Environmental Sciences (DEQ) discovered groundwater from four wells located in Milltown had elevated concentrations of dissolved arsenic that exceeded drinking water standards (> 50 ug/l). In 1983, the Milltown

Reservoir was declared a CERCLA (Superfund) site. After several hydrogeologic investigations (Woessner et al., 1984; Woessner and Popoff, 1982) the source of groundwater contamination was determined to be the reservoir sediments. A century of accumulation of upstream mine wastes was found to be a major source of arsenic and other metals in the reservoir sediment pore water, and the underlying and adjacent (north and northwest) groundwater (Atlantic Richfield Company (ARCO), 1992; Harding Lawson Associates (HLA), 1987; Udaloy, 1988; Woessner et al., 1984).

Groundwater in the Clark Fork River valley is derived from the coarse grained valley-fill sediments that are saturated and form a 20 to over 200 ft thick unconfined system. Groundwater flows westward and down valley (Gestring, 1994; Moore and Woessner, 2002; Tallman, 2005; Woessner et al., 1984). Groundwater recharge is principally from the perched and leaking river systems, and likely, some small quantity of lateral inflow from the surrounding mountain boundaries. Groundwater discharge to the rivers is limited with most groundwater leaving the area by underflow through Hellgate Canyon.

Beginning in the early to mid 1990's feasibility studies were initiated to assess what actions were needed to manage the Milltown Reservoir site and identify the extent and nature of the groundwater plume (Atlantic Richfield Company (ARCO), 1995; Atlantic Richfield Company (ARCO), 2002; Harding Lawson Associates (HLA), 1987; Westwater Consultants et al., 2005). In December of 2004 the Environmental Protection Agency and the State of Montana made the decision to remove the Milltown Dam and 2.5 of the 6.6 mcy (million cubic yards) of contaminated sediments in the reservoir. The State of Montana developed a stream restoration plan for the Clark Fork River within and above the sediment excavation area, and plans to implement it in concert with the remediation. Remediation and restoration plans were designed to be completed in stages over a number of years (Envirocon, 2006; Westwater Consultants et al., 2005). Remediation will require a number of drawdowns of river and reservoir stages until the final river channel and stage configurations are achieved.

The communities and neighborhoods of West Riverside, Pine Grove, Milltown, Bonner and Piltzville are located adjacent to the reservoir. Residents in these communities rely on over 400

shallow domestic wells that tap the valley fill unconfined aquifer for water supply. A desire to determine how river and reservoir drawdowns and the final river configuration will impact the operation of these wells (continue to supply drinking water to residences) has prompted this work.

1.2 Previous Groundwater Modeling Efforts

Groundwater models come in many forms. They can be conceptual (mainly descriptive), and formulated in the framework of a basic water balance, or complex and quantitative. Though more complex groundwater models are always based on a conceptual understanding of the hydrogeologic system (inputs, outputs and changes in storage), in order to quantitatively describe how a groundwater system works and to forecast or predict the cause and effect of actions that change the system, numerical tools are often used to build a two or three-dimensional groundwater model. Such models are used to understand how hydrologic source and sink terms are interrelated (interpretive), and to make predictions (forecast or predictive) (Anderson and Woessner, 1992). They require extensive calibration and testing against previously collected comprehensive data sets (calibration data sets). The work described in this report extends previous efforts that attempted to use numerical models to understand how and what factors control the groundwater system in the vicinity of the reservoir (Gestring, 1994), and how changes in reservoir and river stages are likely to effect groundwater levels (Brick, 2003). The following discussion will briefly describe these two earlier efforts.

Both previously developed single layer numerical groundwater models addressed groundwater flow in two dimensions (Brick, 2003; Gestring, 1994). Gestring's model used the north bank of the reservoir as the eastern area model boundary and a groundwater level contour (water table elevation) for the western aquifer boundary located in Hellgate Canyon (Figure 3). The stated purpose of his flow modeling effort was to assess the transport of inorganic contaminants that flow out of the Milltown Reservoir Sediment Superfund Site and mix with groundwater in the vicinity of Milltown. He produced a two-dimensional steady state representation of the groundwater system calibrated to November 1992 water level data. Based on his results he concluded that a significant portion of water was transmitted around the northern end of the Milltown dam cut-off wall and then likely discharged into the first 600 feet

of the Clark Fork River below the dam. The model also indicated that leakage from the Clark Fork and Blackfoot rivers contributed approximately one half the water found in the underlying aquifer (for the modeled period). Additionally 13,000 to 20,000 acre-ft/yr of contaminated water was estimated to migrate from the fine-grained reservoir sediments through a narrow high conductivity zone north of the dam.

Brick's model extended from just above Piltzville to Bandmann Flats (Figure 3). The purpose of Brick's model was to evaluate how proposed dam removal was likely to affect groundwater levels in the valley area. Brick used a refined representation of the basal bedrock boundary derived from geophysical investigations (Atlantic Richfield Company (ARCO), 1995; Nyquest, 2001), boreholes associated with dam repairs provided by Montana Power Company, and bedrock depths from bridge construction diagrams. Using a steady state model calibrated to Gestring's May 1993 data she first simulated a representation of the groundwater system with the dam and reservoir in place. She then generated a steady state representation of the groundwater levels after dam and reservoir removal with a new planned channel configuration in place (based on the conceptual design for alternative 7A) (Atlantic Richfield Company (ARCO), 2002). Based on data available at the time of her work, Brick concluded that a slight shift in groundwater flow paths would occur. Additionally, her simulations showed a water table would decline 10 to15 feet in the area currently occupied by the reservoir, about seven feet north of the reservoir in the Milltown area, 3-5 feet in West Riverside, and 2-3 feet of decline in the Piltzville area (Figure 4). She estimated error in her prediction as plus or minus 3 feet. Brick also listed a number of model limitations:

- Two-dimensional modeling of a three-dimensional system,
- Steady-state modeling does not account for seasonal variation,
- The distribution of hydraulic conductivity in the aquifer is not well known and evidence from observation wells suggests that the aquifer is highly heterogeneous,
- Leakage for the river and reservoir can be estimated, but is not known,
- There are sparse head data and no hydraulic conductivity data from the gravel aquifer in the reservoir area, thus predictions in this area may be less accurate.

2.0 Developing a Three Dimensional Conceptual and Numerical Model

The previous 20+ years of investigations and the two models described above provided the basis for the development of the preliminary three-dimensional groundwater model introduced in this report. The following sections will present the processes and methods used to formulate both a site conceptual model and the three-dimensional numerical model. We first evaluated existing reports and data sets, identified data gaps, initiated efforts to obtain needed information, developed and supported a conceptual model of the valley groundwater system, and built and calibrated a numerical groundwater model of the project area. In an attempt to keep the body of the report focused on the numerical modeling and its results, we describe approaches to data organization, gathering and interpretation, and present overall results together. Appendices B to E are used to report data sets and specifics related to methods and data interpretations.

The process of developing an appropriate site hydrogeologic model is iterative as data sets are always limited. As data were collected and evaluated they were fed into preliminary conceptual and numerical models, then results were evaluated, further data gaps were identified, and new data were collected. Models were then reformulated and the process repeated until acceptable representations of the system were obtained (Figure 5).

2.1 Data Collection and Interpretation

It was recognized that to more clearly understand three-dimensional groundwater conditions existing data sets needed to be organized and evaluated, and data gaps identified and a process to fill those gaps planned and executed. Project budget constraints limited new data collection efforts focusing efforts principally on analyses of existing data.

2.1.1 Geologic Framework

Additional geophysical surveys completed in the last few years and well/coring logs near the dam suggest the bedrock base of the aquifer may be highly irregular, and as such, likely provides an important control on the three-dimensional movement of groundwater. In addition, hydrologic properties of the sediments have been reported to vary widely and no clear links with aquifer lithology and/or valley locations have been established. To most cost effectively refine both aquifer basal boundaries and aquifer stratigraphy, new geophysical surveys were conducted.

2.1.2 Bedrock Boundary Development

The geometry of the lateral and bottom boundaries of the unconsolidated valley aquifer was revised from previous work by compiling and analyzing available gravity data, four seismic lines processed by Gradient Geophysics (Gradient Geophysics, 1991), historical borehole data, construction site borings, well logs, and topographic projections of mountain slope bedrock into the subsurface. Historical bedrock elevation data based on geophysical and drilling results were sparse for the area below the Milltown Dam, and from the Stimson Mill site through Hellgate Canyon. No valley depth to bedrock data are known to exist between Turah and the Duck Bridge area with a few exceptions where wells penetrate bedrock near the valley edges.

A geophysical gravity bedrock investigation was undertaken that extended from Turah Bridge (the eastern end of the study area), to the eastern edge of the reservoir, and north up the Blackfoot River (Figure 6, yellow dots). A total of 197 new gravity observations were obtained using a Scintrex CG3 Microgal Gravity Meter.

These data were combined with several sets of unpublished gravity data obtained by students from The University of Montana (Sheriff and others, 2007), and with findings from the National Geophysics Data Center and the U.S. Defense Mapping Agency (NGS/DMA) to build a regional map of the gravity. The gravity measurements were then reduced to the Complete Bouguer Anomaly using a series of corrections taking into account the Earth's imperfect shape (topography) and rotation, the location on the spheroid (location of where the data were collected on the earths oval surface), elevation above sea-level, the gravitational attraction of the rocks between the observation point and sea-level, and the surrounding topography. Before the data could be modeled the regional gravity affect were removed from the Complete Bouguer Anomaly data to find the residual gravity anomaly (the gravity effect due only to the density contrast between the valley fill and the bedrock). This residual anomaly was used to find the bedrock topography of the basin using the gravity modeling program GI3 (Cordell and Henderson, 1968). The subsequent surface was constrained with known and minimum depths to bedrock, seismically determined depths, and knowledge of the valley geology to produce the final simulated/calibrated bedrock elevations (Figure 7a). The total data set evaluated included

over 700 observations processed using standard techniques (Evans, 1998; Janiszewski, 2007; Nyquest, 2001).

With this data set a bedrock surface model was developed. Due to the nature of gravity determined depth to bedrock processing, the final simulated bedrock topography is smoothed in relation to the true surface. It has been observed from well borings and well logs that, in places this bedrock surface is highly variable, can contain areas of weathered bedrock, has up to 40 degree slopes as indicated by well logs for adjacent valley wells, and in some places valley fill may contain large boulders resulting in gravity and or errors in drilling interpretations of bedrock depths. The small scale spacing of some of these features is not duplicated in the final simulated bedrock surface. The mean residual between known depths to bedrock and calculated depths to bedrock for this model was 1.97 feet with a standard error of the estimates of 29.1 feet. The trend line fit to the plot of known depths verses calculated depths has a slope that departs from 1 by 0.007. It is evident from Figure 6 that the data distribution north of and below the dam have a greater frequency. The confidence in the simulated depth is greater where the frequency of distribution is large (number of spatially collected data points is greater per unit area). The area above Duck Bridge may contain greater errors due to the lack of any established depths to bedrock within the central portion of the valley. Simulated depths to bedrock at the valley margins did not match well with topographic slopes and valley edge well data. Furthermore, the limited data within and proximal to Hellgate Canyon resulted in the model under predicting alluvium depths in the canyon. Slope projections, well logs, and a seismic line were used to constrain bedrock depths in Hellgate Canyon.

The modeled bedrock surface and corresponding modeled thickness of the alluvium (Figure 7 7a and 7b) are irregular, apparently reflecting a complex erosional and depositional history. A single buried sediment filled channel is not evident. Instead bedrock highs appear to compartmentalize deeper alluvial deposits. A bedrock shelf at the lower end of the reservoir appears to extend below the reservoir sediments, and bedrock of Bonner Mountain is present at its southern edge extending towards the Milltown area. In addition, the bedrock surface is elevated in a portion of the West Riverside area. Figures 7a and 7b also suggest that a low in the bedrock surface is present in the Bandmann flats area along the southern valley boundary. It

was determined that this feature is an artifact of the original modeling effort as few data points were collected in this area of the valley. An additional data collection effort was initiated and the re-interpreted gravity data suggests this area has a more uniform depth than portrayed in the original interpolation (approximately 200 ft) (Sheriff and others, 2007).

2.1.3 Aquifer Stratigraphy

An interpretation of the geometry of the unconsolidated valley fill sediments was further refined by using 89 well and borehole logs collected from previous reports (Brick, 2003; Gestring, 1994; Woessner et al., 1984), Montana's Ground-Water Information Center (http://mbmggwic.mtech.edu/), and from domestic well owners. The well logs were compiled into a database, and cross-section and fence diagrams constructed using RockWorks® Borehole Software (Figure 8; Appendix B).

Based on the review of hundreds of well logs, we were able identify lithologies that could be lumped into a smaller number of units. Commonly, an upper sand and gravel layer was found to overly a discontinuous zone of silt and sand. Such deposits are observed in Hellgate Canyon, in areas just upstream of Milltown, and in portions of West Riverside. A third lower unit of the valley fill is a heterogeneous mix of sand, gravel and clay. Throughout the valley intermittent clay and sandy clay lenses are found in the eastern portion of West Riverside, in the Piltzville area, and at the junction of Crystal Creek and the Clark Fork River valley. Due to the lack of wells drilled in Bandmann Flats and in areas of the Clark Fork flood plain above Milltown Dam, the stratigraphy is not as well known and it is often extrapolated based on a single well log or distal well information. As these grouping have similar sedimentalogical and hydrogeological properties, simplified cross sections were developed using these hydrostratigraphic units (Figure 9). Correlations based on these cross sections were used to distribute hydrogeologic properties in the numerical model.

2.1.4 Refining Groundwater System Properties, and Controls on Flows and Rates of Exchange

Previous efforts focused on examining water levels and groundwater flow directions in the vicinity of Milltown and the reservoir. This modeling effort focused on a larger project area

requiring additional data collection and interpretation. Previous individual research and consulting efforts were evaluated and combined into a project hydrogeologic data set. An additional site wide water level monitoring network was initiated, characterizations of the groundwater exchange locations and rates along river channels and within the reservoir were developed, and aquifer properties were quantified and their three-dimensional distributions estimated.

To refine our understanding of factors controlling water table behavior, a network of monitoring wells, river staff gauges, and stream-groundwater exchange sites (vertical hydraulic gradient measurement sites) was initiated in March of 2006. Water levels were collected from a 74 wells at 56 locations and 20 staff gauges (Figure 10). All instrumented sites were surveyed in or converted to the Montana State Plane Coordinate System FIPS 2500 North American Datum (NAD) 1983 with the Geodetic Reference System 1980 Ellipsoid and the National Geodetic Vertical Datum (NGVD) 1988.

The monitoring network was set up in cooperation with the Montana Department of Environmental Quality and the Missoula County Water Quality District as part of the Milltown Reservoir Sediments Operable Unit Remedial Action Monitoring Plan (Envirocon, 2006). The network design provides the highest resolution proximal to the reservoir, and less detail at increasing distances from the reservoir. A number of these same network wells were also monitored during previous studies (Gestring, 1994; Harding Lawson Associates (HLA), 1987; Tallman, 2005; Woessner et al., 1984). Data from our current monitoring and historical data sets were compiled into a single database containing 226 wells with 718 measurement days converted to a single vertical datum (NGVD 88) and a horizontal datum (NAD 83 Montana State Plane 2500, Appendix C). Included in the database are the reservoir pond and tailrace elevations as well as the available USGS river stage data for the 718 measurement days.

Ground water levels at 22 wells were recorded at intervals no greater than 60 minutes using Solinst® continuous water level recorders (recording pressure transducers corrected with readings from a separate Solinst® barlogger). At all network wells from June 1st to about July 15th, 2006

weekly measurements were collected using an electric water level tape. After July 15th, 2006 monthly monitoring was initiated.

Errors associated with water level measurements include measurement error (e.g. electronic tape wrapping around pump cords), operator error (e.g. different personnel reading tape at different times), and instrument error (e.g. sensitivity adjustment on the electronic tape and varying length calibration). These water level measurement errors are less than 0.2 ft with additional errors propagating from survey errors (0.07 ft), continuous water level recorder errors (0.25 ft), and interpolation with respect to time errors (0.05 ft). The sum of these individual errors is ~ 0.57 ft. When errors are all assumed to be independent the error is ~ 0.33 ft.

To build a relationship between stream stage and ground water elevations, a network of surface water stage gauges was established. Surface water elevations were monitored at three sites (Blackfoot River at Bonner 12340000, Clark Fork River at Turah 12334550 and Clark Fork River above Missoula 12340500) by the USGS, in the reservoir and tailrace (North West Energy, 2007), and at project installed staff gages placed along the river banks as part of this effort. Stage is being measured at a total of 20 locations (Figure 10).

Stage 1 drawdown was initiated on June 1st, 2006 following peak river flows (Figure11). It was suspended from July 7th, 2006 to September 18th, 2006 and then resumed. It was completed on November 12th when the river became the only control on reservoir stage. The maximum drawdown from full pool was ~12 ft. Water level data were continuously compiled and analyzed by constructing and evaluating well, river and reservoir hydrographs, and water table maps (Figure 12).

To analyze the seasonal variation in groundwater levels and the observed affect of the Stage 1 drawdown on the groundwater system, hydrographs were plotted for monitoring locations. In addition to observed water level changes collected as part of this effort (2006-2007 blue line), and historical water level data were also plotted on the same graph for the appropriate time period (from 1982 to 2005, shaded area). Then water level data from Gestring's (1994) study, when available, were indicated to examine historical data trends (Figure 13).

Post Stage 1 drawdown water levels (March 2007 lowest position of the water table) where compared to the historical ranges of water levels measured for the same time period (when the Milltown Reservoir was at full pool), and an estimate of observed Stage 1 drawdown impact was established. The impacts established from historical water level and post drawdown water level hydrographs were plotted in Arc GIS 9.2 and a drawdown surface was interpolated using the spline method (Figure 14). The aerial distribution of computed changes to the water table during the 2006-2007 study period shows the largest impacts occurred adjacent to and down gradient from the reservoir, a decline of 5 to 6 feet. West Riverside and Milltown had water levels decrease about four feet below historical measurements and in the Piltzville area about 2 feet of new drawdown was observed. The Bandmann flats area experienced about a three feet water level decline. Some of this water level decline, particularly in West Riverside may also have resulted from the Bonner Dam removal.

The computed impacts to groundwater levels assumed the historical groundwater level data were recorded during a period with river flows that are similar to those occurring during the 2006-2007 period. This appears to be the case as the1992-1993 data set collected by Gestring (orange line in Figure 13). His study occurred during a period of low river baseflow, a condition we also encountered (2006-2007; Figure 15).

2.1.5 Surface Water / Groundwater Relationships

Previous investigations suggested that reservoir and river leakage to the underlying aquifer is a major component of recharge to the aquifer. However, locations and rates were poorly defined. We collected data to better quantify this process by instrumenting river bed segments.

The exchange of water between surface water and groundwater was examined by measuring vertical hydraulic gradients (VHG), streambed seepage rates, and mapping water table positions near stream channels and comparing them with adjacent stream stage elevations. Three-dimensional vertical hydraulic gradients were determined in the Clark Fork and Blackfoot river channels using clusters of in stream mini piezometers located every ~3000 feet down stream from site boundaries (Tallman, 2005). Vertical gradients were used to develop a conceptual model of the spatial distributions of surface water and groundwater exchange (Figures 16, 17,

and 18, and 19). Generally, river bed properties were assigned by dividing the distance equally between monitoring points. However, professional judgment was applied based on field observations of stream and floodplain conditions, and knowledge of approximate water table positions in some cases.

The rates of river and ground water exchange were also investigated using in-stream bed temperature arrays. Thirteen 1 1/4 inch diameter by 48 inch long sand points (Mass Midwest Manufacturing, Inc. gravel points) were driven into the stream bed with just the top few inches of the instrument extending above the river bed. Both river temperatures and river bed (water) temperatures were recorded with Thermocron iButton® temperature recording devices installed vertically within these sandpoints (Figure 20) (Johnson et al., 2005). Nine out of thirteen instruments have been recovered. Surface water and bed temperature profiles were then analyzed using the USGS heat transport model to estimate river bed flux rates (Hsieh et al., 2000; Tallman, 2005).

Data analyses involved reproducing the observed saturated river bed temperature signals by using the daily heating and cooling data for the rivers as a source term. A column one-dimensional saturated river bed sediment model was developed and field and literature values assigned (Figure 21). Grid spacing was set at 0.065 feet. The VHG and stream stage were used as hydraulic boundary conditions, the river temperture as the source term, and the groundwater temperature as an intital condition. The model was then calibrated principally by changing the vertical hydraulic conductivity and making minor adjustments to other physical and thermal parameters. Temperature modeling results are presented in (Table 1).

General Area	Instrument Location	Date	Computed River bed hydraulic conductivity (Kv ft/day)	Vertical hydraulic Gradient (VHG)	Computed river bed flux rate ($ft^3/(day\ ft^2)$)
Clark Fork River Above the Dam	CFRA2 (above duck bridge)	8/24/06-11/12/06	9.8	0.75 to 0.89	7.4 - 8.8
	CFRA3 (CE)	5/18/06 – 7/8/06	131	-0.94 to -1.07	123 - 141
	CFRA5 (CCR)	8/24/06 – 11/12/06	13.1	2.39 to 2.69	31.4 - 35.3
	CFRA8 (Turah Bridge)	8/24/06 – 11/13/06	32.8	-0.83 to -0.97	24.7 - 31.8
Blackfoot River	BFR2	7/31/06 – 10/10/06	6.56	-1.55 to -1.93	10.2 - 12.7
	BFR8 (on bank)	6/2/06 – 6/17/06	8.2	-1.24 to -1.29	10.2 - 10.6
	BFR8 (in middle of channel)	10/10/06 – 10/31/06	984	-0.11 to -0.14	113 - 141
Clark Fork River Below the Dam	CFRB6	8/26/06 – 11/17/06	6.56	-1.19 to -1.78	7.8 - 11.7
	CFRB8a	6/20/06 – 8/6/06	23	-1.36 to -1.53	31.4 - 35.3
	CFRB8d	6/20/06 – 8/6/06	21.3	-1.41 to -1.91	30.0 - 40.6

Table 1 Results of temperature modeling. Locations are identified in Figure 16. The vertical gradients larger than one reflect a losing reach that is perched above the valley water table.

The results of the temperature modeling show vertical hydraulic conductivity values that range from about 7 to 984 ft/day and river bed exchange rates that range from approximately 7 to 140 $ft^3/(ft^2 day)$. The Clark Fork River bed above Milltown Dam and the Blackfoot River bed have hydraulic conductivities that range from 10 to 33 ft/day and 7 to 984 ft/day, respectively,

Seepage rates for these river reaches range from 7 to 32 $ft^3/(ft^2day)$ and 10 to 140 $ft^3/(ft^2day)$. The highest seepage rates appear to correspond with portions of the channels where gravel is transported. Lower values appear to be associated with portions of the river that are overlain by the reservoir pool and contain fine-grained sediments. The river below the dam has a coarse river bed system that has been partially sealed by fine grain reservoir sediments (Figure 22). Hydraulic conductivities are lower, 7 to 23 ft/d than found in other sections of the river, however, the computed exchange rates, 8 to 41 $ft^3/(ft^2day)$ appear to be driven by the measured large vertical hydraulic gradients (Gestring, 1994).

Streambed hydraulic conductivity values were also measured by conducting falling head permeameter tests throughout the study area (Landon et al., 2002). Falling head tests that generated horizontal hydraulic conductivity values (Kh) were analyzed using standard methods (Fetter, 2001; Hvorslev, 1951; Landon et al., 2002). The vertical river bed hydraulic conductivity (Kv) was computed from field measured values by assuming it is one tenth of the horizontal conductivity (Anderson and Woessner, 1992). The vertical hydraulic conductivity results range from about 6 to 1100 ft/day.

		Falling Head Method (Fetter, 2001)		Hvorslev (1951) Method	
		Kv/Kh (1/10)			
	Location	Site 1	Site 2	Site 1	Site 2
		Kv ft/day	Kv ft/day	Kv ft/day	Kv ft/day
Blackfoot River	BFR5	25		47	
	BFR6	466		893	
	BFR8	19		37	
	BFR9	23		44	
	BFR11	64		86	
Clark Fork River Above Dam	CFRa2	21		41	
	CFRa3	57	22	109	43
	CFRa4	1071	13	725	25
	CFRa5	112		216	
	CFRa6	7	17	12	32
	CFRa7	17	6	33	12
	CFRa8	49	7	94	15
Clark Fork River Below Dam	CFRb2	36		68	
	CFRb7	163		312	

Table 2 Results of the falling head permeameter tests at listed locations (Figure 16). Site 2 represent a second test completed at the same general location often within one meter of the first data collection point.

The results from these falling head permeameter tests yielded values that were similar to those derived from temperature modeling

2.1.6 Aquifer Properties

Site aquifer properties were obtained from previous aquifer test data reported in the literature, and newly applied interpretation methods, To characterize the transmission properties of the valley fill sediments values of hydraulic conductivity (K) and transmissivity (K times the saturated aquifer thickness, T) are derived. The volume of water in storage is computed using the aquifer porosity and the available water that will enter or be drained (released) for the total volume is defined by the aquifer storativity (S and Sy for unconfined aquifers). Estimates of the magnitude, location and variation of each of these properties are required to quantitatively describe groundwater conditions in the area of study.

Aquifer hydraulic conductivities throughout the valley have been reported to range from 150 ft/day ~ 60,000 ft/day (Atlantic Richfield Company (ARCO), 1995; Land and Water Consulting,

2004; Land and Water Consulting, 2005; Newman, 1996; Newman, 2005; Woessner et al., 1984). General aquifer property values have been complied in Table 3. Vertical hydraulic conductivities of the valley aquifer were assumed to be a tenth of horizontal aquifer conductivities (Fetter, 2001). Aquifer porosity and specific yield selected based on previous studies (Woessner, 1984) and aquifer material properties reported in the literature (Fetter, 1994). Aquifer storativity values were compiled from reported aquifer test analyses results (Land and Water Consulting, 2004; Newman, 1996; Newman, 2005; Woessner et al., 1984).

Aquifer property values were interpolated throughout the study area from locations where aquifer tests were conducted. Values were attributed to geologic settings described on well logs and then extrapolated to similar interpolated geological conditions (Table 3).

Source	well #	K (ft/day)	Transmissivity (ft^2/day)	Kz (ft/day)	Sy	S
[1]	102	3,710 - 3,715	96,400-96,600			
[1]	103	1,770 - 2,100	65,200-55,000			
[1]	105a	290	18,230			
[3]	105b	1,578 - 1,886	882,683-1,040,996		32.94 - .034	0.0477 - 0.006
[3]	105c	1,512 - 1,704	834,221		5.58 - 2.24	0.028 - 0.026
[1]	106	56,700 - 59,400	4,140,100			
[1]	107	13,600 - 14,200	573,000-595,100			
[1]	108	6,500 - 6,800	539,800-595,200			
[1]	109	15,100 - 16,900	1,600,000-1,800,000			
[1]	110	2,200 - 2,580	242,100-208,500			
[3]	906	1,733 - 2,192			0.24 - 0.1	0.0005 - 0.001
[3]	99b	1,872 - 3,072			0.36 - 0.12	0.001 - 0.0008
[4]	west well	1498	9,159 - 34,034			
[4]	east well		46,575 - 89,904			2.54E-14
[5]	R-75	1,269.09 - 1,286.47		226.18 - 235.49	0.12	.00119 - .00012
[2]	HG-32	16,734	903,636			
[2]	HG-33	9,012	877,824			
[6]	mw-6	3,900 - 11,000				
[6]	Mw-7	300 - 400				
[6]	Turah Bridge - Rodin	9000 - 5000	1,400,000 - 780,000 (@ 150' thickness)			
[6]	West-Riverside	14,000 - 83,000				
[7]	West-Riverside	1,826 – 89,201				
[8]	Smw-3	599				0.13
[9]	Canyon river Well	608-5,079	55,293 - 462,171			

Table 3 The compilation of reported hydraulic conductivity values determined throughout the study area.

[1] (Woessner et al., 1984)
[2] (Gestring, 1994)
[3] (Atlantic Richfield Company (ARCO), 1995)
[4] (Newman, 1996)
[5] (Newman, 2005)
[6] (Peak Lag Analysis)
[7] (Flow Tube Analysis)
[8] (Land and Water Consulting, 2004)
[9] (Land and Water Consulting, 2005)

In an attempt to further interpret the possible magnitudes and locations of various zones of similar hydrologic properties, extensive analyses of interpreted cross sections (well logs) were completed, relating lithology to aquifer test results. In addition, groundwater level relationships and groundwater flow path interpretations were also used to compute general locations of hydraulic conductivity zones. Stage peak lag time equations derived by Pinder, Bredehoeft, and Cooper (Pinder et al., 1969) and flow tube analysis were utilized to constrain hydraulic conductivities in key areas where no aquifer test data were available. Stage peak lag time equations evaluate aquifer properties by analyzing the respond of well water levels to changes in upgradient water level changes (Figure 23). The results of the peak lag analysis suggest high hydraulic conductivities occur in a portion of the West Riverside area, ranging from 19,000 to 82,000 ft/day.

Flow tube analysis can also be used to evaluate the distribution of aquifer properties (Fetter, 2001). The analysis assumes that under steady state conditions all water that enters the flow tube leaves the flow tube (Figure 24). A flow tube analysis for the same general area in West Riverside indicates a very high hydraulic conductive zone is present and that values decrease slightly to the west.

2.2 Refined Conceptual Model

The conceptual model for the study area is based on previous work, newly collected and interpreted data, and hydrologic principles. In general, the hydrogeological conceptual model is a simple water budget for a specific area over a designated time period. This budget includes boundary inflows and outflows, and gains and losses of water internally as groundwater and river systems exchange water (Figure 25). An annual groundwater balance for the project area (Table 4) was formulated as follows:

In = Out +/- Change in Storage

$GW_{inCFR} + GW_{inBRF} + GW_{inDC} + GW_{inMC} + BFR_{leak} + CFR_{leak} + Res_{leak} + GW_{inBR} = GW_{outCFR} + GW_{ConsP} + GSW_{out} +/- GW_S$

Where: GW_{inCFR} is lateral groundwater underflow into the model area at Turah Bridge, GW_{inBRF} is lateral groundwater underflow into the model area from the Blackfoot River valley, GW_{inDC}

is lateral groundwater underflow into the model area from Deer Creek, GW_{inMC} is lateral groundwater underflow into the model area from Marshall Creek, BFR_{leak} is seepage (recharge) from the Blackfoot River channel into the valley aqufier, CFR_{leak} is seepage (recharge) from the Clark Fork River channel into the valley aquifer, Res_{leak} is seepage (recharge) from Milltown Reservoir into the underlying aquifer, GW_{inBR} is the seepage into the model domain from a bedrock groundwater system, GW_{outCFR} is lateral groundwater underflow from the Clark Fork River Valley at Hellgate Canyon out of the model domain, GW_{ConsP} is consumed groundwater pumped from wells, GSW_{out} is groundwater seepage into the Clark Fork River within the model area, and +/- GW_S is the net change in groundwater storage (net annual water level changes).

2.2.1 Pre-Model Groundwater Balance

The groundwater balance formulated in Tables 4a and 4b was computed based on field data and previous studies, a pre-simulation water balance. All underflow calculations were computed using Darcy's Law:

$Q=KIA$

Q= Groundwater Underflow

K=hydraulic conductivity of the aquifer

I= groundwater hydraulic gradient

A= saturated cross sectional area of the aquifer

Surface water and groundwater exchanges locations and volumes were derived from point distributions of gaining and losing reaches (Figures 17, 18, and 19) and flux rates determined by temperature modeling. Recharge from precipitation and discharge from evapotranspiration were assumed to be negligible as they were estimated to be a small percentage of the total water balance. The inflow from bedrock is unknown, however, the lack of a geochemical signal in the valley ground water from a bedrock source, observations of drilling water wells into bedrock in the Milltown area and generally observing a reduction of water production to near zero, and the lack of interpreted water table contours paralleling the valley walls suggest that contributions are small relative to the volume of water moving through the unconsolidated valley fill. In addition, numerical model calibration did not require the use of a bedrock flux to calibrate the model. Thus, groundwater inflow form the bedrock boundary is considered not to be a significant

component of the water balance and is not included as a component of the pre-simulation water balance. The prepared water balance is for a one year time period during which the net change in groundwater storage was considered to be negligible (change in storage = 0).

Water Balance Parameter	**Inflow source**	Minimum ft^3/day	Maximum ft^3/day	Possible Error	Range of Values	Previously Determined Values ft^3/day
GW_{inCFR}	GW Underflow Clark Fork River	$6.2e^5$	$1.2e^6$	33%	$4.2e^5 – 1.6e^6$	
GW_{inBRF}	GW Underflow Blackfoot River	$8.6e^4$	$5.2\ e^5$	33%	$5.7e^4$ - $6.9e^5$	$2.7e^5$ (Brick, 2003) $2.4e^4$(Popoff M.A., 1985)
GW_{inMC}	Marshall Creek underflow	140	$1.1e^5$	60%	$5.6e^1$ - $1.8e^5$	$1.1e^5$(Gestring, 1994)
GW_{inDC}	Deer Creek Underflow	$2.8e^4$	$3.1e^5$	60%	$1.1e^4 – 5.0e^5$	$3.1e^5$(Brick, 2003)
BFR_{leak}	Leakage Blackfoot River (BFR4 to BFR6)	$2.0e^6$	$2.3e^6$	50%	$1.0e^6$ - $3.5e^6$	
	Leakage Blackfoot River (I-90 Bridge to BFR4)	$9.8e^5$	$9.8e^5$	50%	$4.9e^5$ - $1.5e^6$	$6e^5$-$1.8e^6$(Gestring, 1994)
CFR_{leak}	Leakage Clark Fork river Below dam to well HGD	$2.3e^6$	$1.2e^7$	54%	$1.1e^6$ - $1.8e^7$	$2.4e^6$-$7.2e^6$(Gestring, 1994)
	Leakage Clark Fork river CFRA3 to CFRA4	$5.9e^6$	$5.9e^6$	60%	$2.4e^6$ - $9.4e^6$	
	Leakage Clark Fork river Above dam CFRA8	$5.7e^5$	$5.7e^5$	60%	$2.3e^5$ - $9.1e^5$	
Res_{leak}	Leakage Reservoir	$1.7e^4$	$3.2e^6$	50%	$8.5e^3$ - $4.8e^6$	$2e^6$(Gestring, 1994) $1.9e^6$-$2.6e^6$(Popoff M.A., 1985) $3.2e^6$(Moore and Woessner, 2002)
	Total Inflow	**$5.7e^6$**	**$4.0e^7$**		$6.7e^6$ - $2.2e^7$	

Table 4a Groundwater inflow balance table results. Individual river leakage and discharge locations can be located in Figure 16.

Water Balance Parameter	Outflow Source	Minimum ft^3/day	Maximum ft^3/day	% Error	Range of Values	
GW_{outCFR}	GW under Hellgate Canyon	$3.3e^6$	$1.5e^7$	33%	$2.1e^6$ - $2.0e^7$	$3.8e^6$-$7.6e^6$(Gestring, 1994) $4.2e^6$(Brick, 2003) $3.3e^6$-$6.6e^6$(Tallman A.A., 2005)
GSW_{out}	GW discharge: Clark Fork River CFRA2	$1.9e^6$	$1.9e^6$	60%	$7.6e^5$ - $3.0e^6$	$4.2e^6$ (Brick, 2003) 3.8-$7.6e^6$(Gestring, 1994)
	GW discharge: Clark Fork River CFRA5	$1.8e^6$	$1.8e^6$	60%	$7.2e^5$ - $2.9e^6$	
	GW discharge: Clark Fork River (CFRB1 to CFRB4)	$2.0e^6$	$2.0e^6$	60%	$8.0e^5$-$3.2e^6$	
GW_{ConsP}	Pumping Wells	$5e^4$	$7.6e^4$	5%	$4.8e^4$ – $8.0e^4$	(Gestring, 1994)
	Total Outflow	$9.0e^6$	$2.0e^7$		$9.1e^6$ - $2.1e^7$	
	Difference	$-3.3e^6$	$2.0e^7$			

Table 4b Groundwater outflow balance table results. Individual river leakage and discharge locations can be seen in Figure 16.

The water balance maximums and minimums were computed based on ranges of field values (e.g. hydraulic conductivity, hydraulic gradients, ranges of computed seepage and inflow rates), measured or assumed errors and uncertainties and professional judgment. Lateral inflow and outflow rates were computed using Darcy's Law and seepage rates were estimated using data from Table 1 and then computing the total area per river section of the saturated river bottom. Though groundwater pumping (consumed water) from the regions domestic wells were estimated, this out term is two orders of magnitude lower than the other components, thus has little affect on the overall water balance. The projected error applied to each term was estimated based on suggested uncertainty in analytical techniques and concerns over extrapolation of single point values.

3.0 Construction of the Numerical Groundwater Model

The process of modeling a hydrogeologic system requires descretizing space and time, and mathematically building the groundwater system inside of a computer. This methodology allows model conditions to be changed and updated more easily than physical modeling (sand tank) approaches. The following material details the generation of the study area model.

3.1 Model Formulation

In order to quantify how staged portions of the remediation operation are likely to affect groundwater levels in the associated aquifer, a three dimensional numerical groundwater model was formulated. The numerical model was developed using Ground Water Vistas graphical user interface to the USGS MODFLOW code (Environmental Simulations Inc. (ESI), 2004; Harbaugh A.W. et al., 2000).

3.2 Model Framework

The numerical groundwater model consists of 1,052,800 cells of which 53,192 are active. A large model area was selected so that model area could be expanded in future simulations and, if appropriate, the model could be connected to an existing model of the Missoula Valley Aquifer (Tallman, 2005). As a rectangular grid is required, a large portion of the model overlies the adjacent mountains, areas not simulated and represented by inactive cells.

The area was discretized into 150 ft by 150 ft cells and 7 layers (Figure 26a). Bottom elevations for each layer were assigned based on a November 2006 potentiometric surface (low water month). The bottom elevation of layer 1 was assigned to be 12 ft below this water table surface with layers 2 to 6 each 10 ft below the bottom of the layer above. The model base is represented by gravity interpolated bedrock elevations. The contact between the groundwater bearing valley fill sand and gravel and the bedrock was assigned as a no flow boundary.

The unconfined valley aquifer and the rivers were allowed to exchange water at 808 river cells that were segregated into seven reaches. In the reservoir area, exchange of groundwater and reservoir water was also represented using river cells and an additional 3 river reaches. Lateral flux boundaries were assigned using measured or interpolated groundwater levels at

Turah Bridge, the northern edge of the Stimson property (Blackfoot River valley), and Hellgate Canyon. Additional groundwater underflow was simulated as injection wells where side drainages intersect the valley. An extraction well was used to simulate periods of the sediment dewatering proximal to the reservoir (initiated in November 2006).

3.3 Model Boundaries

3.3.1 Bedrock

The model area is bound by bedrock. Each layer is laterally constrained by no flow cells which simulate locations of valley edge bedrock. The bottom elevation for each cell in the deepest layer, layer 7, is based on interpolated bedrock topography. The bedrock topography is reflected through each layer (Figure 26b). Bedrock boundaries were converted to no flow cells using Arc GIS 9.2 and imported into the model structure.

3.3.2 Specified Head

Three specified head boundaries form the boundaries of the aquifer at Turah, near the mouth of the Blackfoot Canyon, and in Hellgate Canyon. The specified head boundaries represent equipotential lines at these locations for either steady state or transient conditions. Constant head boundaries are not allowed to change at these locations during steady state simulations, or during each transient stress period. The water table elevation at these boundaries were extrapolated from the nearest wells, this being HGD in Hellgate Canyon, Rodin at Turah, and RSW-4 where the Blackfoot River enters the valley (Figure 10).

3.3.3 Wells

Injection wells were used to simulated groundwater underflow along the mountain boundaries where Deer Creek (310,000 ft^3/day) and Marshal Creek alluvial filled valleys (91,000 ft^3/day) enter the valley (Figure 26b). Due to the limited availability of information necessary to estimate underflow, a single injection well discharge was used at each location to represent steady state and transient conditions. Recharge from other smaller surface water drainages and diffuse bedrock recharge was assumed to be negligible and not simulated. A dewatering well

located in the reservoir was simulated in the transient runs to representing periods of sediment dewatering conducted by Envirocon (started in November of 2006) (Appendix D).

3.3.4 Rivers

The rivers were represented as 11 different reaches Figure 27. The reaches began and ended at established river stage monitoring sites. At river cell locations, the river bed exchange rate was adjusted by varying the conductance of the river bed which is determined by (McDonald and Harbaugh, 1984):

$$C = \frac{KLW}{M}$$

Where

C = River Conductance
K = Riverbed hydraulic conductivity
L = Length of river cell
W = Width of river cell
M = Thickness of river cell

The exchange rate within a model cell was determined using the conductance term and the head difference between the river stage and groundwater (head in a model cell). When a river cell becomes disconnected from the groundwater (the elevation of the assigned base of the river bed sediments is greater than the simulated groundwater head in the cell) the head difference between the river stage and the assigned base of the river bed sediments (3 feet in this model) is multiplied by the conductance to determine the rate of river seepage, a value that remains constant for the period the stream stage remains constant. The river bed conductance term is usually poorly known and during model calibration it is fitted to derive observed groundwater conditions. Values used in this work were constrained by field estimates (see the previous sections on river bed property measurements). Below Milltown Dam, the river was divided into three different river reaches. The computed conductance of these reaches was assumed to decrease down river from reach to reach.

3.3.5 Reservoir

The leakage of water from the reservoir and into the underlying groundwater (layer 1) was simulated using river cells. The river cells were broken up into three different reaches to

establish a reasonable gradient within the reservoir. The reaches extended up to the Duck Bridge. A package of reservoir sediments was assigned a thickness based on sediment survey information (River Design Group, 2007)(Figure 28). These values were used to generate conductance terms and to compute exchange rates.

3.4 Aquifer Parameterization

Aquifer hydraulic conductivity values from the literature and this effort ranged from 300 to 90,000 ft/day. Parameterization of the model cells was based on the location of field tests, interpretations of the geologic cross sections, and likely distributions of sediment types based on perceived deposition environments.

For transient simulations storage coefficients are required. The unconfined system represented by layer one was assigned a specific yield of 0.15. As the remaining layers remain saturated throughout the simulation a specific storage value of $1e^{-6}$ was assigned to cells in layers 2 through 6. The average bulk porosity of the modeled sediments was assigned as 0.2. All storage and porosity values remained constant for all model runs.

4.0 Model Execution and Calibration

The three-dimensional model was constructed and parameterized based on field observed water levels, measured and interpolated aquifer properties and geometries, and application of basic hydrogeologic principals. The MODFLOW code was solved using the PreConditioned Conjugate Gradient 2 solver package (Hill, 1990). The solver was limited to a maximum of 50 inner iterations and a maximum of 5000 outer iterations and the head change criterion was set to 0.01 to minimize run time. The residual criterion and relaxation parameter were set to one and the Cholesky matrix preconditioning method was used. The simulated water balance results were consistently stable and differences between inflow and outflow components were less than 0.02 percent. The model was calibrated to historical and current conditions using standard techniques (Anderson and Woessner, 1992)

The calibration process requires the setting of pre-simulation calibration targets and then performing an iterative process comparing model results with set calibrations targets. Targets

include water levels measured at monitoring points and lumping statistics such as the mean absolute error (Anderson and Woessner, 1992), locations and rates of losing and gaining stream reaches, and the calculated fluxes of the pre-model water budget. Targets are specified for both steady state and transient calibrations (Table 5). Qualitative calibration evaluations are also applied including matching of measured and modeled water table maps, and, in transient simulations, matching simulated and measured hydrographs at monitoring points. In addition, modeled parameter values are expected to fall within estimated values based on field measurements and literature values, and within the known and interpreted geologic settings.

Calibration Parameter	**Calibration Target**	**Target Type**
Groundwater Levels	Absolute residual mean error +/- 4.5 ft	Quantitative
Water Balance Underflow	Within estimated range (Tables 4a & 4b)	Quantitative
River and Reservoir Leakage	Within estimated range (Tables 4a & 4b)	Quantitative
Location of Gaining and Losing River Reaches	+/- 0.5 mile	Qualitative
Match of Simulated and Measured Water Table Maps and Hydrographs (transient)	Observed closeness of fit	Qualitative
Aquifer Parameter Distribution	Supported by field data and geologic data sets	Qualitative

Table 5 Listing of Calibration Parameters and Targets.

The designation of an acceptable match between simulated and measured-interpolated groundwater conditions is still subjective. The level of quantitative match to targets is not standardized as the purpose of the model will suggest the needed degree of match. For this project the values listed in Table 5 are based on the realization that drawdowns of the reservoir may result in a maximum of 10 to 15 ft of groundwater level change (end of Stage 2), so the targets should be less than this. In addition the overall groundwater level change across the entire model area is about 150 ft, thus the absolute residual mean error criteria is a match of heads within 3% of the total measured head variation.

The calibration process used in this modeling effort included calibration to recent steady state conditions, transient conditions, and history matching to both steady state and transient 1992-1993 data (Gestring, 1994) (Figure 29).

An additional analysis was preformed to evaluate the sensitivity of model results to variations in input parameters. Once completed the calibrated steady state model was used to derive estimates of final Stage 2 drawdown effects of groundwater levels. Two scenarios examining the effect of varying sensitive parameters on predictions were also evaluated.

The calibration process involves assigning boundaries and parameters then running the model and comparing model results with calibration targets. The process proceeds by then adjusting parameters, boundaries and/or model geometry and re-running the model; once again simulated results are compared to the targets. This process continues until an acceptable match is achieved. Calibration was performed using manual trial and error, and automated parameter estimation techniques (Anderson and Woessner, 1992).

Once the steady state model was calibrated, the steady state heads and fluxes were input as initial conditions in a transient simulation. Once again an iterative calibration process was used to calibrate the transient model. The calibrated parameters and model structure of the transient model were then fed back into the steady state model to check to see if the new parameter distributions generated during transient calibration fit the steady state calibration. This process was repeated until both the steady state and transient models were considered calibrated with a common set of parameters (Figure 29).

As a further evaluation the calibrated model was then applied to an independent data set (not used for calibration), Gestring's 1992-1993 measurements. These data only included information for the Milltown area to Hellgate Canyon (Figure 3).

4.1 Calibrated Groundwater Flow Model

The model calibration resulted in a supportable three-dimensional representation of the groundwater conditions within the region of investigation. The calibrated parameter distributions and calibration statistics related to steady state, transient and history match conditions are presented in the next sections.

4.2 Calibrated Parameter Distributions

The final calibrated model hydraulic conductivity distributions represented the aquifer with values that ranged from 75 to 60,000 ft/day (Figure 30). Areas of low hydraulic conductivities are proximal to the confluence of the Clark Fork and Blackfoot River rivers. Regions of high conductivity are located in West Riverside and near the mouth of Hellgate Canyon. Initial assignment of interpolated field and literature derived hydraulic conductivities underwent slight modifications during model calibration. The final distribution is supported by well log interpretations, basic sediment depositional process theory, observed water level response, and measured and interpreted flux rates.

4.3 River Bed Conductance

The riverbed conductance in the final calibrated model ranges from 98 to 16,500 ft^2/d (Figure 31). Reservoir conductance in reach 9 is 7200, in reach 10 is 2250, and reach 11 is 1800 ft^2/d (Figure 27). The conductance in reach 9 may be higher in some sections than simulated as this area was represented by only a few field measurements.

4.4 Steady State

Our steady state model simulated conditions for March 31, 2006. The model was calibrated to measured heads and the pre-modeling estimated water budget terms.

Twenty four calibration targets were used to evaluate steady state calibration. These heads were distributed in multiple layers as follows: 4 in layer 1; 3 in layer 2; 4 in Layer 3; 6 in layer 4; 4 in layer 5; 1 in layer 6, and 2 in layer 7. The match of measured to simulated steady state heads show a residual mean of -0.73 ft, an absolute residual mean of 1.63 ft, and a standard deviation of 0.02 (Figure 32).

Simulated heads for 18 of the target wells were within 1.75 ft of the observed water levels (absolute residual mean of 0.79 ft with a standard deviation of 0.60 ft) (Figure 33) (Appendix E). The overall simulated water table position compared well with the observed water table map (Figure 34).

Acceptable calibration of identified gaining and losing river reaches (simulated within 0.5 miles of measured boundaries) was achieved (Figure 35). Below the Milltown Dam the short stream reach identified as a gaining stream was simulated to occupy slightly less river reach length than the observed area. Above the Milltown Dam the simulated vertical exchanges with the Clark Fork River and groundwater are slightly different than those interpolated from point field measurements. However, generally, simulated conditions meet calibration criteria (Figure 17,18, and19).

The simulated steady state water budget (Table 6) compared favorably with the pre-model estimated steady state budget (Tables 4a and 4b). The simulated water budget slightly underestimated seepage from the Clark Fork River into the underlying groundwater and the flow of valley groundwater into gaining portions of the river. Overall the simulated inflow and outflow fell within computed estimated pre-model ranges.

	Estimated range (ft/day)	Modeled value (ft/day)
GW_{inCFR}	$4.2e^5 – 1.6e^6$	$1.3e^6$
GW_{inBRF}	$5.7e^4$ - $6.9e^5$	$5.7e^4$
GW_{inMC}	$5.6e^1$ - $1.8e^5$	$9.0e^4$
GW_{inDC}	$1.1e^4$ -$5.0e^5$	$3.1e^5$
BFR_{leak}	$1.5e^6$ - $4.9e^6$	$2.0e^6$
CFR_{leak}	$3.7e^6$ - $2.8e^7$	$3.2e^6$
Res_{leak}	$8.5e^3$ - $4.8e^6$	$1.9e^6$
Total Inflow	$5.6e^6$ - $4.1e^7$	$8.9e^6$
Outflow	**Estimated range (ft/day)**	**Modeled value (ft/day)**
GW_{outCFR}	$2.2e^6$-$2.0e^7$	$8.1e^6$
GSW_{out}	$2.3e^6$-$9.1e^6$	$7.1e^5$
Total Outflow	**$4.5e^6$-$2.9e^7$**	**$8.8e^6$**

Table 6 Comparison of the pre-model estimated (includes error estimate) and simulated steady state water balance. Values shown in red fell outside of the estimated pre-model range.

4.5 Transient

The calibrated steady state heads, boundaries and fluxes were used as initial conditions during transient model calibration. The comparison of simulated heads to observed heads (March 31, 2006 to April 21, 2007), and the pre-modeling estimated water balance revealed the model does a reasonable job of simulating observed conditions under this more demanding evaluation. For the transient simulation 60 observed heads were used as calibration targets. They were distributed as follows: 23 in layer 1; 7 in layer 2; 8 in Layer 3; 7 in layer 4; 8 in layer 5; 3 in layer 6, and 4 in layer 7. Comparisons of modeled to measured heads using lumping statistics for each model stress period are presented in Figure 36. These results show the head match during the initial few stress periods was poorer than in later periods of the modeling effort. This is most likely partly a result of the early model stress periods being too long, resulting in an incomplete representation of flow and head conditions during spring runoff when river stages and

groundwater levels were changing rapidly. However, head residuals did stabilize as time progressed suggesting general transient conditions are appropriately represented.

The comparison of observed and simulated heads over time at calibration targets provides an additional method to assess the representativeness of the numerical model (Figure 37). Results show relatively good fits of simulated water level positions with observed levels at most sites

The simulated water budget compared well with the estimate budget. An example of the budget represented by the last time step computed in the transient simulation is presented in Table 7.

	Estimated range (ft/day)	Modeled value (ft/day)
GW_{inCFR}	$4.2e^5 – 1.6e^6$	$1.2e^6$
GW_{inBRF}	$5.7e^4 - 6.9e^5$	$1.8e^5$
GW_{inMC}	$5.6e^1 - 1.8e^5$	$9e^4$
GW_{inDC}	$1.1e^4 - 5.0e^5$	$3.1e^5$
BFR_{leak}	$1.5e^6 - 4.9e^6$	$1.5e^6$
CFR_{leak}	$3.7e^6 - 2.8e^7$	$4.1e^6$
Res_{leak}	$8.5e^3 - 4.8e^6$	$1.0e^6$
Total Inflow	$5.6e^6 - 4.1e^7$	$8.3e^6$
Outflow	Estimated range (ft/day)	Modeled value (ft/day)
GW_{outCFR}	$2.2e^6 - 2.0e^7$	$7.2e^6$
GSW_{out}	$2.3e^6 - 9.1e^6$	$8.5e^5$
GW_{ConsP}	$4.8e^4 - 8.0e^4$	$1.7e^5$
Total Outflow	$4.5e^6 - 2.9e^7$	$8.2e^6$

Table 7 Transient water balance presented for the last stress period of April 21, 2007. Estimated range includes error estimates. Values in red are outside the estimated range.

4.6 History Matching

As a further evaluation of the calibrated model it was used to simulate observed conditions for two independent data sets: Gestring's steady state conditions, and his sparse transient data set (1992-1993). In this approach the reservoir elevation and river elevations were set along with measured steady state boundary conditions based on Gestring's values. The model was then executed without parameter changes and simulated results were compared to his observed data sets. The same approach was applied to his transient head measurements.

Results of the steady state analyses using 53 targets show heads were reproduced within suggested acceptable ranges (Figure 38). A water balance comparison was not developed as Gestring's model did not include the entire extent of the project site.

The match of historical simulated and observed water table maps is presented in Figure 39. The simulated water table is slightly higher than the observed water table. However, the general surfaces compare favorably. Some of the differences in water table elevations are most likely an artifact of Gestring's use of a more heavily populated monitoring well network in this area.

The results of transient head history matching (83 targets) are shown in Figure 40. The head residual and absolute residual remained within acceptable calibration criteria (Table 5). This evaluation suggests the model reasonably represents the processes controlling groundwater occurrence and movement in the project area.

5.0 Sensitivity Analyses

Once our numerical model was calibrated, and before we attempted forecasting impacts of drawdowns, we completed an analysis to determine which aquifer parameters values had the largest effect on the model calibration, a sensitivity analyses. This information highlights the specific parameters that principally control the model calibration for the given set of model conditions. Results suggest which parameters need to be well defined. If instead they are considered poorly defined, additional spatial and temporal resolution of those parameters may be needed to limit uncertainty in model results.

The sensitivity analysis was performed using our steady state calibrated model. It focused on three groups of parameters: vertical (Kz or Kv) and horizontal aquifer hydraulic conductivities Kx=Ky =Kh), aquifer storage properties (S), and river bed conductance values. All values were set to range 20% above and below the values used in our calibrated model. The hydraulic conductivity in each zone was varied separately while all other parameter remained constant.

The results of the sensitivity analysis indicate that the model is most sensitive to horizontal aquifer hydraulic conductivity and river bed conductance, and least sensitive to variations in vertical aquifer hydraulic conductivity and storage values (Figures 41, 42, 43). Of the different horizontal aquifer hydraulic conductivity zones evaluated, the model was most sensitive to zone 27. This zone encompasses the Bandmann Flats area in the western area of the model (Figure 30). The sensitivity of the steady state model to the river bed conductance was greatest in reach 5 (Figure 27). This reach extends up gradient from Duck Bridge.

Conceptually, the range of uncertainty in model predictions could be reduced if reasonable ranges in parameter uncertainties could be refined by additional analyses and/or more complete field data. The calibration process is intended to build evidence that the formulated model produces a reasonable representation of the system, recognizing that error and uncertainty are inherent in the modeling process. With these points in mind, we now present our predictions of the impacts of remediation drawdowns on the groundwater system.

6.0 Forecasts

The model was used to simulate the groundwater levels that would result after the planned Stage 2 drawdown was complete. We used our March 31, 2006 calibrated steady state model and replaced the pre-drawdown river stage and reservoir levels with new data sets developed by evaluating how the planned total reservoir drawdown of 19 ft (after Stage 2 was completed) would reduce surface water levels. Surface water elevations in river reach 1 and river reach 2 (Figure 21) were modified to reflect the new stages and gradients anticipated in those areas. In addition, an area of the river cells used to simulate the reservoir sediments east of Milltown Dam were eliminated as dewatering and sediment removal are planned in these areas (Figure 44) (Envirocon, 2006).

By using the steady state representation of the March groundwater system the predicted water table position likely represents the lowest groundwater position that will be observed during the year, a condition that would have the largest impact on domestic wells. We also observed from field data collected during the 2006 drawdown that the water table responds almost immediately to the reservoir changes (days to weeks).

The new reservoir and river configuration was first simulated using the same boundary conditions as the calibrated steady state model. We observed that the specified head boundary used to represent conditions in the Blackfoot River canyon limited groundwater level responses in the adjacent area. We replaced that boundary condition with a general head boundary calibrated to the fluxes modeled in the calibrated steady state model. Model boundaries in Hellgate Canyon and at Turah Bridge were left as specified heads as they were considered distance boundaries, and not likely to have an observable impact on model results (Anderson and Woessner , 1992). Model results are presented as predicted drawdowns computed by subtracting the simulated heads for the Stage 1 and 2 drawdown (total combined drawdown) from the simulated March 31, 2006 steady state heads (prior to Stage 1 and Stage 2 drawdowns).

The predicted aquifer response to the completed Stage 2 drawdown of the Milltown Reservoir can be viewed in Figure 45. The results show 7 - 8 feet of drawdown in the northwest area of Piltzville, 2 - 3 feet of drawdown in the southwest area of Piltzville, 12 - 14 feet of drawdown in Milltown, and 10 - 11 feet of drawdown in Bonner and the area of Stimson Lumber Company. Downstream of the reservoir, the impact is predicted to be 8-9 feet in West Riverside, 5-8 feet in the area near Pine Grove, 3 - 5 feet in Bandmann Flats, and 2 -3 feet in East Missoula.

The effects of the 19 foot drawdown propagate approximately 2 miles up stream of the dam, and to Hellgate Canyon. In Figure 45, the area just below Milltown Dam has a simulated area with 2 to 4 feet of drawdown (blue region) surrounded by an area of greater drawdown. The area contains a buried bedrock high. In the Blackfoot River canyon, at the north end of Stimson property there is a simulated area (dark orange) mapped as having a greater drawdown than the surrounding region. Once again a buried bedrock high is present at that location. It is unclear if

these small areas of the model are representative of likely impacts or if they are an artifact of model formulation or discretization. The over all trends should be viewed as more representative of likely impacts than the simulated changes in a few cells of the model.

Within the time frame of the year 1 work, we focused on generating a supportable calibrated model of the project site. A next logical step would be to generate a number of additional calibrated models with expected errors and uncertainties in model parameters built into them. This would permit us to place a confidence interval on predicted results. Using two scenarios, we did attempt to illustrate how variations in model sensitive parameters are likely to impact model predictions at this site. We fully realize the two scenarios we set up need to be re-run and first calibrated under the prescribed conditions, then used to predict. However, as we stated, that was not completed in this phase of the project.

As an illustration, two additional predictive scenarios were evaluated (see Figure 29, Stage 2B and Stage 2C). We ran a prediction that increased all aquifer conductivities by 20% and decreased all river bed conductance terms by 20% to see what effect this would have on predicted groundwater drawdowns. We anticipated this scenario would result in larger predicted drawdowns. In a second scenario, we decreased aquifer hydraulic conductivities by 20% and increased river bed conductances by 20%. We anticipated this scenario would result in smaller than originally predicted drawdowns. For each scenario, the parameters were changed in the March 2006 steady state predictive model and final heads computed (Figure 46 a and b). Predicted impacts under the prescribed conditions showed anticipated changes in heads. Generally, values computed for the first scenario produced heads up to 6 feet lower in places than those predicted from our calibrated modeling. Scenario two values were generally about 6 feet higher than calibrated model predictions. This result (Stage 2C) is somewhat unrealistic as groundwater levels were observed to drop below predicted scenario two elevations during Stage 1 drawdown at some locations (see Figure 15 for observed Stage 1 drawdown impacts). Clearly, a more robust uncertainty analysis is needed to frame modeling predictions and aid decision makers. Future work should develop multiple calibrated representations of the project site, a process that would allow us to better bound predictions.

.

In addition to the predicting the degree of water level change from the operational drawdowns, we completed a flow direction analyses by comparing the calibrated modeled March 31, 2006 water table surface and groundwater flow paths with the predicted low water table surface and flow paths (Figure 45 model conditions)(Figure 47). These results suggest that the configuration of the post Stage 2 water table position may result in a more northerly movement of groundwater from the lower reservoir area, and a more down valley flow of groundwater in the Piltzville regions, than originally occurred (pre-drawdown).

7.0 Model Limitations

As with most modeling efforts data sets are incomplete and the system is not fully characterized. This results in a degree of uncertainty in model results. By recognizing weaknesses in our understanding of the physical and hydrogeologic systems, steps can be taken to target data collection and testing efforts to reduce model uncertainly.

Our calibration efforts brought to light factors that appear to require additional refinement. These include investigating how uncertainty in the gravity generated bedrock boundary model; the assigned number, value and location of hydraulic conductivity zones, and the variation in river bed leakage properties impact model calibration and predictions.

The configuration of the bedrock boundary underlying the unconsolidated aquifer may have as much as +/- 30 ft of error associated with it. This is partly a function of the density of the survey points and limited availability of calibration borings in areas outside of Milltown and the reservoir area. Also the lack of high resolution surface elevation data upstream of the reservoir and west of Pine Grove reduced the resolution of the gravity model. The current gravity model also doesn't represent steep bedrock slopes well. The impact of these factors on model predictions is unknown and needs to be evaluated. If significant changes in bedrock boundary elevations (+/- 30 ft) are found to change the degree of model calibration, additional refinement of this boundary may be required.

The values reported for hydraulic conductivities in the study area are generally in the 100 to 1000's of ft/d. Our current model has 21 hydraulic conductivity zones. However, depositional

relationships among zones are poorly understood. Flow tube and peak delay analyses suggest the presence of high hydraulic conductivity zones in the West Riverside area; however, no actual aquifer tests have been executed in this area to confirm these conditions. Clearly, additional characterization of aquifer properties in targeted areas would refine the current calibrated hydraulic conductivity distribution.

A third area of concern relates to how the relationship between stream stage and bed characteristics is represented in the model. Field data suggest that as stream stage changes seepage rates change in a non-linear fashion. When the stream becomes perched or in sections where it is always perched, the seepage rate appears to be influenced by underlying unsaturated zone properties, changes in bed characteristics during different flow regimes, and/or changes in river temperature. Though model calibration can be achieved by varying seepage properties when field data are available, unfortunately, how these rates may change during un-monitored future drawdowns are unknown. In addition, the river characteristics of remediated or restored stream sections are expected to be somewhat different than those characterized under current investigations. Overall, we only have limited field data describing the relationship between stream stage and river leakage.

The model assumed the bedrock is not a significant source of recharge to the valley fill aquifer. This is partly supported by the results of drilling into bedrock in the Milltown area. However, few wells penetrate the bedrock along the sides of the valley. Further justification of this assumption is needed.

It is recommended that these identified limitations be addressed in additional hydrogeologic investigations and modeling studies. Clearly, a more robust uncertainty analysis is also needed to provide a framing of modeling results and to aid decision makers.

8.0 References Cited

Anderson, M.P. and Woessner, W.W., 1992. Applied goundwater modeling, simulation of flow and advective transport. Academic Press, 382 pp.

Atlantic Richfield Company (ARCO), 1992. Summary of Four-Step Process, Addressing Wetlands Issues in Upper Clark Fork River Superfund Sites, Letter from Ms. Sandra Stash, ARCO, Anaconda, MT to Mr. Donald Pizzini and Mr. Robert Fox, USEPA, Helena, MT.

Atlantic Richfield Company (ARCO), 1995. Milltown Reservior Sediments Operable Unit, Final Draft Remedial Investigation Report. .

Atlantic Richfield Company (ARCO), 2002. Milltown Reservior Sediments Site Final Combined Feasibility Study. Report prepared for Arco by EMC2, Bozeman, MT.

Brick, C., 2003. Preliminary groundwater modeling to estimate effects of dam and sediment removal on the alluvial aquifer in Milltown, Montana. Clark Fork Coalition. Report.

Cordell, L. and Henderson, R.G., 1968. Iterative three-dimensional solution of gravity anomaly data using a digital computer. Geophysics, 33(4): 596-601.

Envirocon, 2006. Remedial design work plan, Final.

Environmental Simulations Inc. (ESI), 2004. Guide to Using Groundwater Vistas, Version 4

Evans, C.A., 1998. A constrained gravity model of the Central Missoula Valley and shape of the Ninemile Fault. Masters Thesis, University of Montana, Missoula, MT, 66 pp.

Fetter, C.W., 2001. Applied hydrogeology, 4th ed. Macmillan Publishing Company, New York, NY, 598 pp.

Gestring, S.L., 1994. The interaction of the Clark Fork River and the Hellgate Valley Aquifer near, Milltown, Montana. M.S. Thesis. Geology Department, University of Montana.

Gradient Geophysics, 1991. Missoula-Milltown area seismic refraction determined bedrock depth data, processed for Land and Water Consulting, Inc., unpublished.

Harbaugh A.W., Banta R.B., Hill M.C. and McDonald M.G., 2000. Modflow-2000, The U.S. Geological Survey Modular Ground-water Model—User guide to Modularization Concepts and the Ground-water Flow Processes. U.S. Geological Survey Open File Report 00-92. .

Harding Lawson Associates (HLA), 1987. Milltown Reservoir Data Report Supplemental Investigations conducted under the Feasibility Study, Report prepared for Montana Department of Health and Environmental Sciences Solid and Hazardous Waste Bureau, Helena, Montana.

Hill, M.C., 1990. PreConditioned Conjugate-Gradient 2 (PCG2), A computer crogram for solving ground-water flow equations. Report 90-4048, Denver, Colorado.

Hsieh, P.A., Wingle, W. and Healy, R.W., 2000. VS2DHI- A graphical software package for simulating fluid flow and solute or energy transport in variably saturated porous media, USGS Water Resources Investigations Report 9.

Hvorslev, M.J., 1951. Time lag and soil permeability in ground-water observations, U.S. Army Waterways Experiment Station Bulletin 36, Vicksburg, Mississippi.

Janiszewski, F.D., 2007. Seismic reflection and gravity constraints on the bedrock configuration in the greater East Missoula Area. Masters Thesis, University of Montana, Missoula, MT, 108 pp.

Johnson, A.N. et al., 2005. Evaluation of an inexpensive small-diameter temperature logger for documenting ground water-river interactions. Ground Water Monitoring and Remediation, 25(4): 68-74.

Land and Water Consulting, I., 2004. Aquifer/GroundwaterAnalysis, Aquifer Test of Plywood Processing Well Impacts from Drawdown of the Blackfoot River, Prepared for the Stimson Lumber Company Bonner, Montana.

Land and Water Consulting, I., 2005. Well #1 Pumping Test Results And Water Availability Report, Prepared for Canyon River Development, LLC, Missoula, Montana.

Landon, M.K., Rus, D.L. and Harvey, F.E., 2002. Comparison of instream methods for measuring hydraulic conductivity in sandy streambeds. Ground Water 39(6): 870-885.

Lewis R.S., 1998. Geologic map of the Butte 1^o x 2^o Quadrangle. Montana Bureau of Mines and Geology.

McDonald, M.G. and Harbaugh, A.W., 1984. A modular three-dimensional finite-difference ground-water flow model. U.S. Geological Survey Open-File Report 83-875, 528 pp.

Moore, J.N. and Woessner, W.W., 2002. Arsenic contamination in the water supply of Milltown, Montana, In: A.H. Welch and K.G. Stollenwerk (editors), Arsenic in Ground Water: Geochemistry and Occurrence. Kluwer Academic Publishers, Boston.

Nelson, W.H. and Dobell, J.P., 1961. Geology of the Bonner Quadrangle, Montana. U.S. Geological Survey Bulletin, 1111-F: 235.

Newman, H., 1996. Groundwater Source and Availability of Two Wells Serving Canyon Pines Homeowners Association, Piltsville, Montana, Prepared for Canyon Pines Homeowners Association, Missoula, Montana.

Newman, H., 2005. Technical Report for Beneficial Water Use Permit for Turah Meadows SUbdivision, Turah, Montana, Aquifer Test Results Seepage Loss Estimates and Augmentation Plan for Turah Meadows Subdivision, Turah, Montana, Missoula, Montana.

North West Energy, 2007. Milltown Dam Daily Readings. In: U.o. Montana (Editor). Northwest Energy, Missoula, Montana.

Nyquest, D.L., 2001. A depth-to-bedrock model of the Hellgate Canyon and Bandmann Flats area, East Missoula, Montana using constrained inversion of gravity data. M.S. thesis. Geology Department, University of Montana, pp. 186.

Pinder, G.F., Bredehoeft, J.D. and Cooper, H.H., 1969. Determination of aquifer diffusivity from an aquifer response to fluctuations in river stage. Water Resources Research, 5: 850-855.

Popoff M.A., 1985. A case study of the hydrogeology and groundwater contamination of Milltown Valley, Montana, University of Montana.

River Design Group, I., 2007. Proposed land profile for the Clark Fork River segments; Milltown Reservoir sediment wedge evaluation data and survey points, Unpublished Spreadsheet.

Sheriff, S.D. and others, 2007. University of Montana gravity data compilation for the Missoula-Milltown region. University of Montana.

Tallman A.A., 2005. Sources of Water Captured by Municipal Supply Wells in a Highly Conductive Aquifer, Western Montana, Masters Thesis. Department of Geology, University of Montana, pp. 291.

Tallman, A.A., 2005. Sources of Water Captured by Municipal Supply Wells in a Highly Conductive Aquifer, Western Montana, Masters Thesis. Department of Geology, University of Montana, pp. 291.

Udaloy, A.G., 1988. Arsenic mobilization in response to the draining and filling of the reservoir at Milltown, Montana. M.S. Thesis. Department of Geology, Universtiy of Montana.

Westwater Consultants, I., River Design Group, I. and Geum Environmental Consulting, I., 2005. Restoration Plan for the Clark Fork and Blackfoot River near Milltown Dam – October 2005.

Woessner, W.W. et al., 1984. Arsenic Source and Water Supply Remediation Action Study, Milltown, Montana. Final Report for Solid Waste Bureau, Montana Dept. Health and Environmental Sciences, Helena, montana.

Woessner, W.W. and Popoff, W.A., 1982. Hydrogeologic Survey of Milltown, Montana and Vicinity. Report for the Water Quality Bureau, Department of Health and Environmental Sciences, Helena, MT.

9.0 Appendices

Appendix A Figures

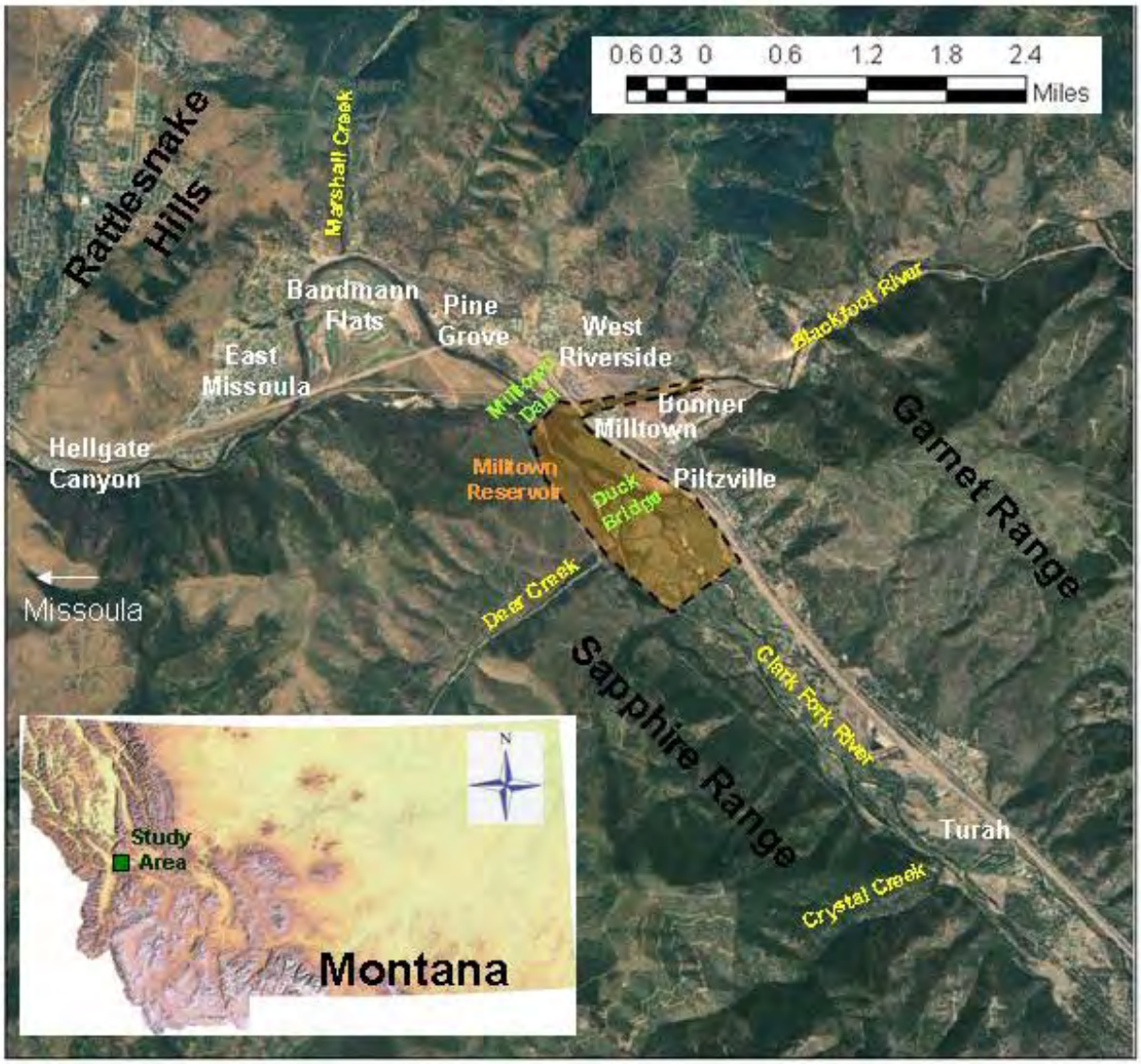

Figure 1ES Study area location map. The study area is located in North Western Montana east of Missoula and west of Turah. The Milltown Reservoir is bounded by Milltown Dam to the west, the Clark Fork River channel just east of the Duck Bridge and the Blackfoot River arm of the reservoir northeast to the Blackfoot River Canyon

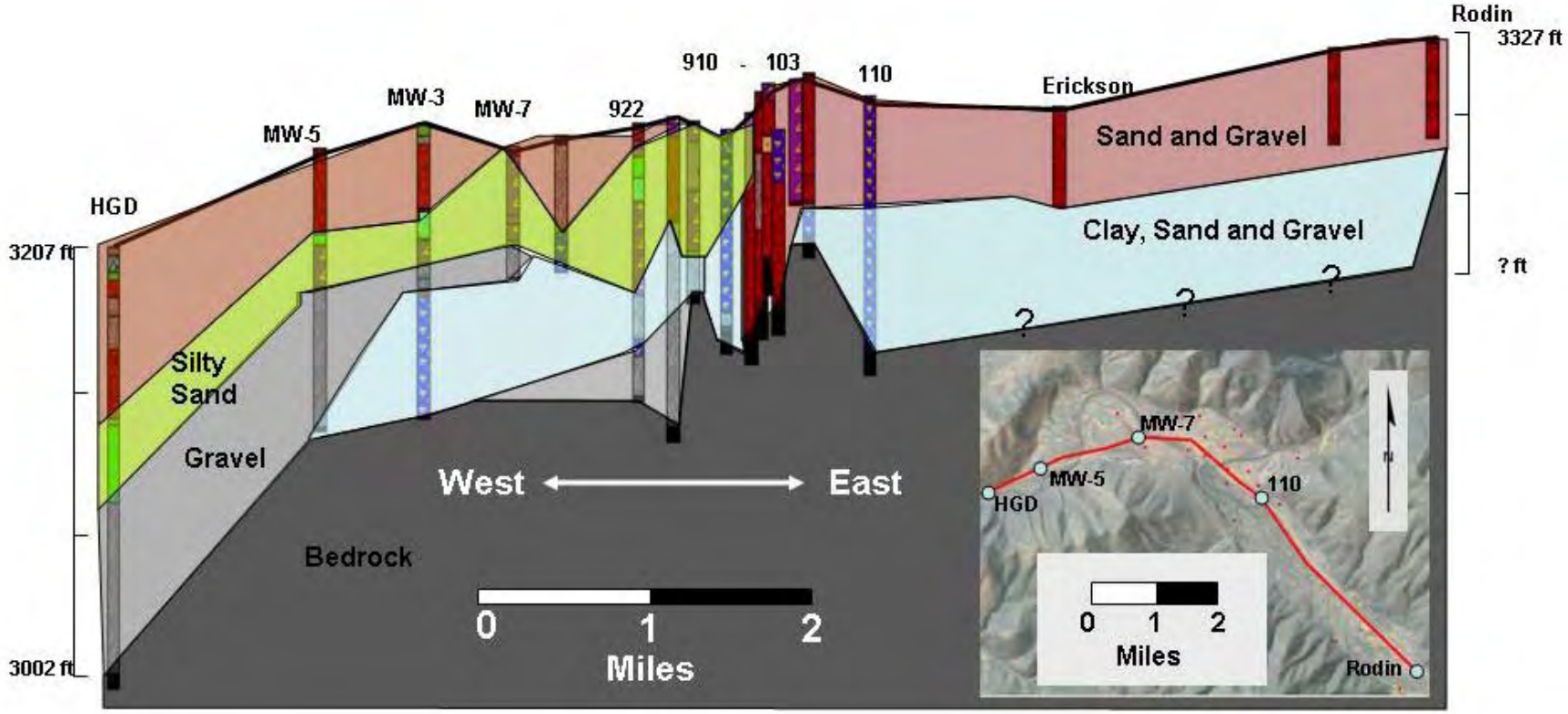

Figure 2 ES Hydrostratigraphic cross section interpreted from well logs.

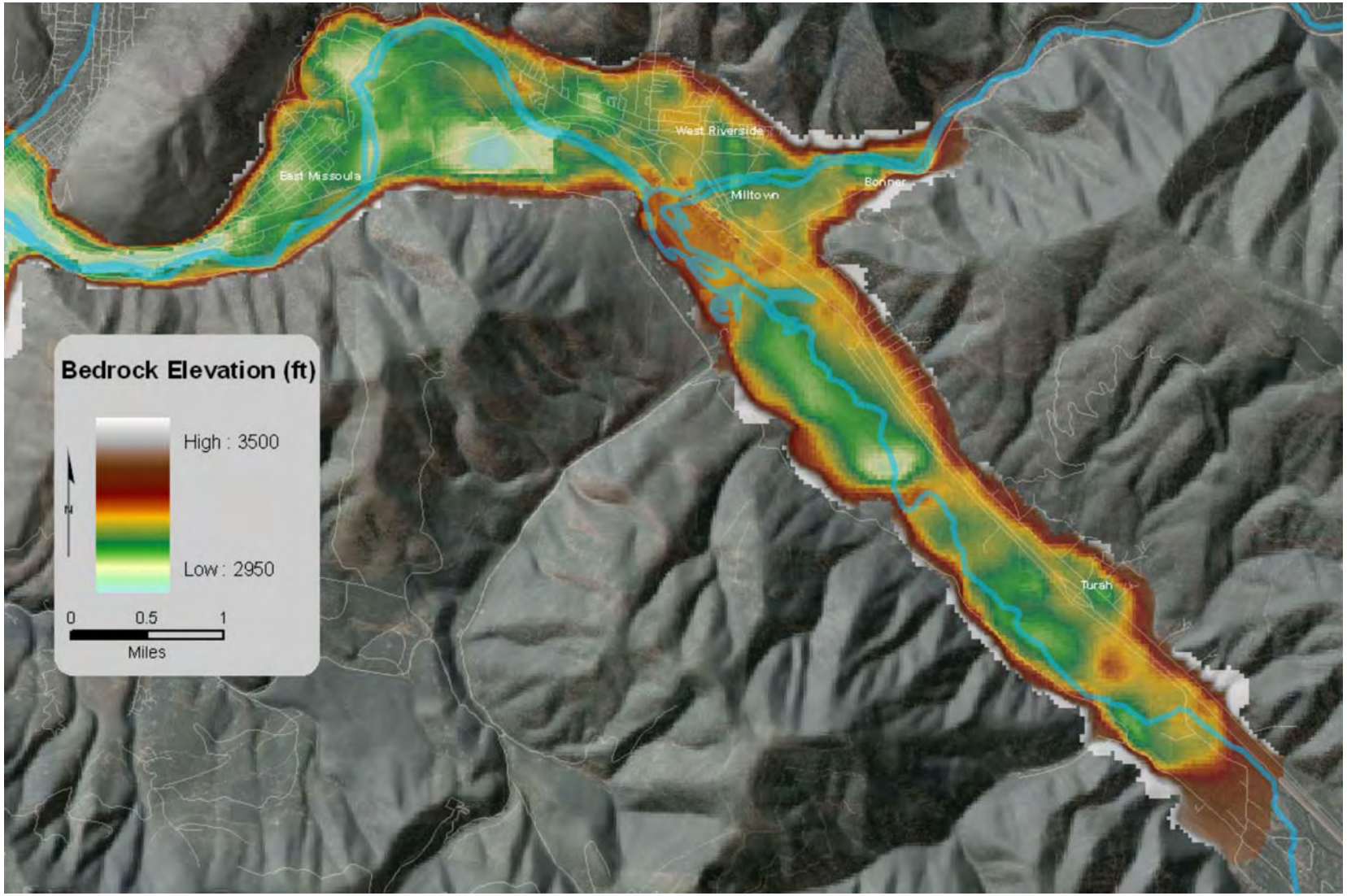

Figure 3ES Bedrock elevations derived from a compilation of gravity data, four seismic lines processed by Gradient Geophysics, historical borehole data, well logs, and topographic projections into the subsurface. Known depth to bedrock was used to condition the data. However, bedrock depth may actually vary up to + or – 30 feet in areas outside of the area immediately adjacent to the reservoir.

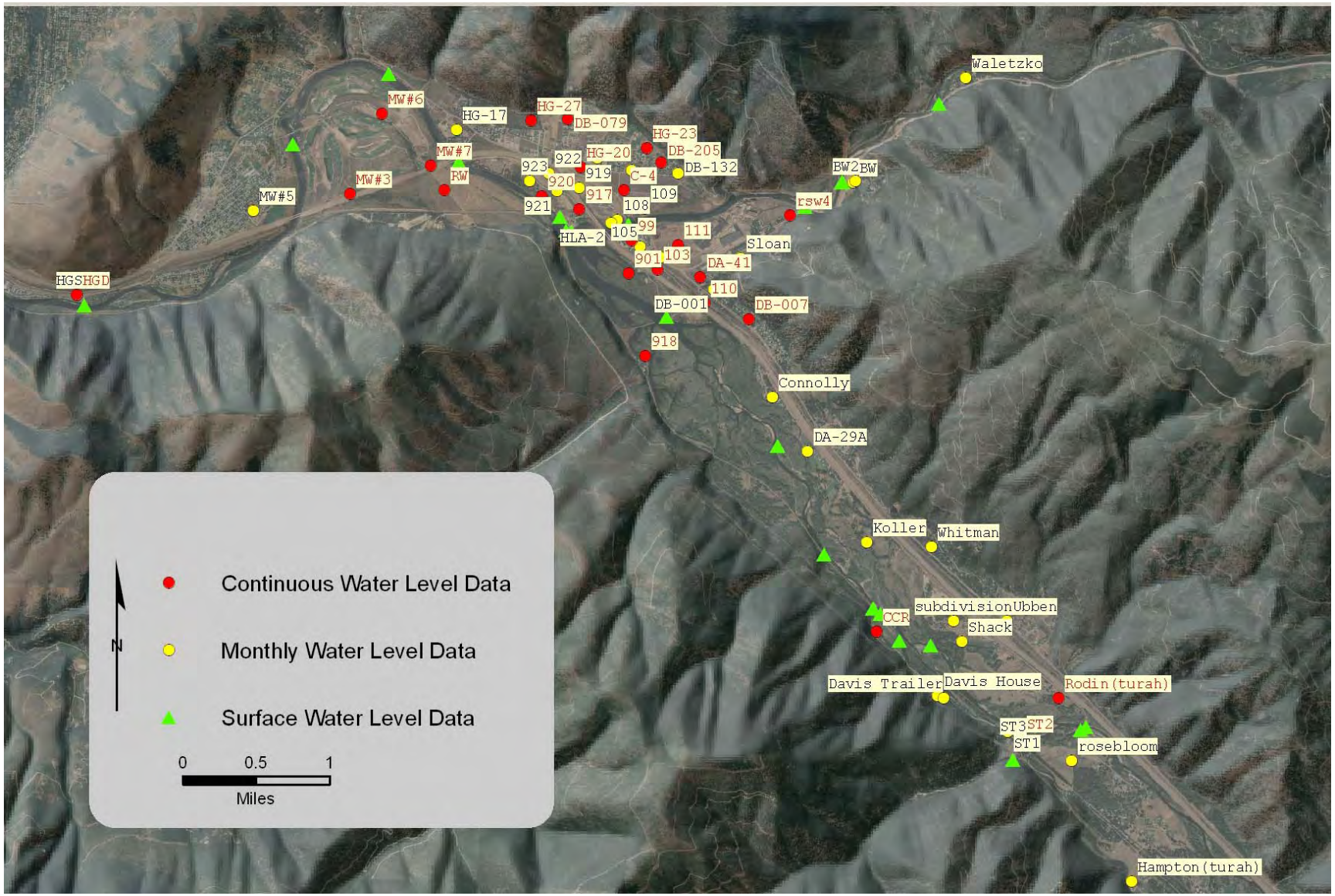

Figure 4ES Location map of the current monitoring network

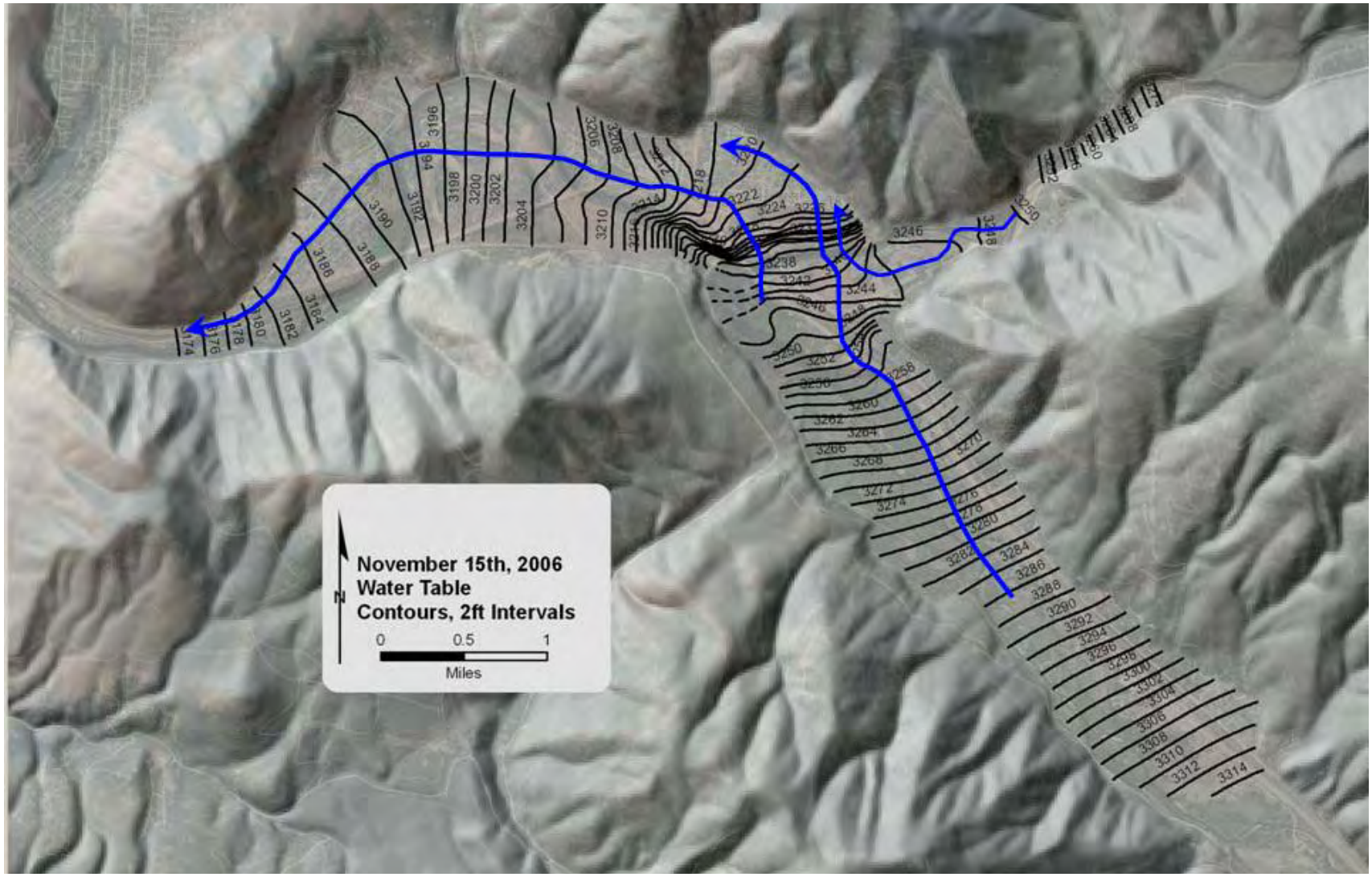

Figure 5ES Water table map for November 15, 2006. Flow is generally down valley from the east to the west and from the Blackfoot River canyon to the west.

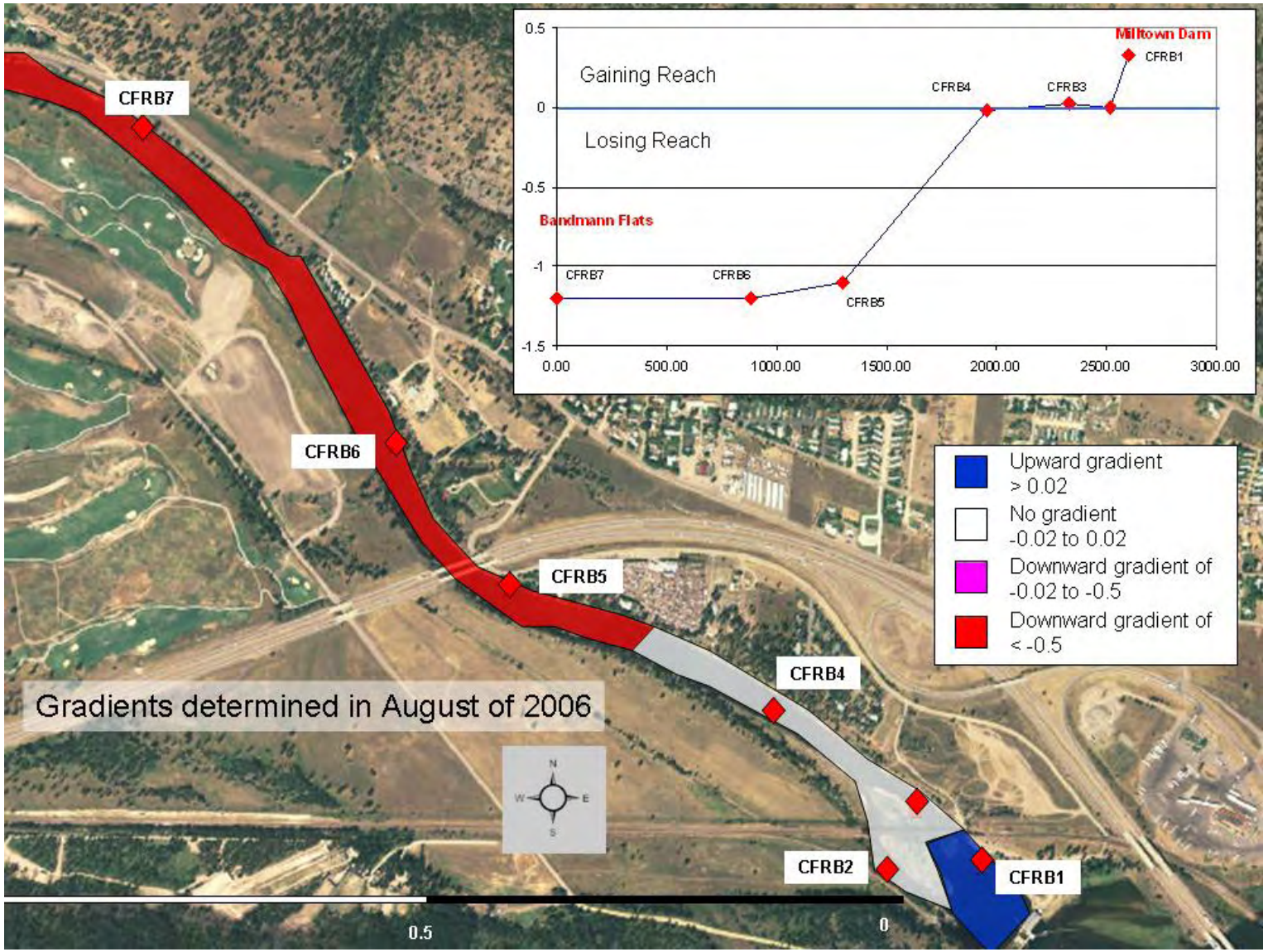

Figure 6ES Conceptual distribution of vertical hydraulic gradients collected from instruments installed in the river bed between Milltown Dam and Bandmann Flats. Negative gradients indicate zones of river water seepage to the underlying groundwater system (losing stream section).

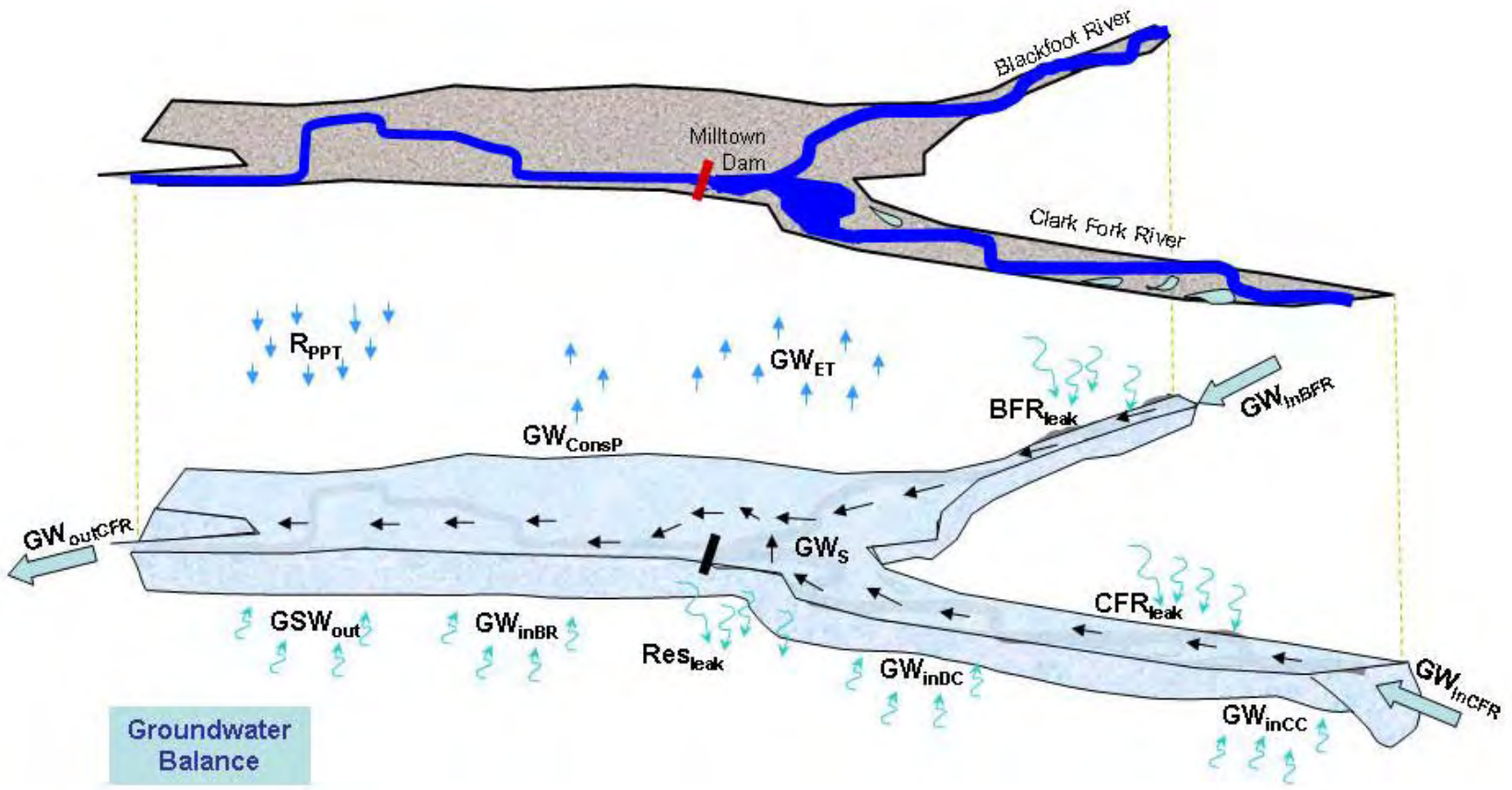

Figure 7ES Generalized illustration of the conceptual model.

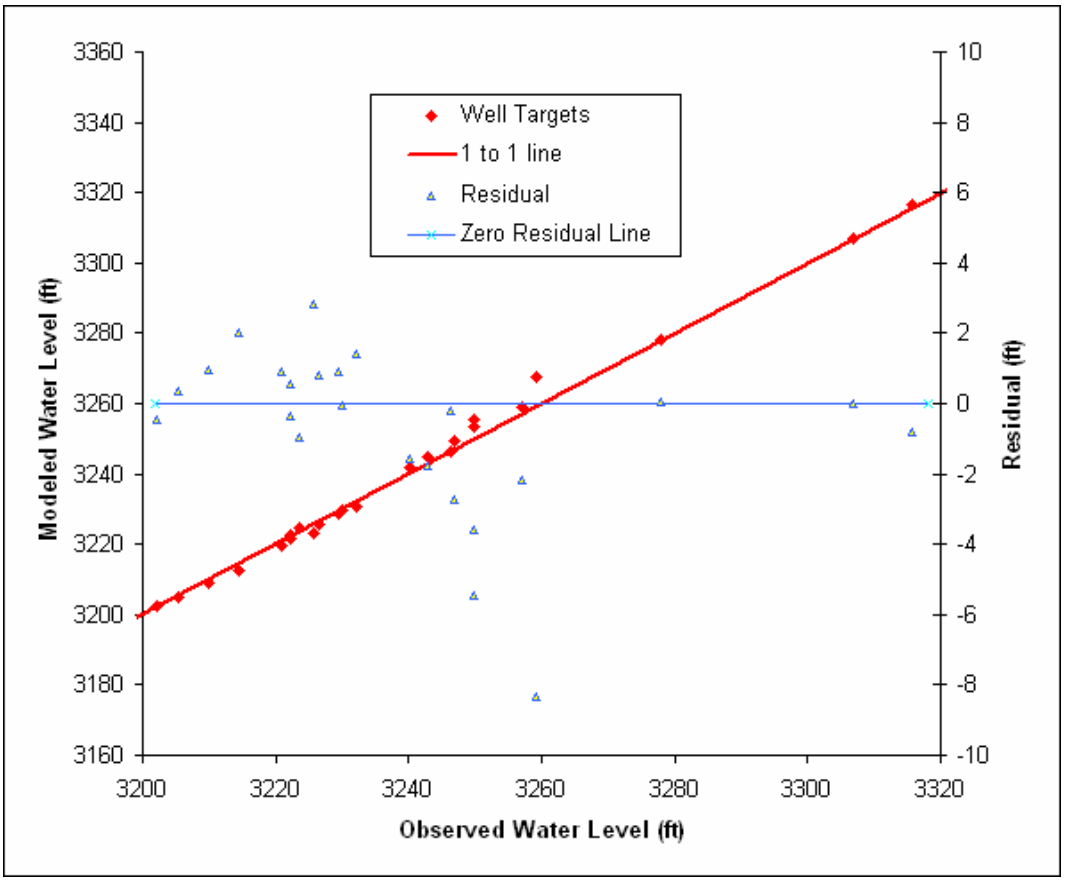

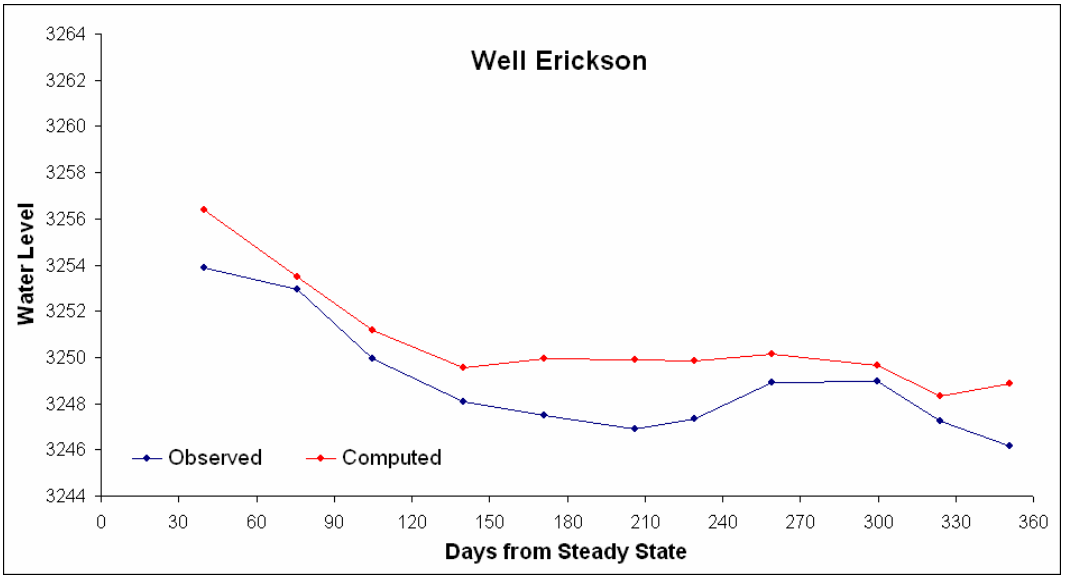

Figure 8ES Example of Head calibration steady state and a transient hydrograph match.

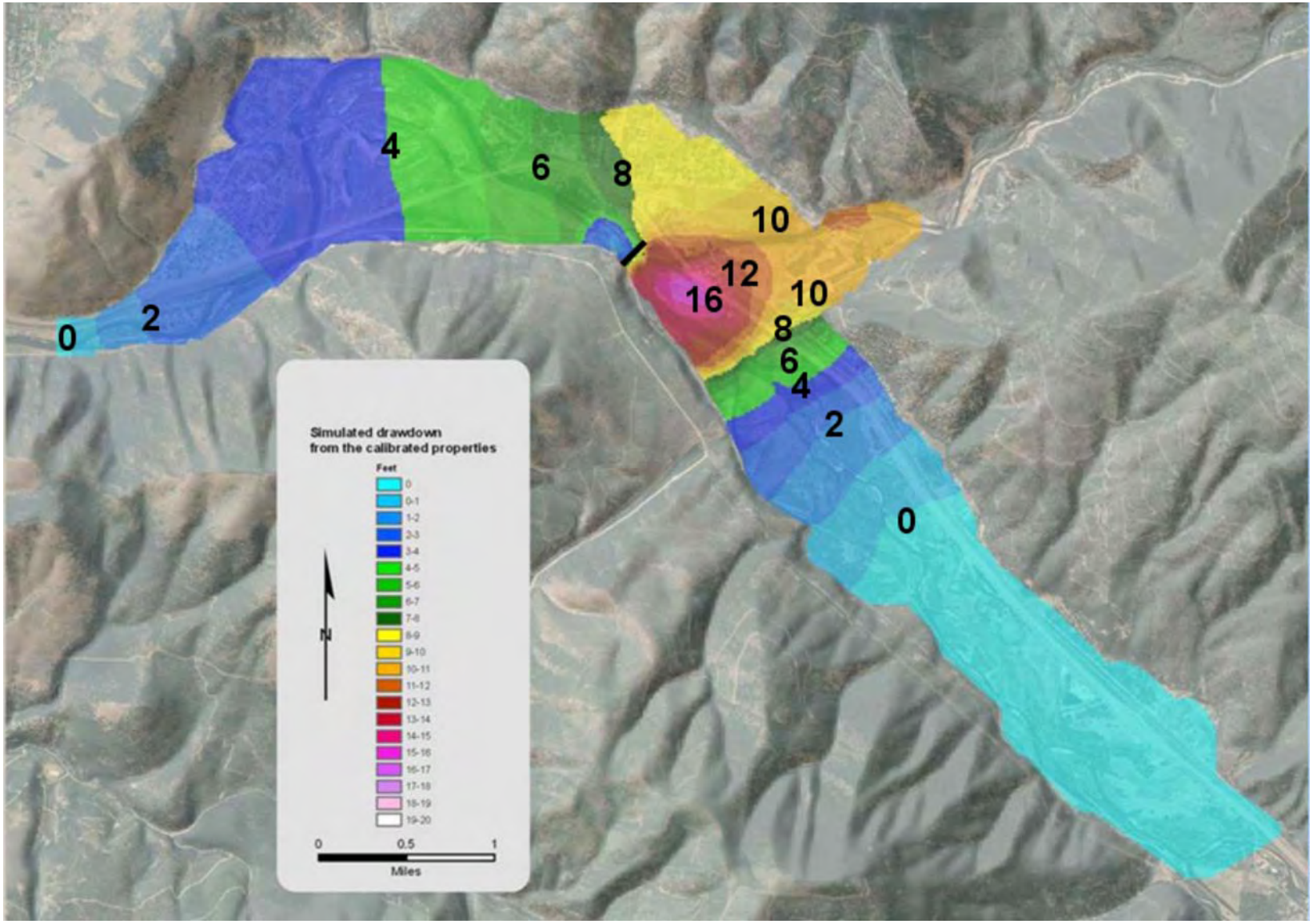

Figure 9ES Simulated drawdown (predicted reduction) of the water table position. The map was created by differencing the calibrated pre-remediation steady state water table from the predicted post Stage 2 reservoir water table. Numbers represent midpoint groundwater levels reductions in feet.

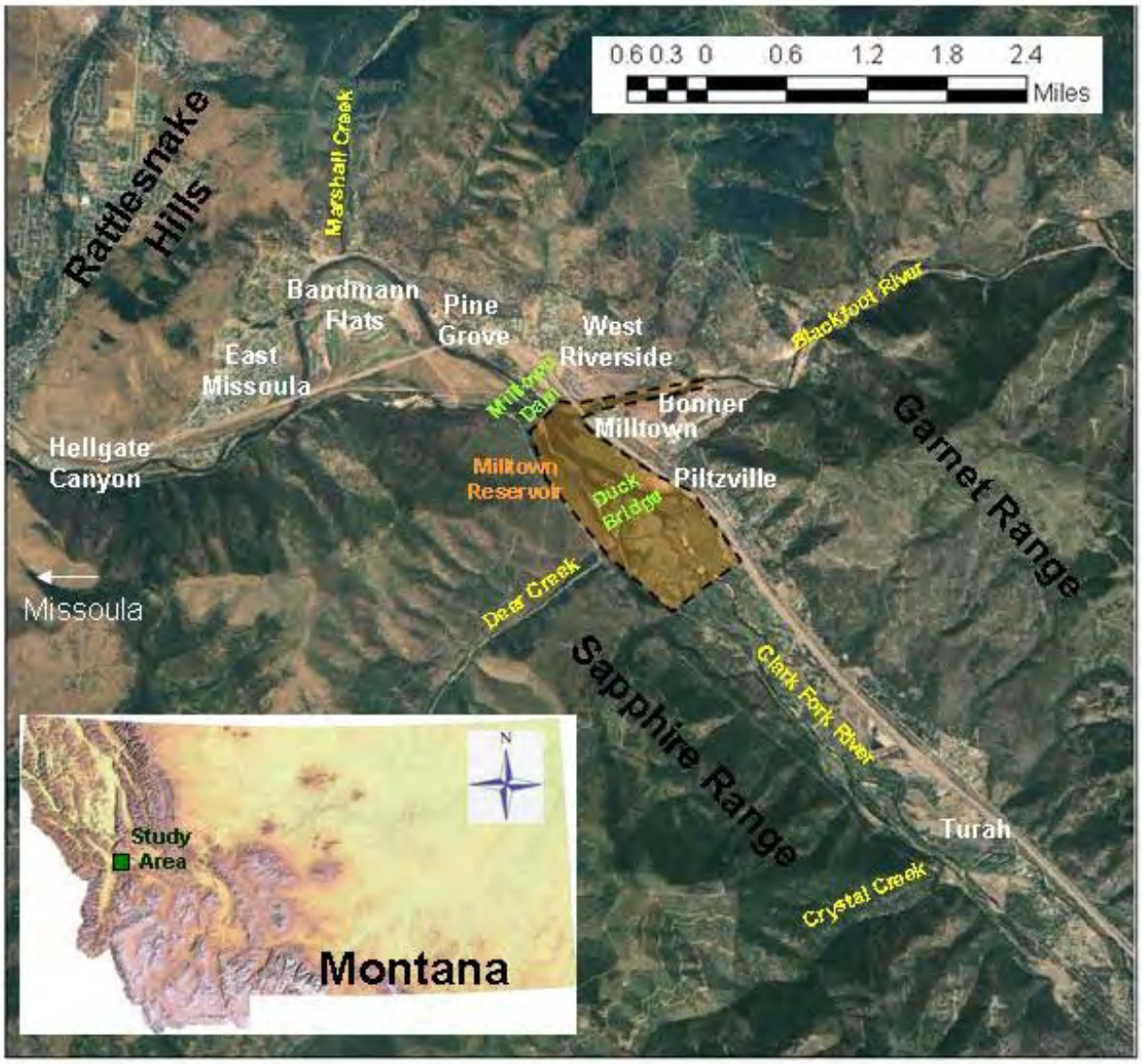

Figure 1 Study area location map. The study area is located in Northwestern Montana east of Missoula and west of Turah. North is at the top of the map.

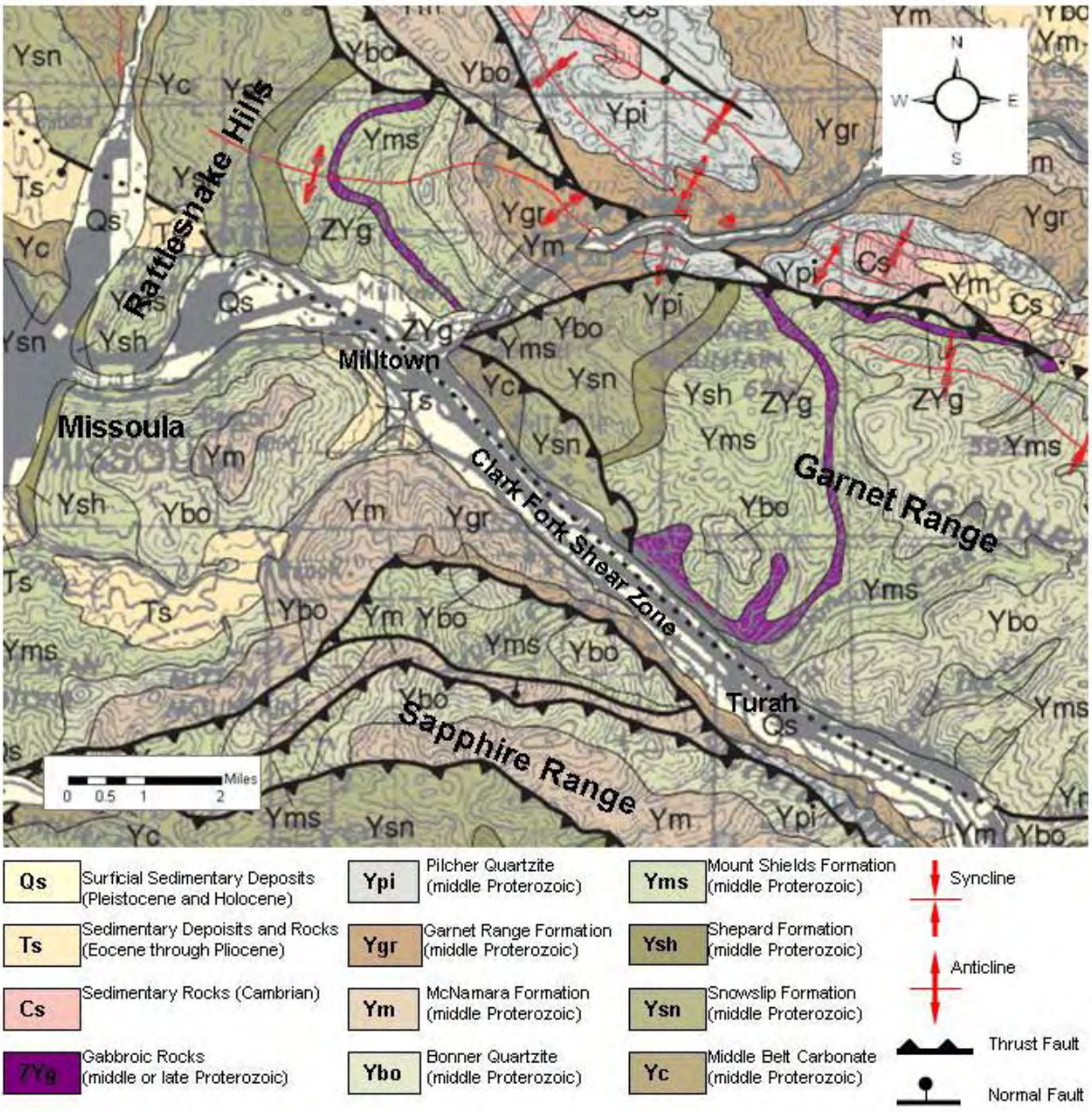

Figure 2 Geologic map of the study area after (Lewis R.S., 1998). This map shows the geologic complexity of the area.

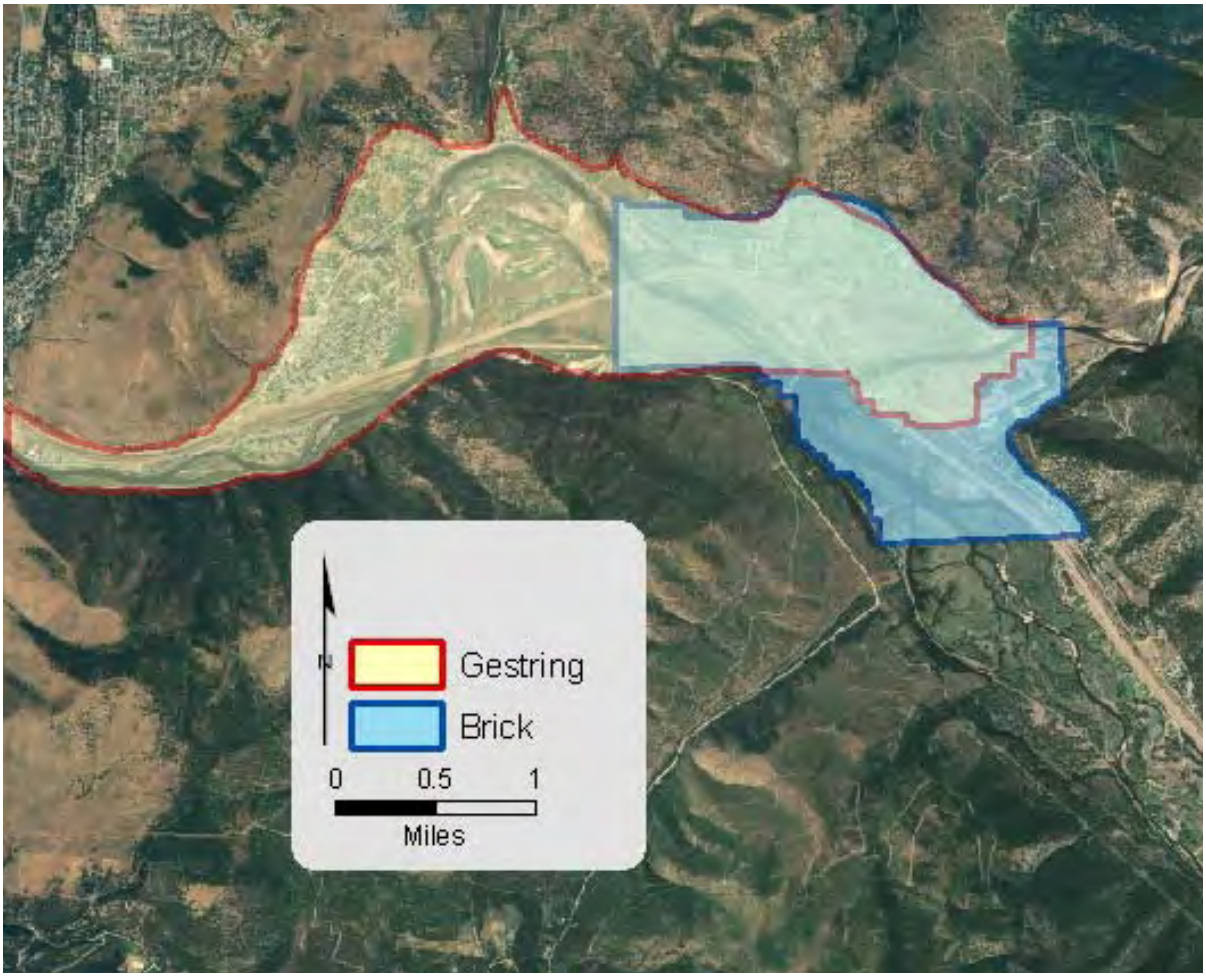

Figure 3 Representation of the areas previously modeled. The yellow region was previously modeled by (Gestring, 1994) and the blue region was previously modeled by (Brick, 2003) , with the green area being overlap from both models.

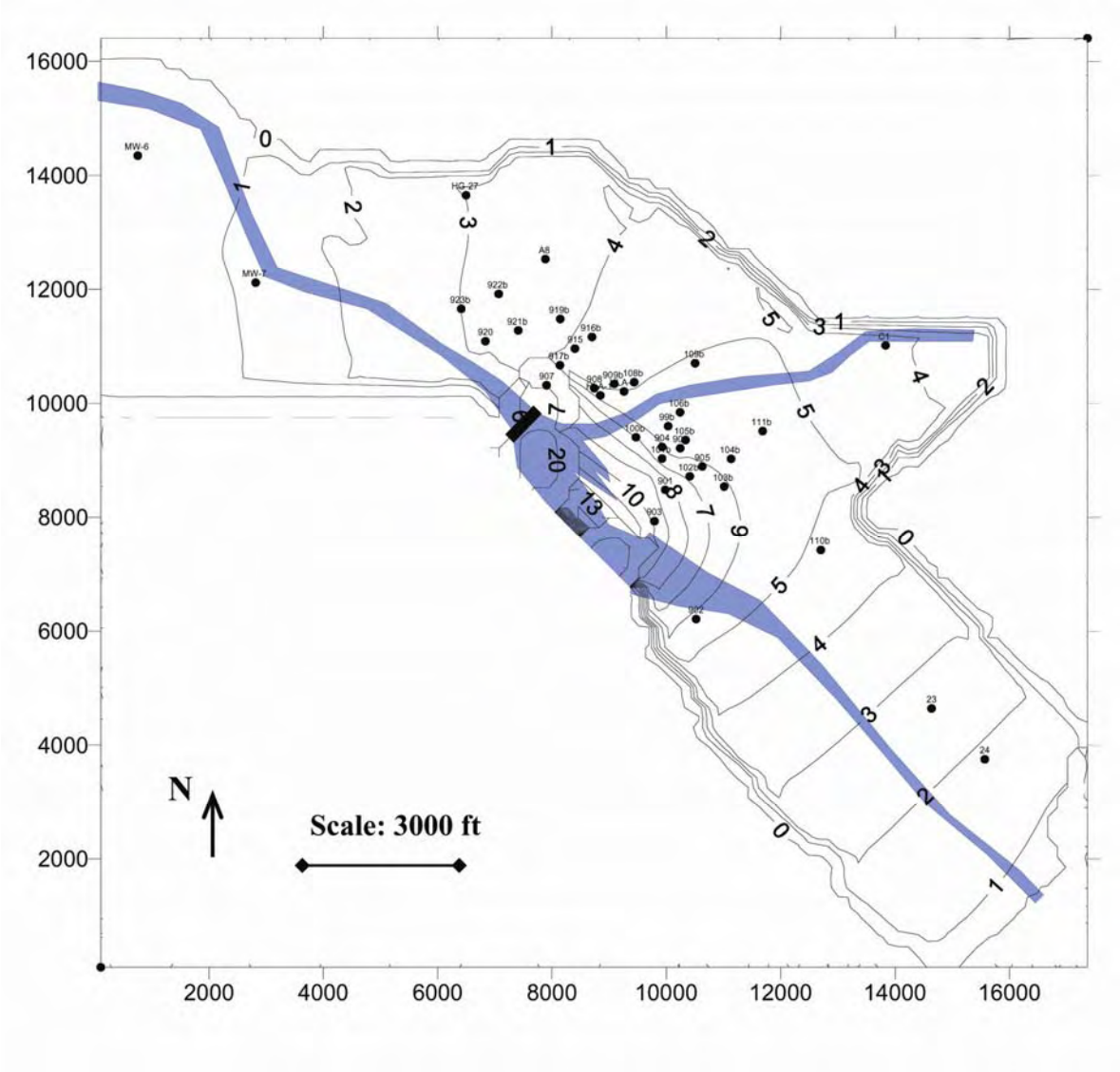

Figure 4 Contour map of predicted water table decline after dam and sediment removal as planned in 2002 (Brick, 2003).

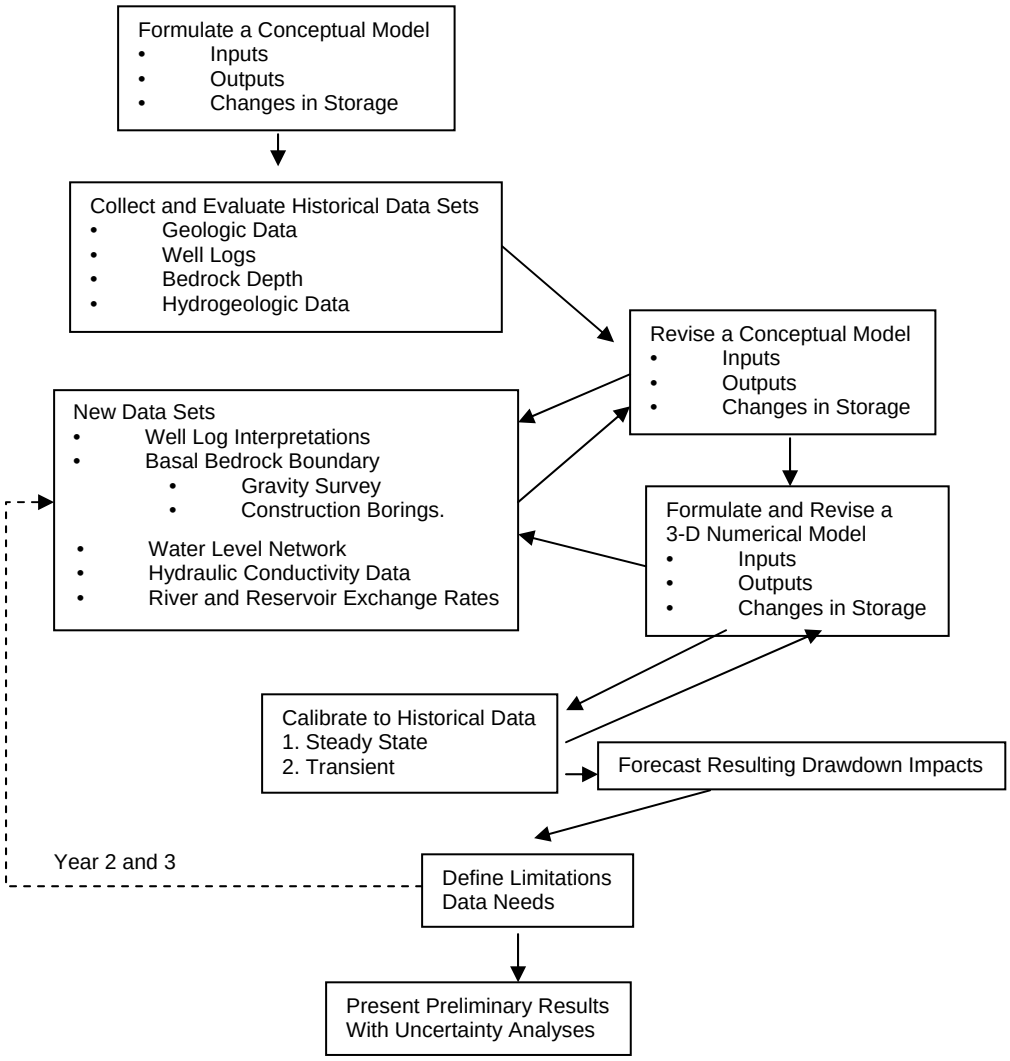

.

Figure 5 Flow chart illustrating the iterative process used to complete the groundwater modeling effort.

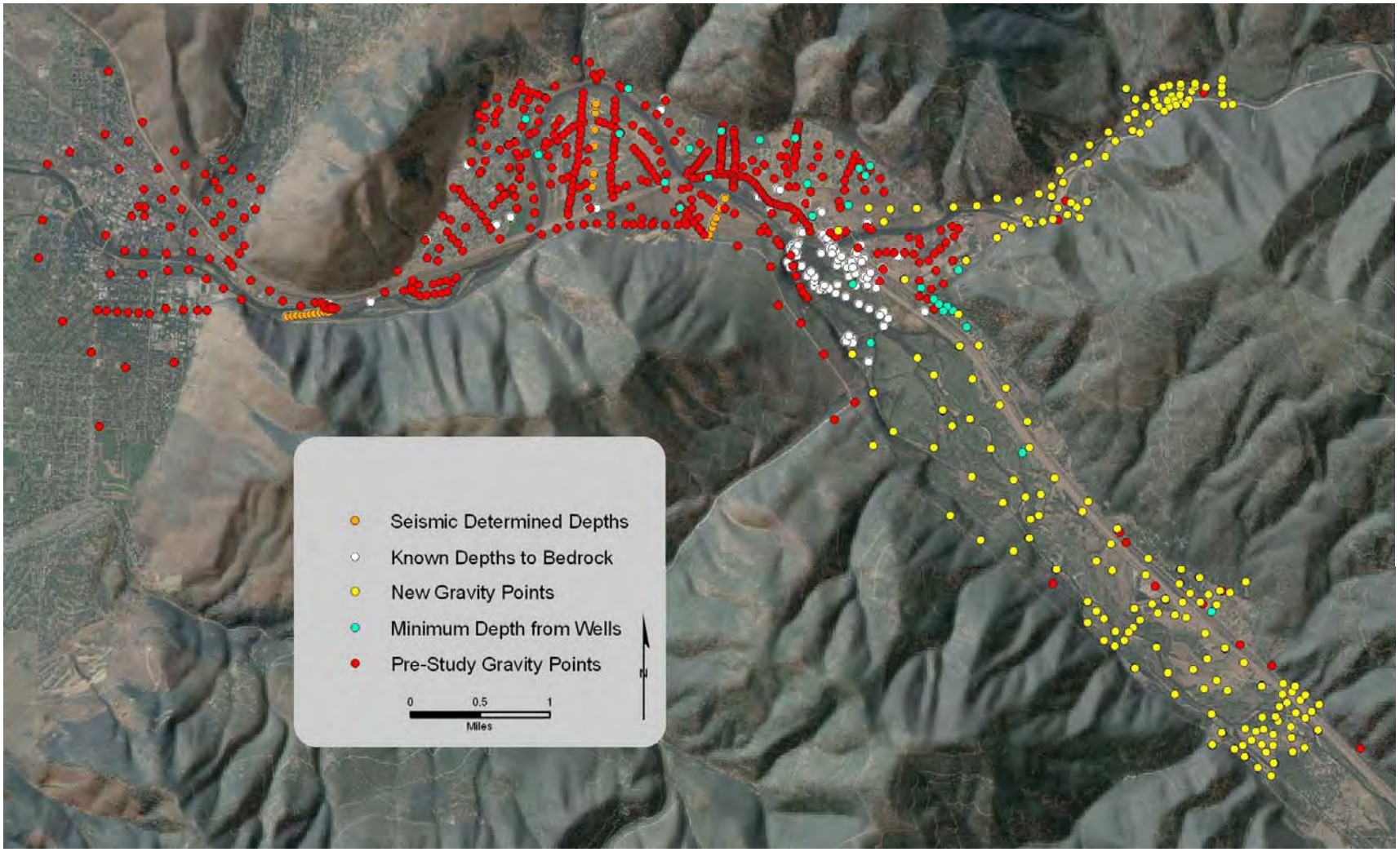

Figure 6 Geophysical data and known bedrock depth from borings and wells logs used to estimate bedrock depths.

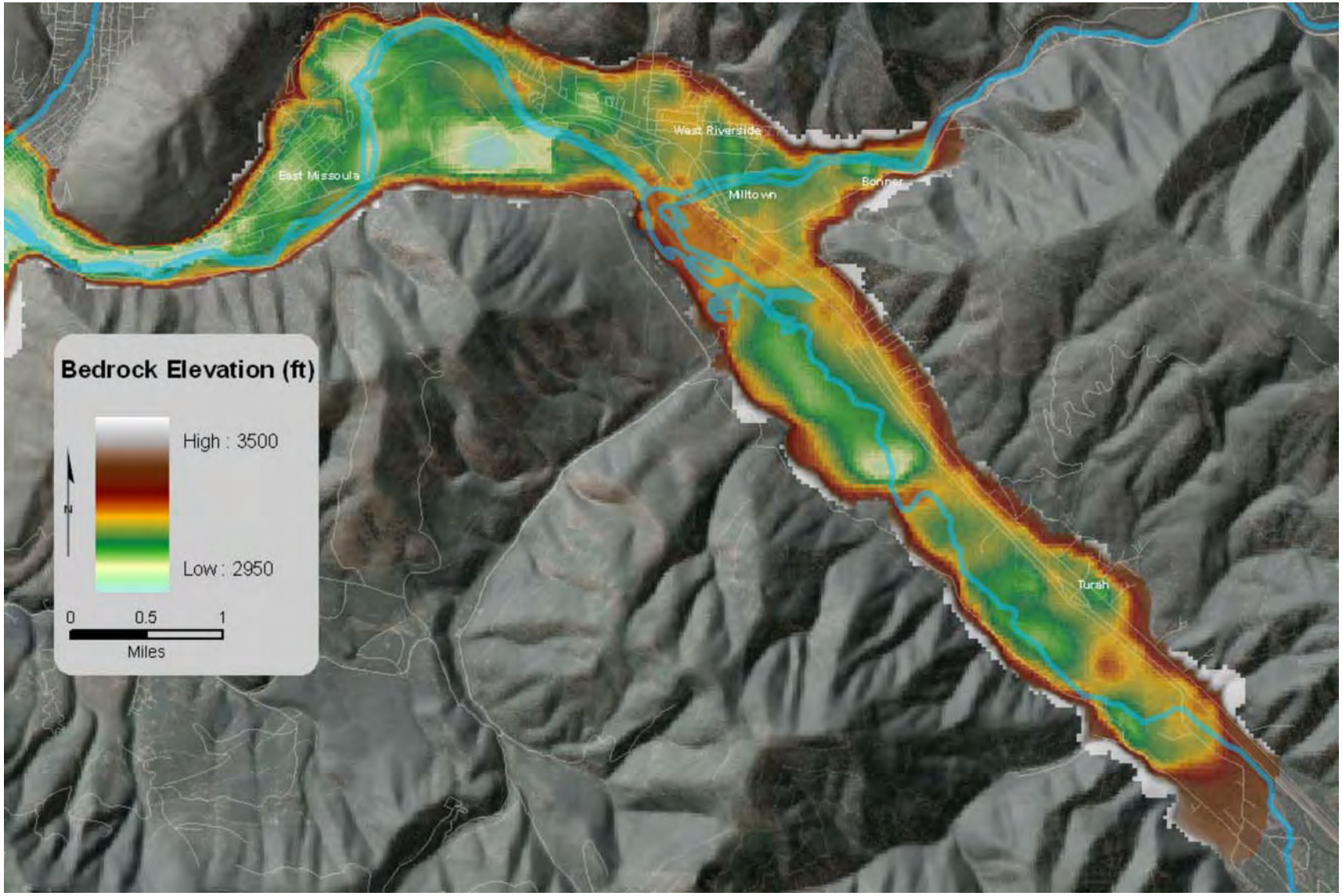

Figure 7a Bedrock elevations derived from a compilation of gravity data, four seismic lines processed by Gradient Geophysics, historical borehole data, well logs, and topographic projections into the subsurface. Known depth to bedrock was used to condition the data. However, bedrock depth may actually vary up to + or – 30 feet in areas outside of the area immediately adjacent to the reservoir area. Rivers are shown in light blue.

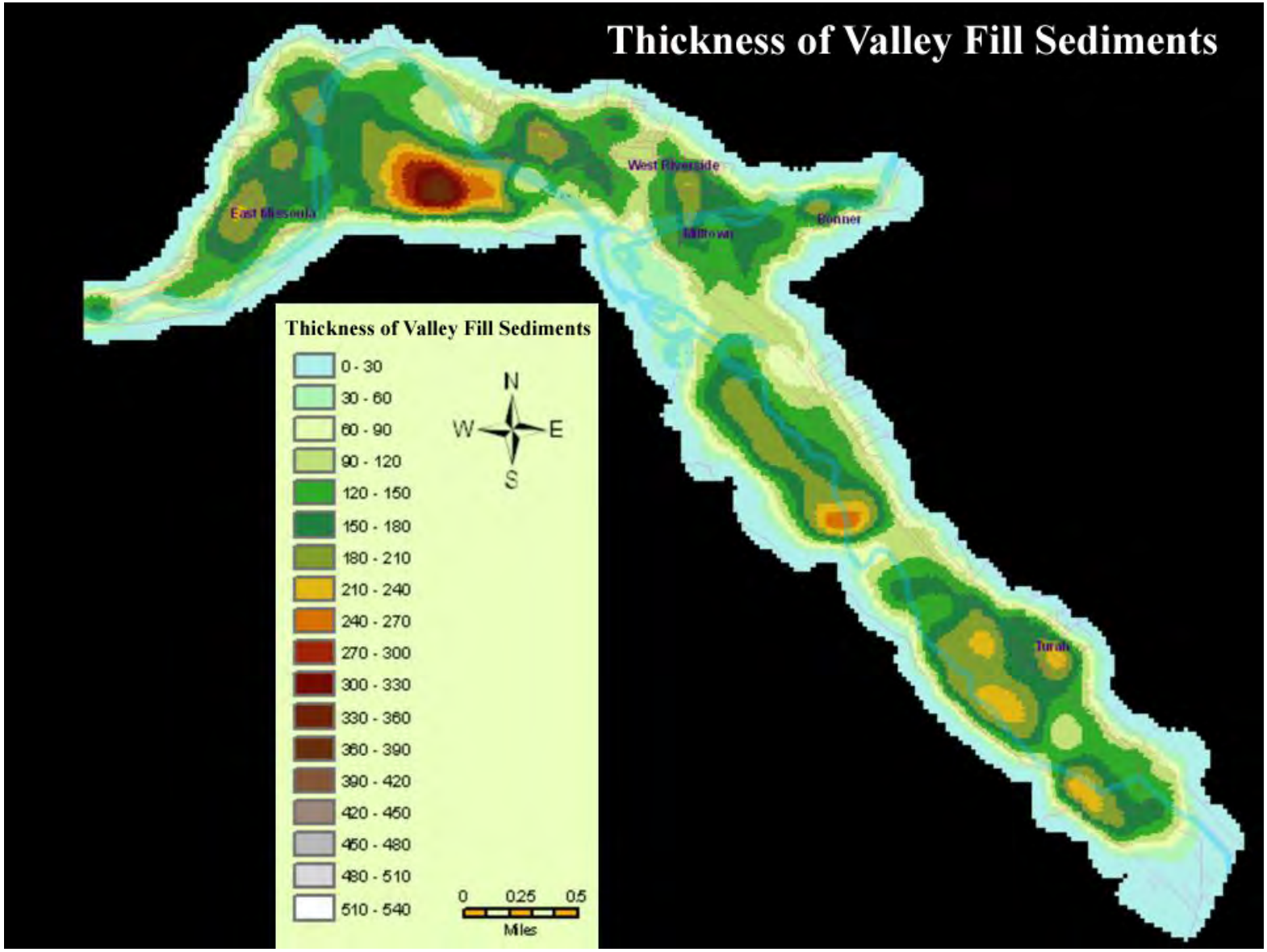

Figure 7b Thickness of unconsolidated valley fill material derived by subtracting land surface elevations from the modeled bedrock surface (Figure 7a). Uncertainty in modeled bedrock elevations and surface topography introduce errors in mapped thickness of +/- 30 to 35 ft.

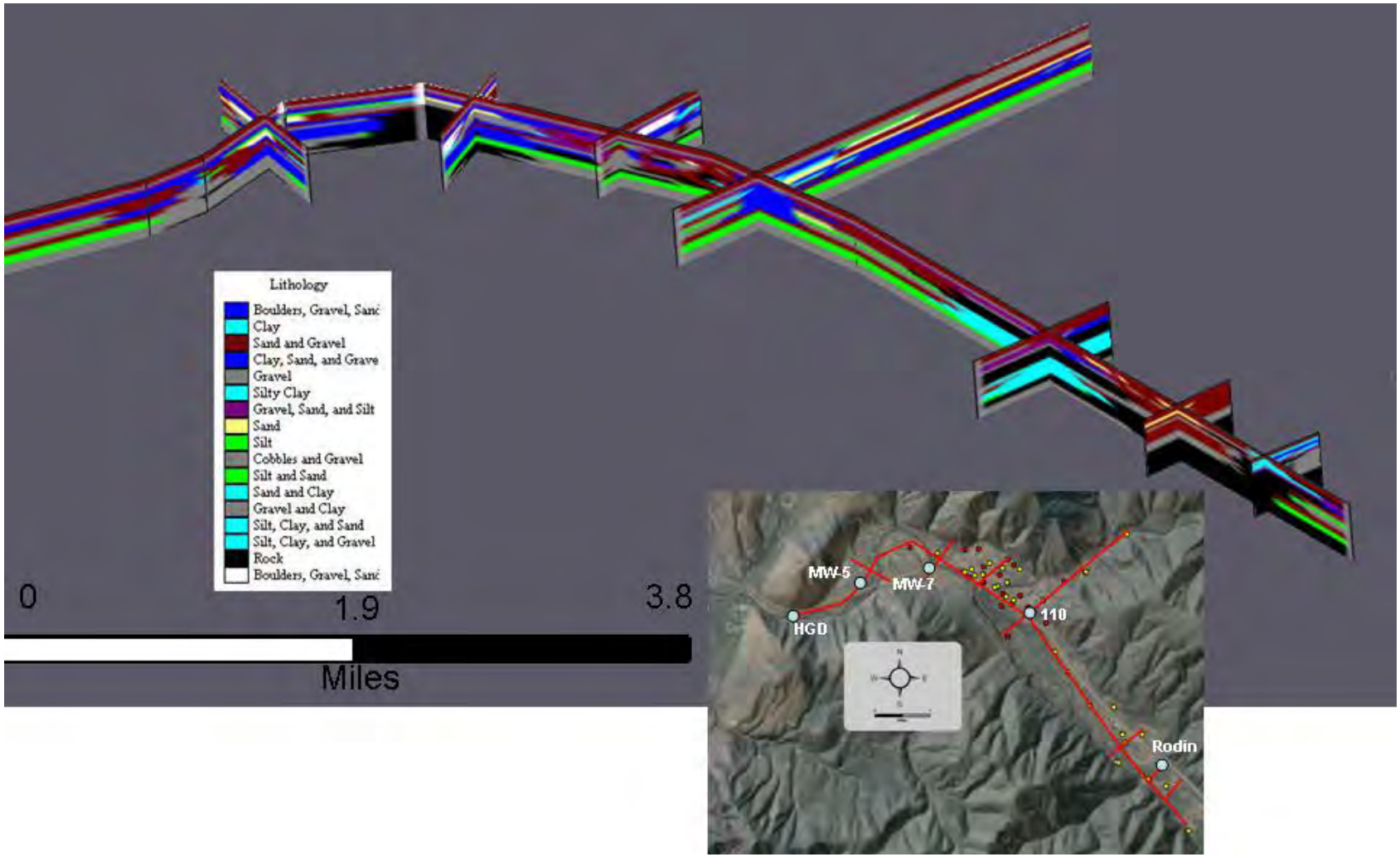

Figure 8 Fence diagram model generated by RockWorks® Borehole Software. The cross section has a 485 ft vertical scale with a base elevation of 3000 ft and an exaggeration factor of 5. Vertical scale is plotted on the reference map. Though well logs often generally describe geologic properties the interpreted lithology can be represented as bedrock in black, aqua blue suggests silt is present, green is silty sand, yellow sand, and grays and browns denote gravel or sand and gravel.

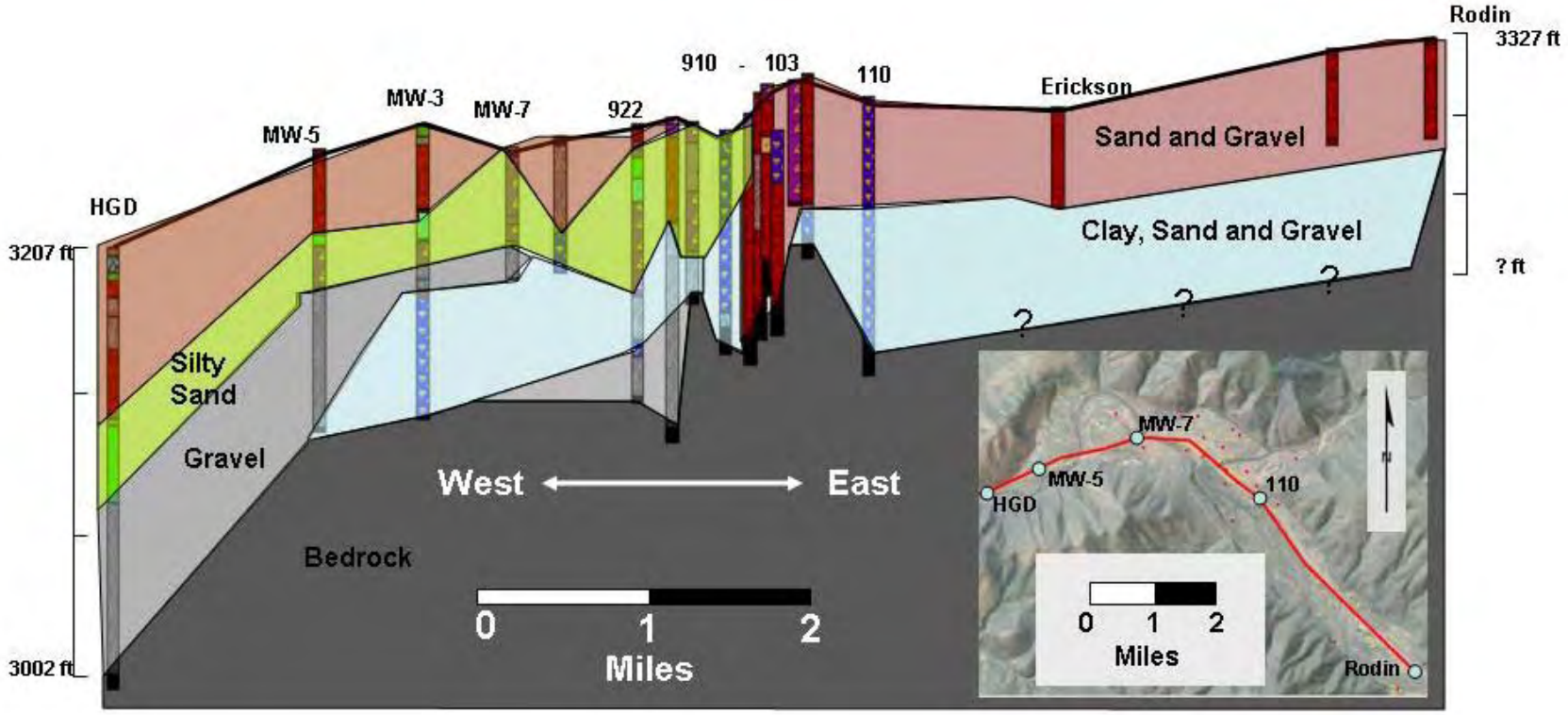

Figure 9 Hydrostratigraphic cross section interpreted from well logs from the Turah Bridge are to Hellgate Canyon.

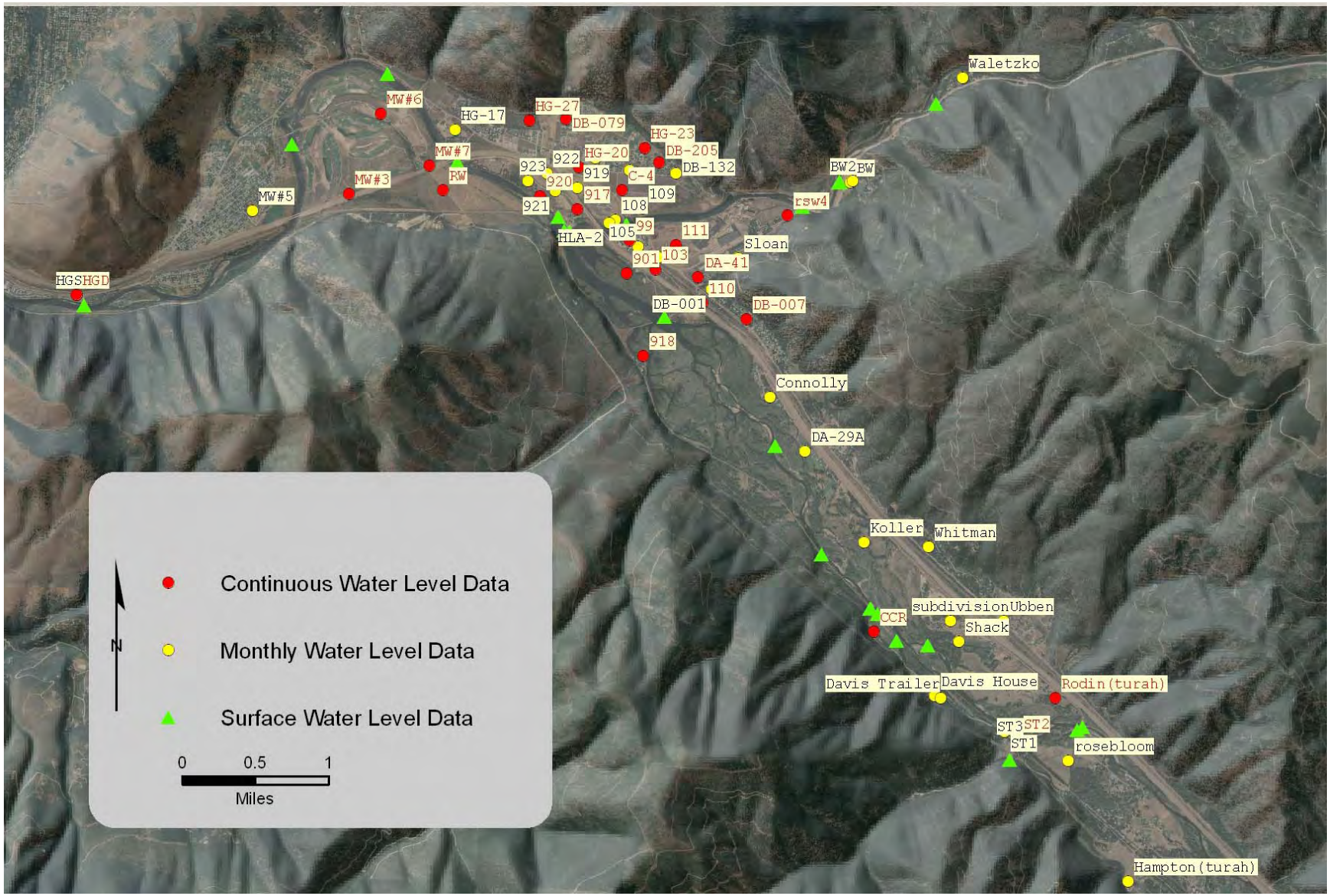

Figure 10 Location map of the current monitoring network

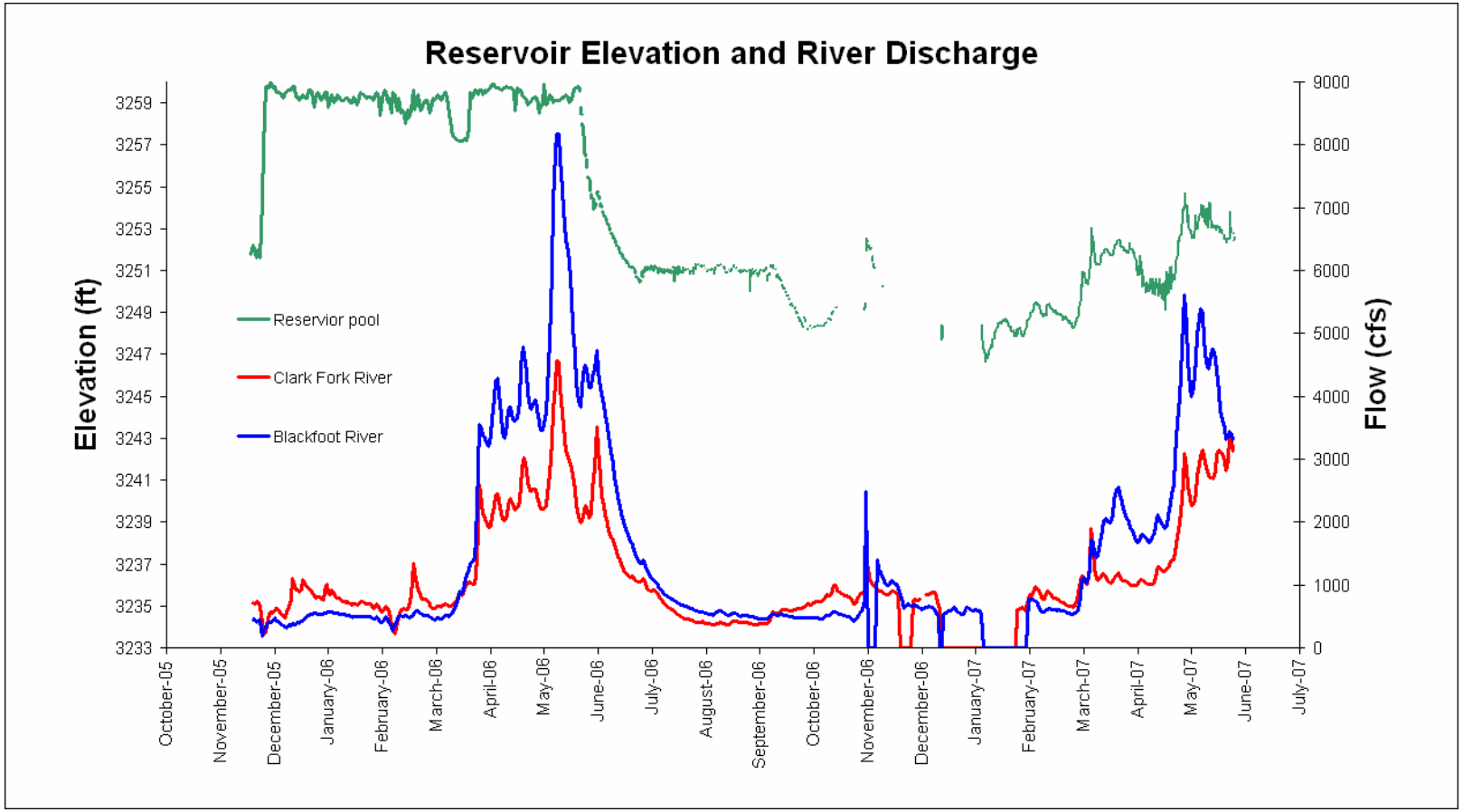

Figure 11 A hydrograph illustrating the stage of the Clark Fork River and Blackfoot River, river discharges, and the elevation of the Milltown Reservoir pool prior to, during, and after Stage 1 drawdown (initiated June 2006).

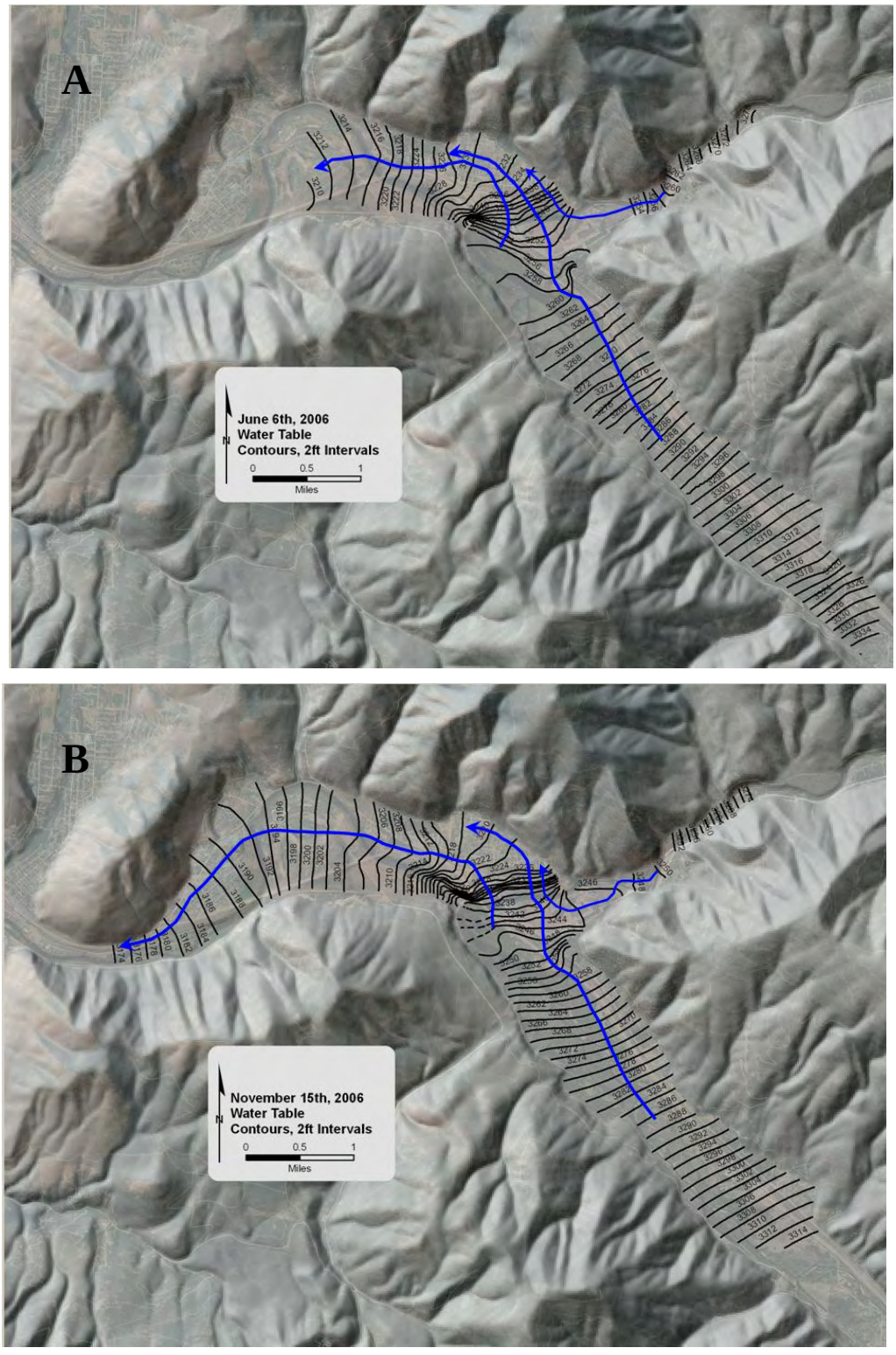

Figure 12 Water table maps A) June 6, 2006 and B) November 15, 2006. The well network data used to develop the June map included fewer data points than the November plot as the monitoring network was not fully developed in June. Groundwater flow is indicated by the blue arrows, and is generally down valley.

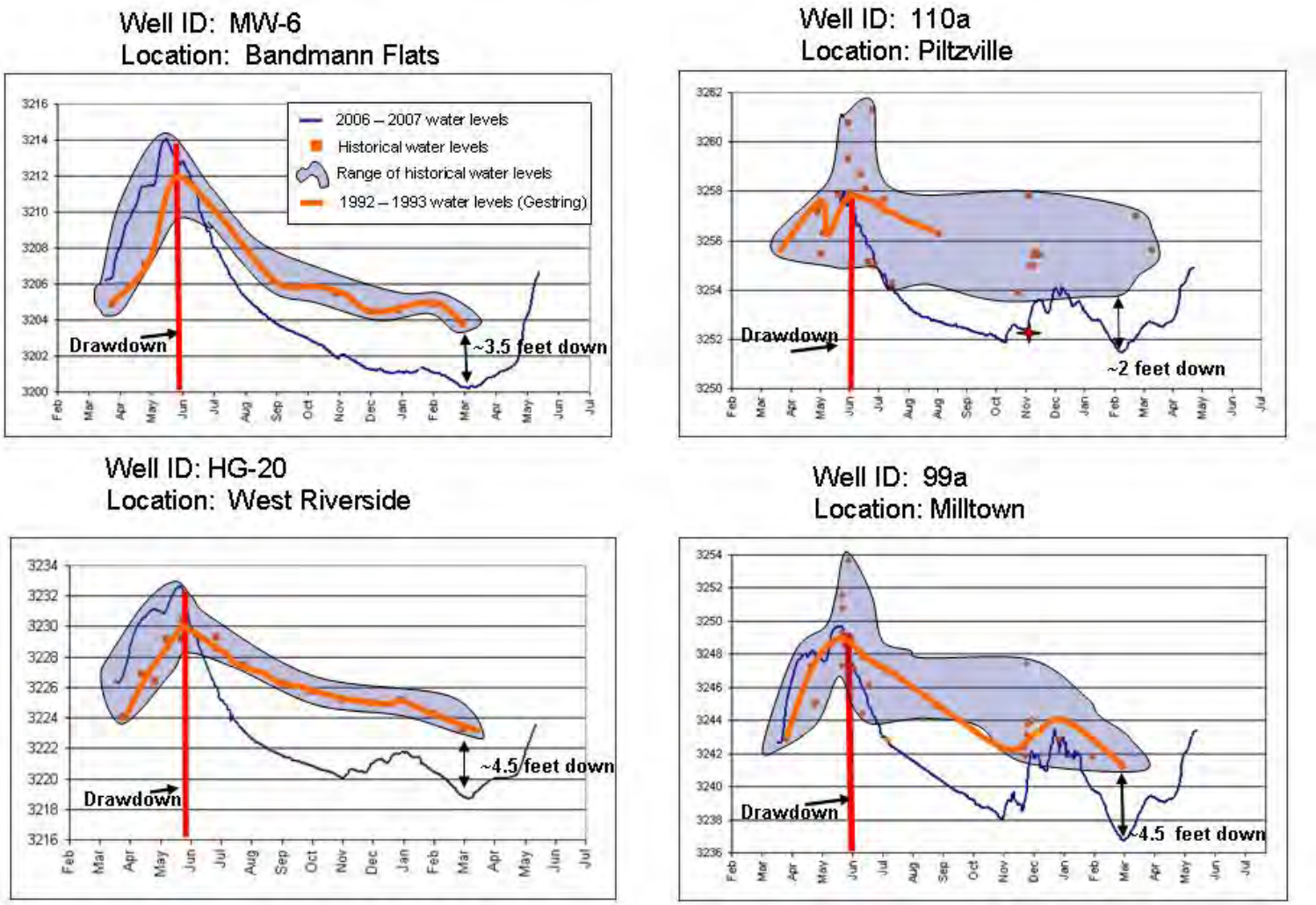

Figure 13 Hydrographs of selected wells showing measured water table response during this effort (2006-2007), the timing of the start of the2006 reservoir and river Stage 1 drawdown (red line), the observed historical pre-drawdown water level behavior and value (Gestring, 1992, orange line), and the historical range of pre-drawdown water level fluctuations using data sets from 1982 to 2005 (see Appendix C to determine ranges represented for each well). The observed drawdown difference between historical (Gestring, 1994) and the observed 2006-2007 water levels at low water in March 2007 is indicated by the double arrow.

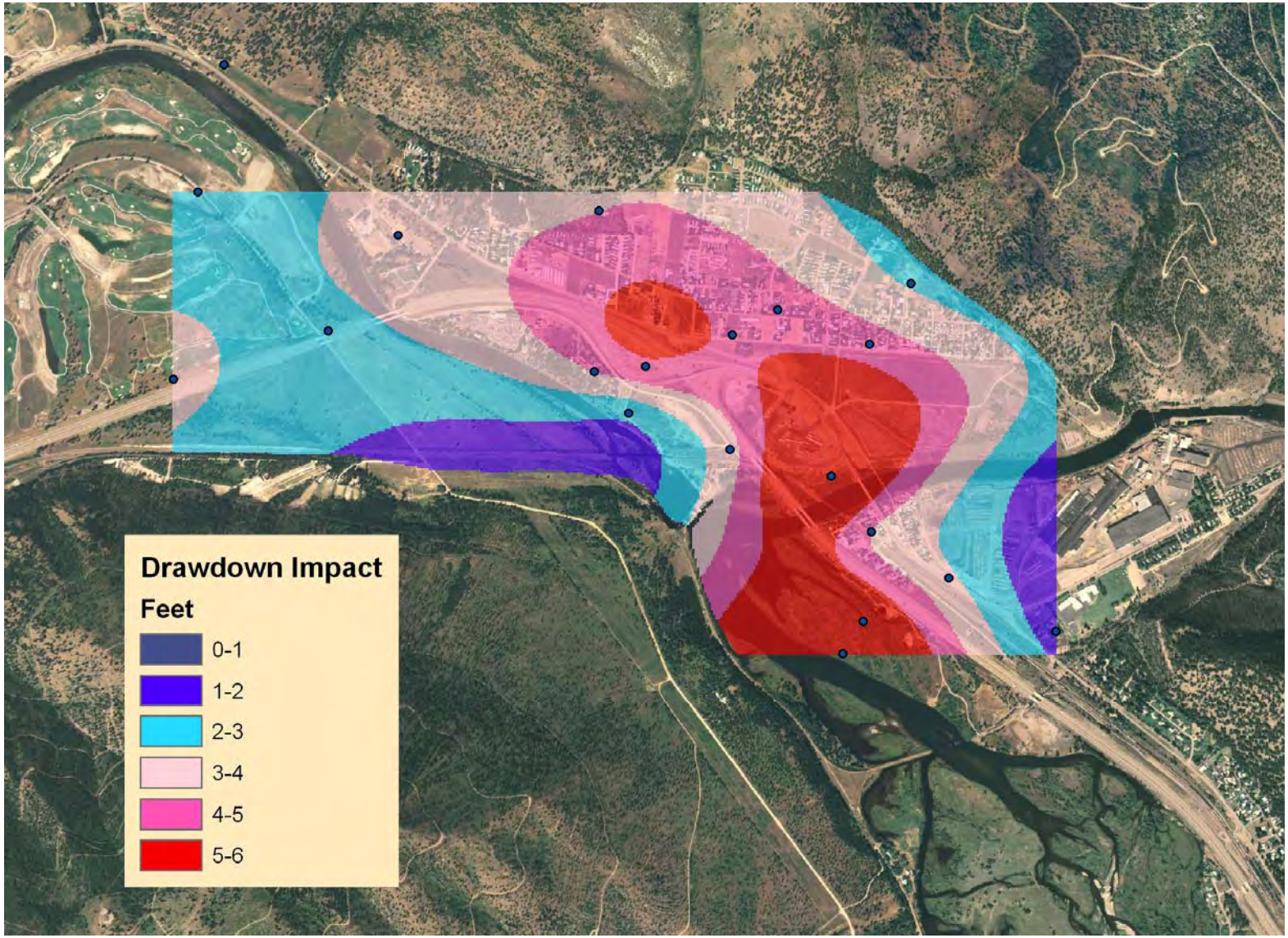

Figure 14 Observed impacts of lowering water levels below March historical levels as a result of Stage 1 remediation drawdowns. March 2007 data were compared with March 1993 data (Gestring, 1994). The plot covers Gestring's study area,

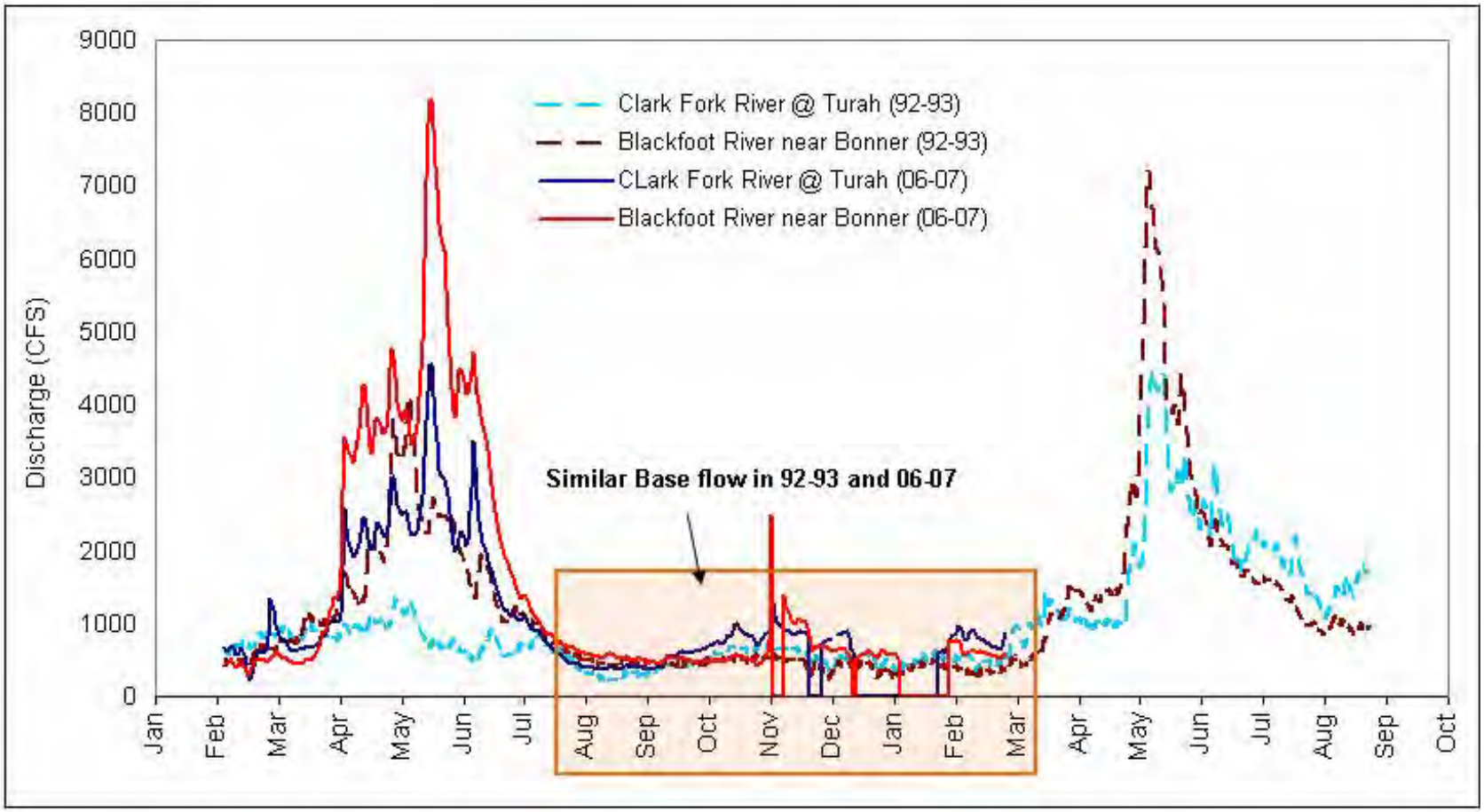

Figure 15 Stream hydrographs for the Clark Fork River and the Blackfoot River for 1992-1993 and 2006 to 2007. The shaded block indicates baseflow periods.

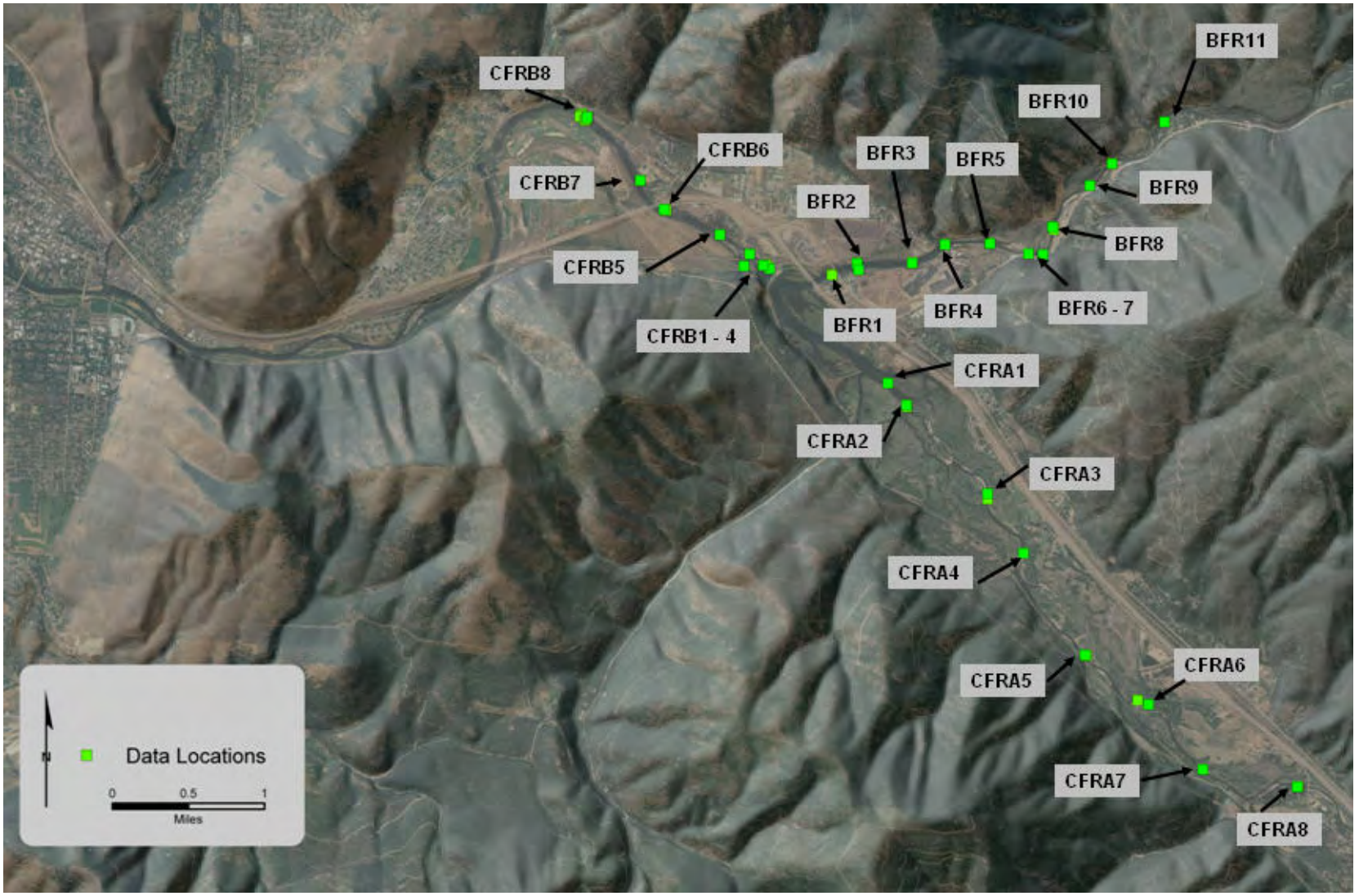

Figure 16 A map illustrating the locations where river VHG's and seepage rates were investigated.

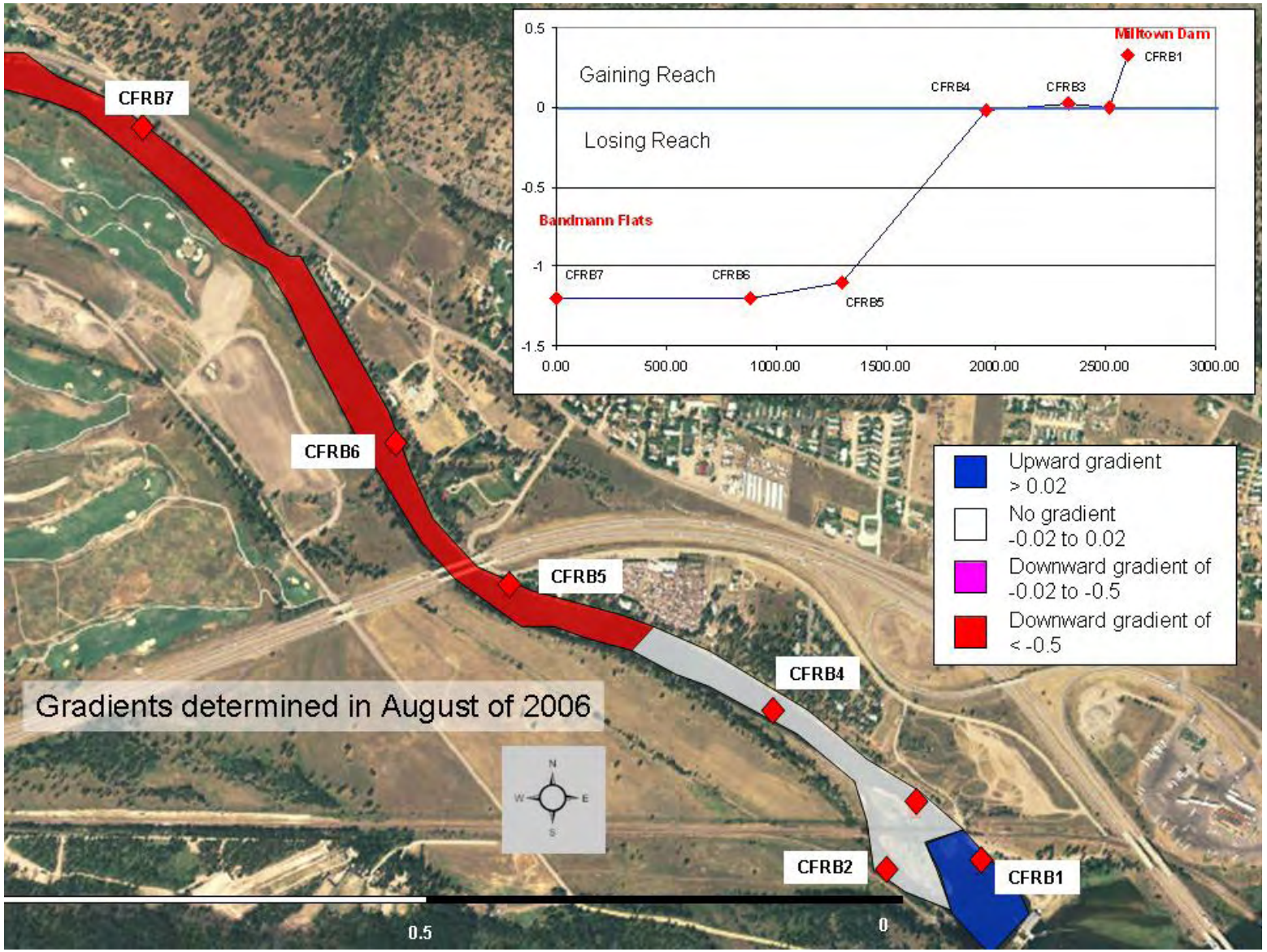

Figure 17 Conceptual distribution of vertical hydraulic gradients collected from instruments installed in the river bed between Milltown Dam and Bandmann Flats. Negative gradients indicate zones of river water seepage to the underlying groundwater system (losing stream section).

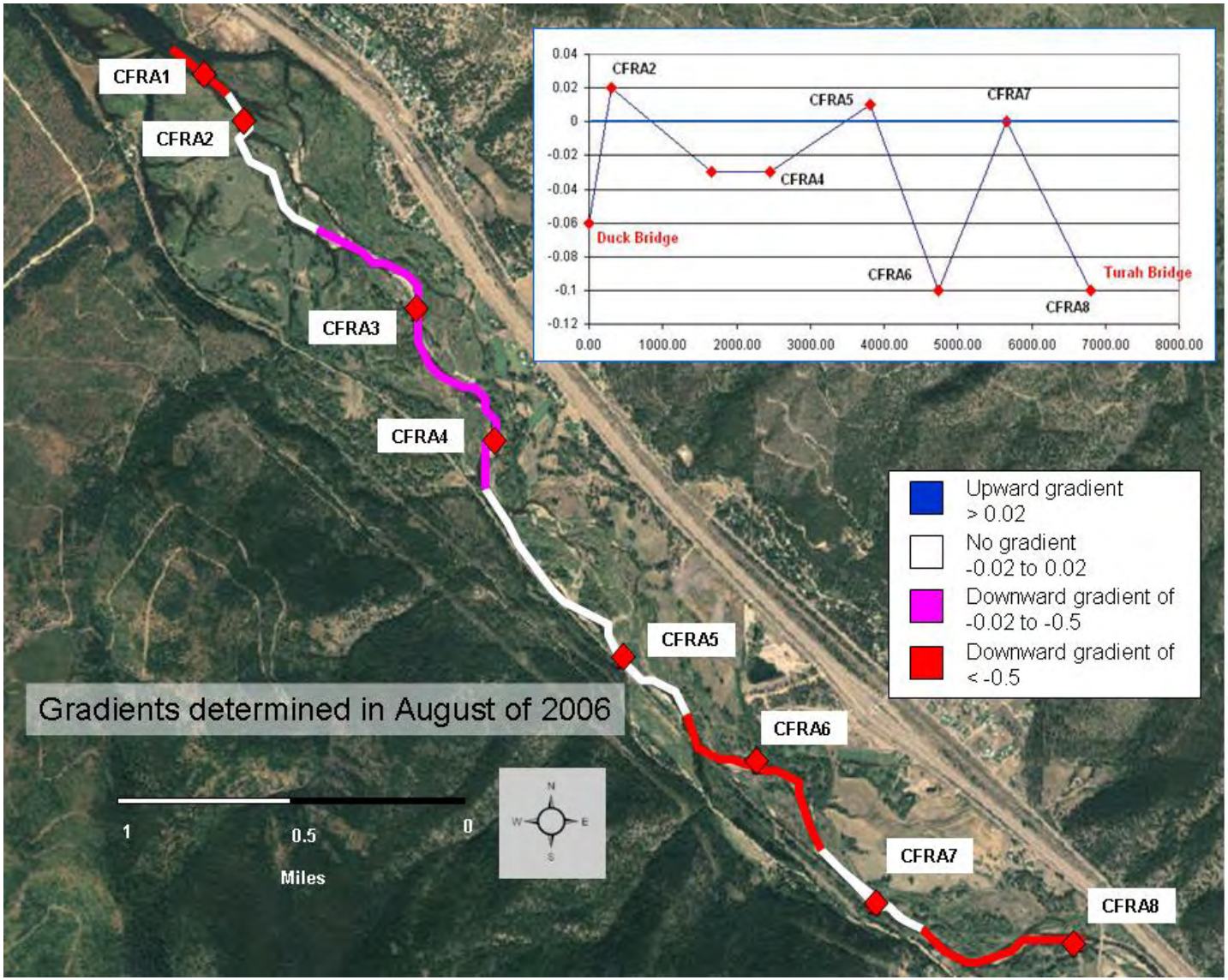

Figure 18 Conceptual distribution of vertical hydraulic gradients between Turah Bridge and Milltown Dam. Negative gradients indicate zones of river water seepage to the underlying groundwater systems (losing stream section).

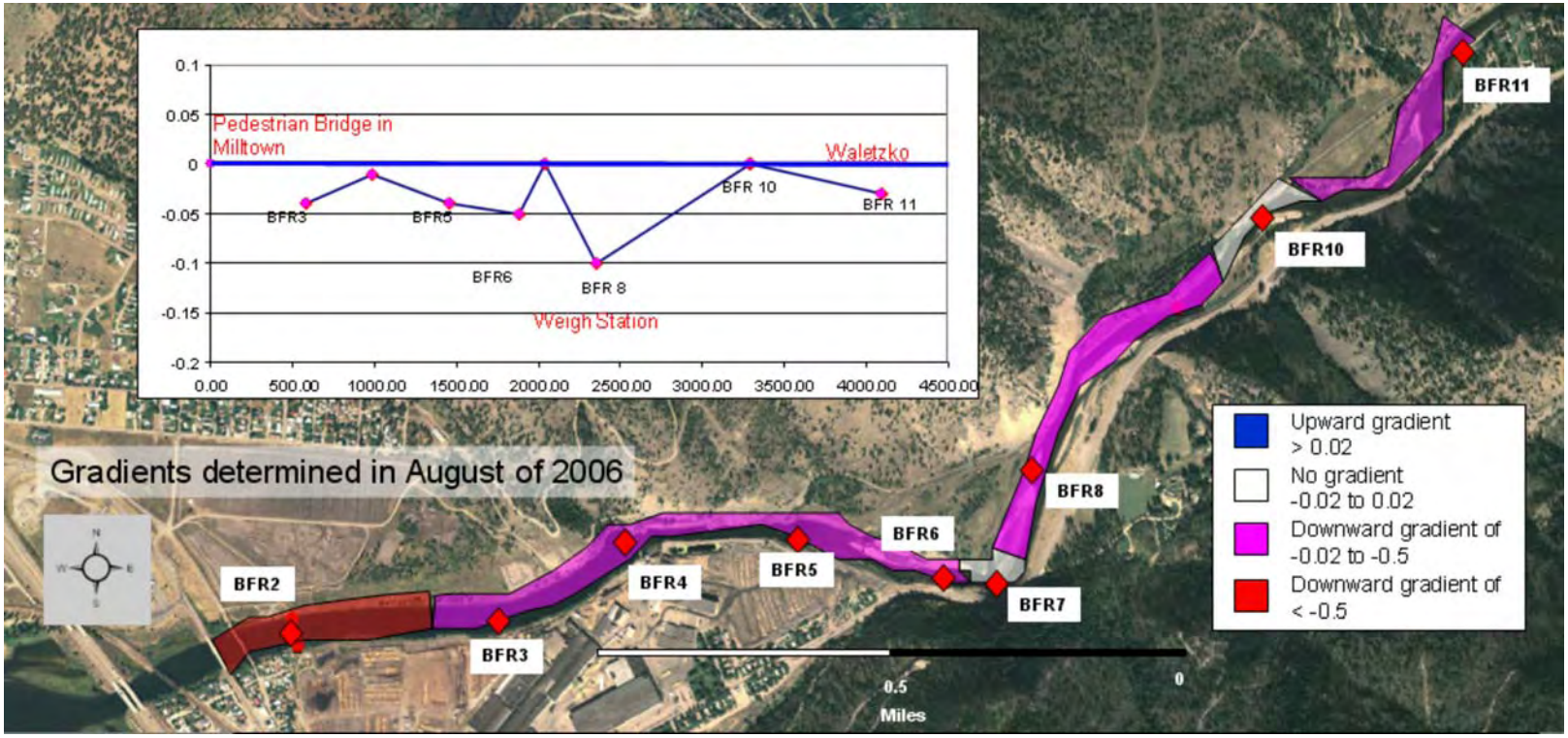

Figure 19 Conceptual distribution of vertical hydraulic gradients on the Blackfoot River above Milltown Dam. Negative gradients indicate zones of river water seepage to the underlying groundwater systems.

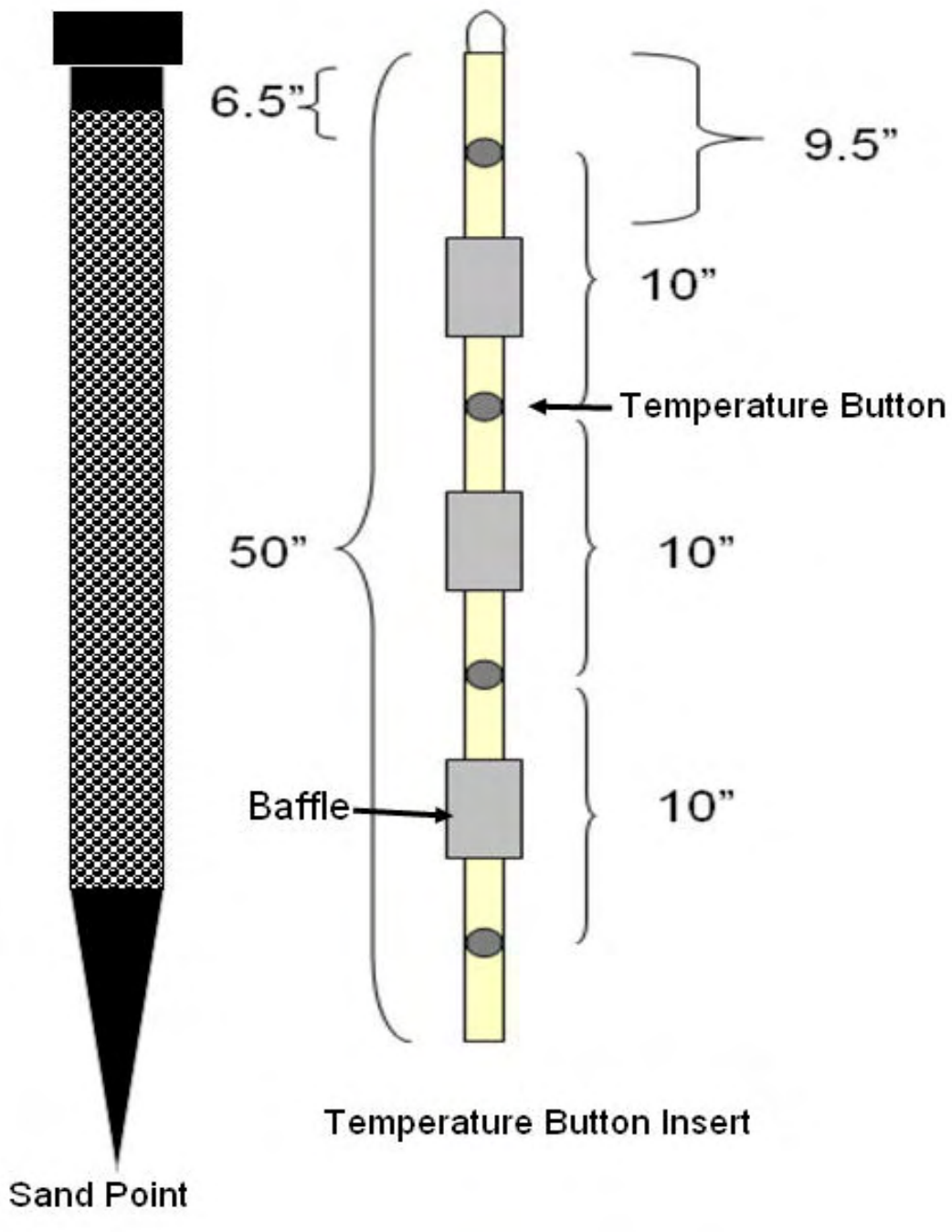

Figure20 Illustration of a sand point and PVC constructed insert (see Johnson et al., 2005 for details).

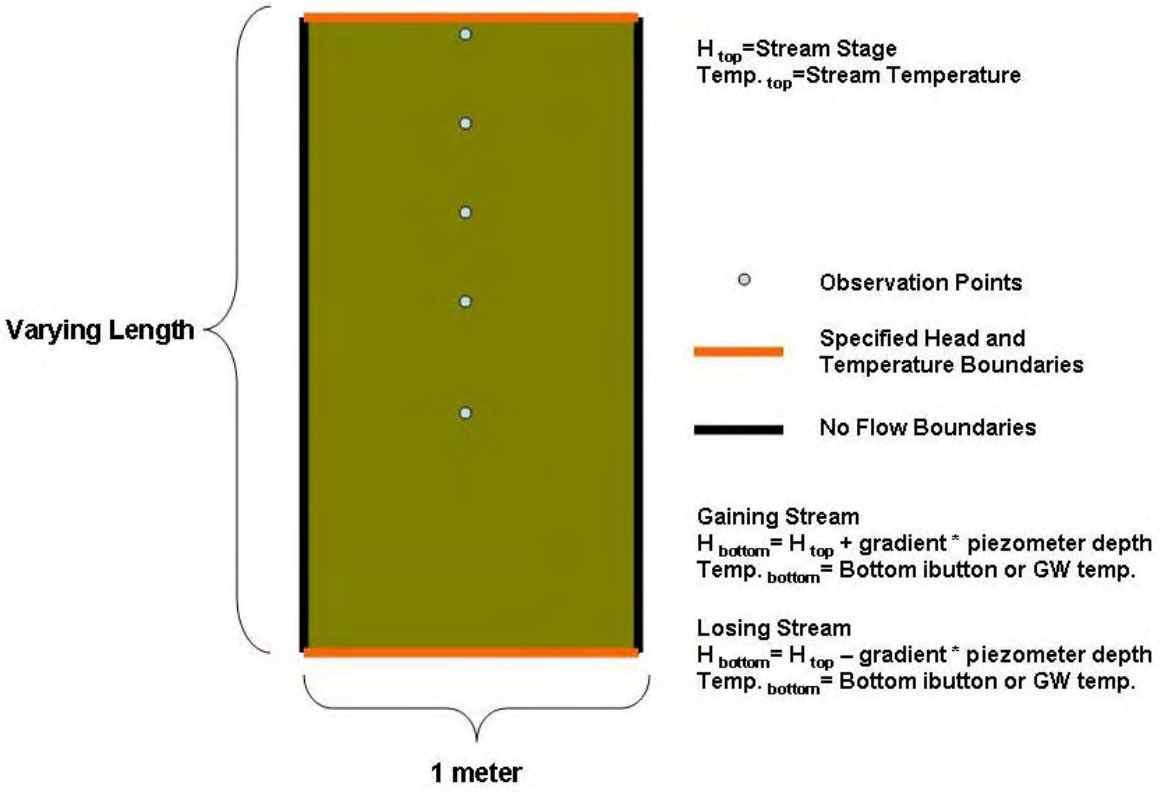

Figure 21 Diagram of the one dimensional heat transport model.

Assumptions made using the VS2DHI heat transport model:

1. Water enters and leaves the river only in a vertical direction (1D flow)
2. Sediments in the streambed have uniform hydraulic and thermal properties
3. Vertical hydraulic gradients do not vary with time
4. The metal sandpoint casing does not measurably influence heat conduction

Figure 22 A picture of the riverbed morphology below Milltown dam. The photo shows the coarse river bed armored with fine grained reservoir sediments.

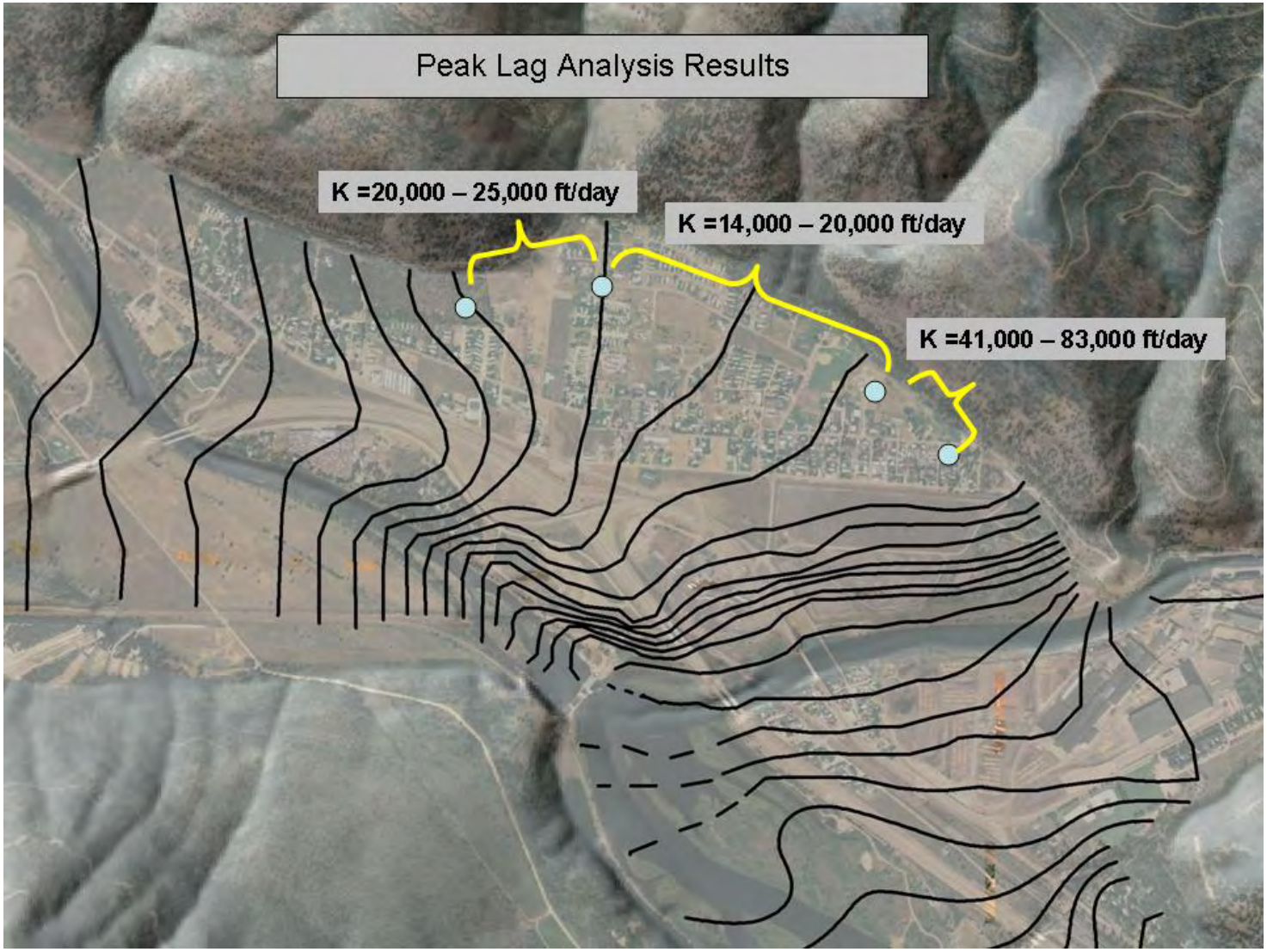

Figure 23 An illustration of the wells used in conducting the peak lag analysis. Water table map is contoured from 3/31/06 water level measurements (contour interval equals 2 ft).

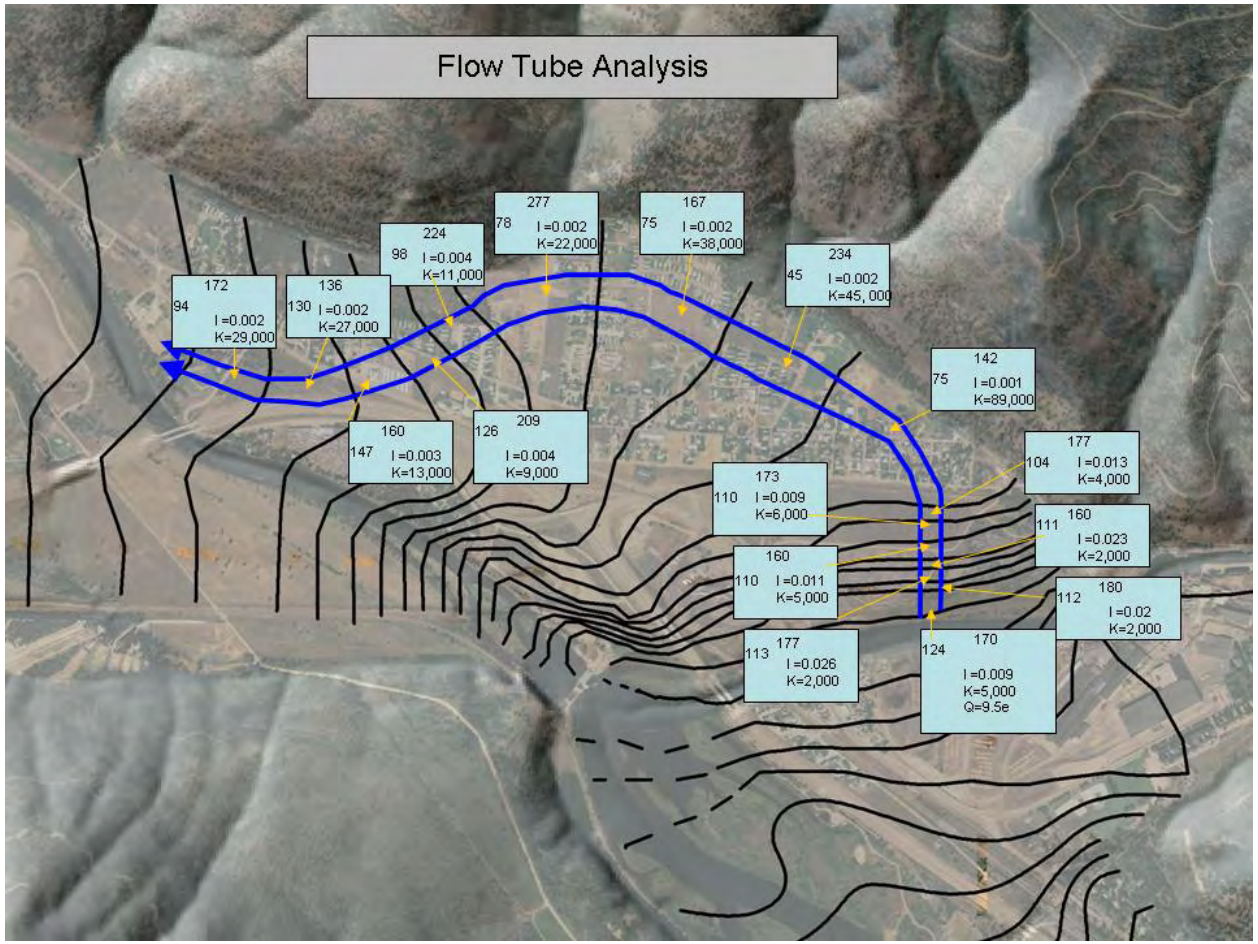

Figure 24 An illustration of a flow tube used to estimate the relative hydraulic conductivity values and trends in the neighborhoods of West Riverside and Pine Grove. Water table map is contoured from 3/31/06 water level measurements (contour interval equals 2 ft).

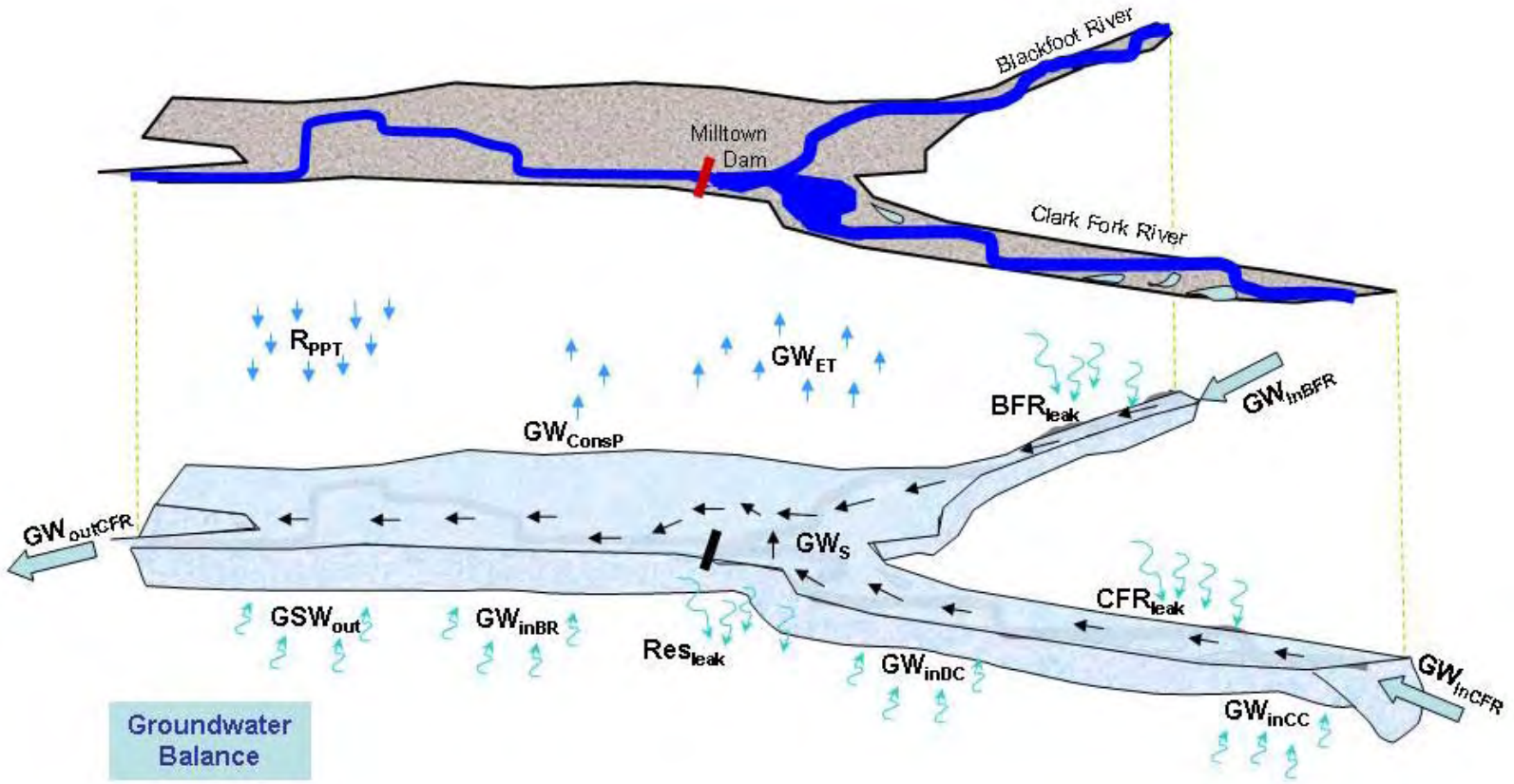

Figure 25 Generalized conceptual model.

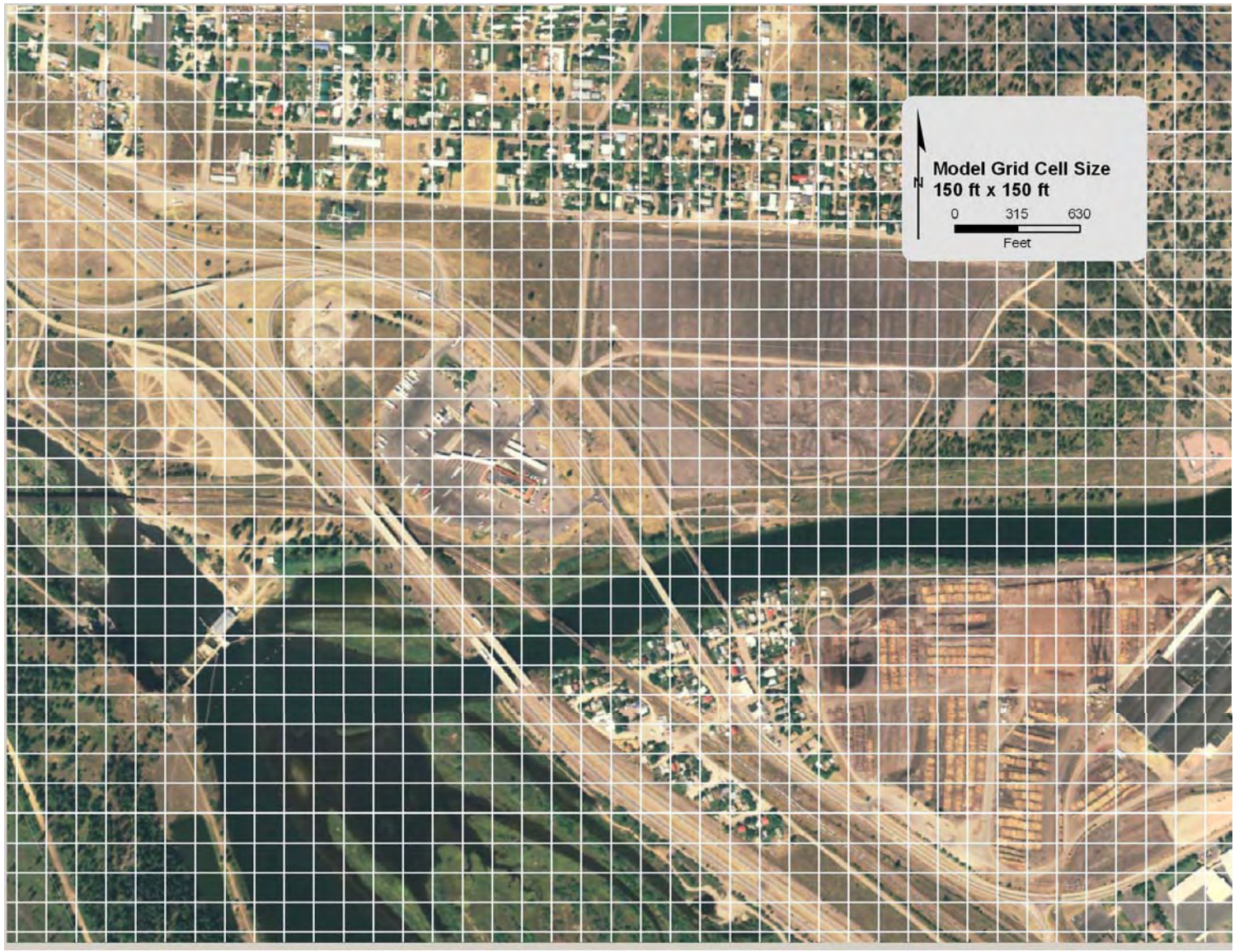

Figure 26a Illustration of the size and spatial distribution of model cells.

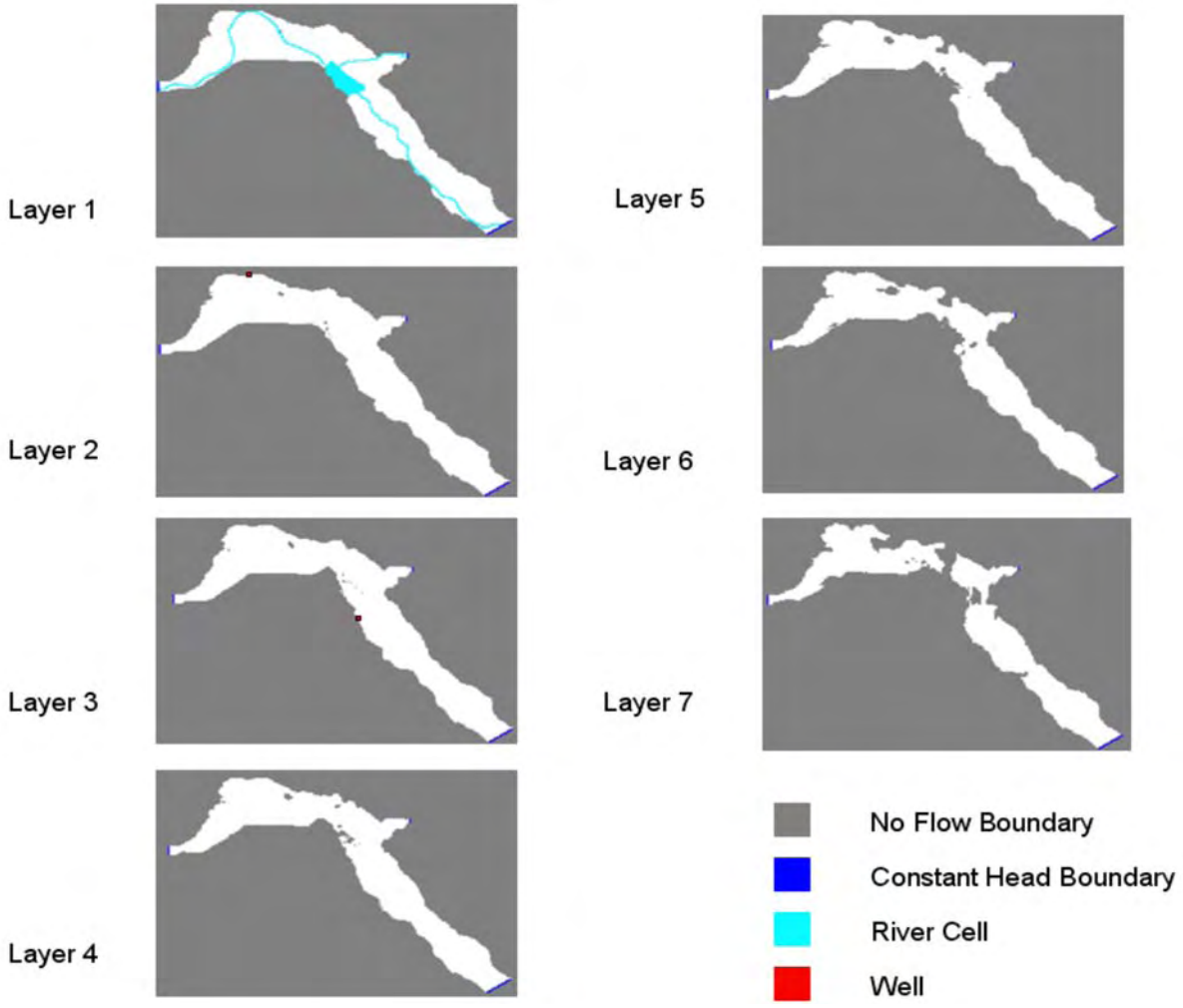

Figure 26b Illustration of boundary conditions for each layer of the numerical groundwater model. Initial model runs used constant head boundaries representing single equipotential lines at the southeastern Turah Bridge, northeastern Blackfoot River valley and western Hellgate Canyon boundaries. Remaining boundaries were simulated as no flow except where small yield injection wells were used to represent minor tributary groundwater underflow entering the valley aquifer. River cells were used to allow exchange of water between the river and groundwater in Layer 1. Note as the layer bases encountered bedrock highs portion of layers would become inactive (no flow gray areas).

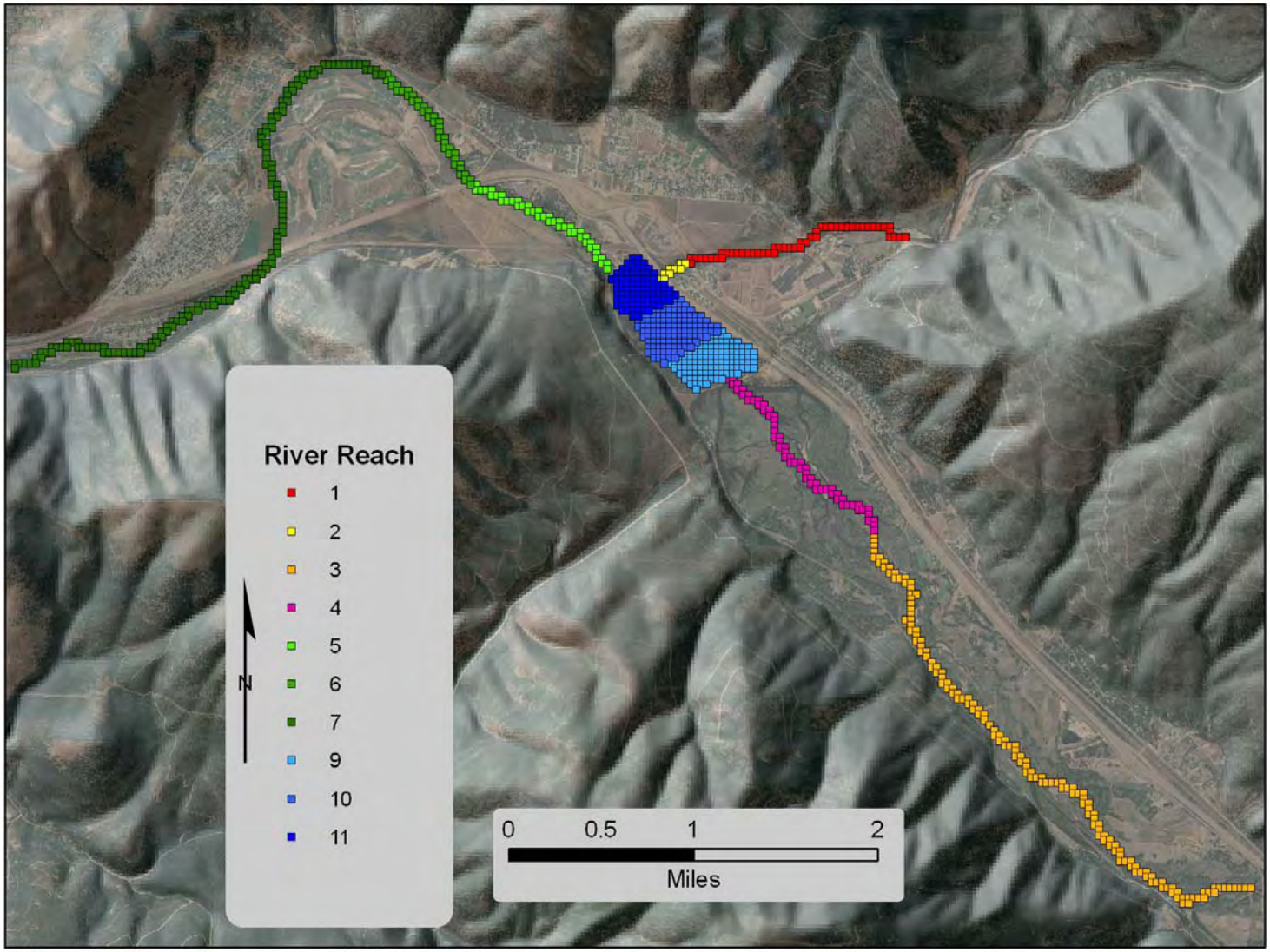

Figure 27 11 river reaches were used to simulate river/groundwater exchange rates and locations.

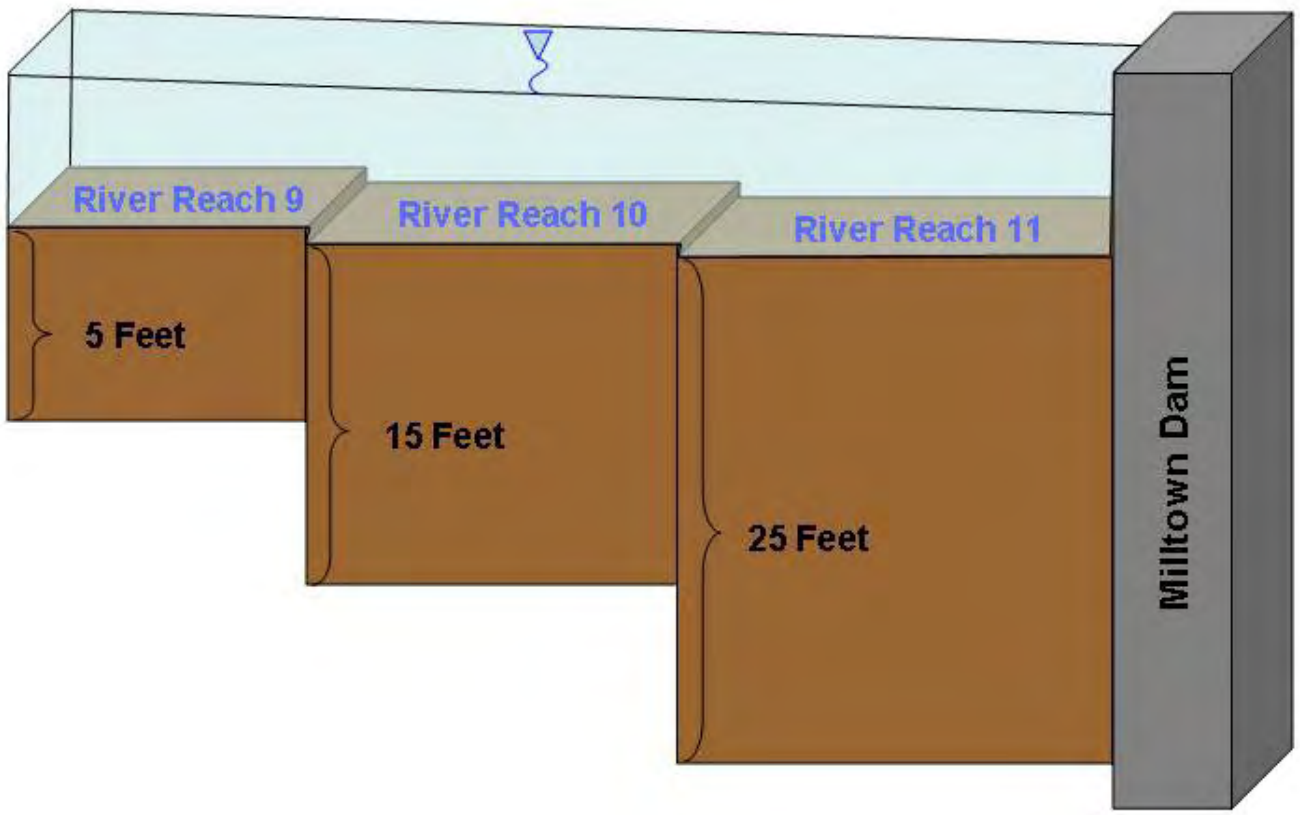

Figure 28 Schematic of the river bed thickness assignments used to compute conductance terms for reservoir/groundwater exchange in layer 1 reservoir sediments (Figure 27).

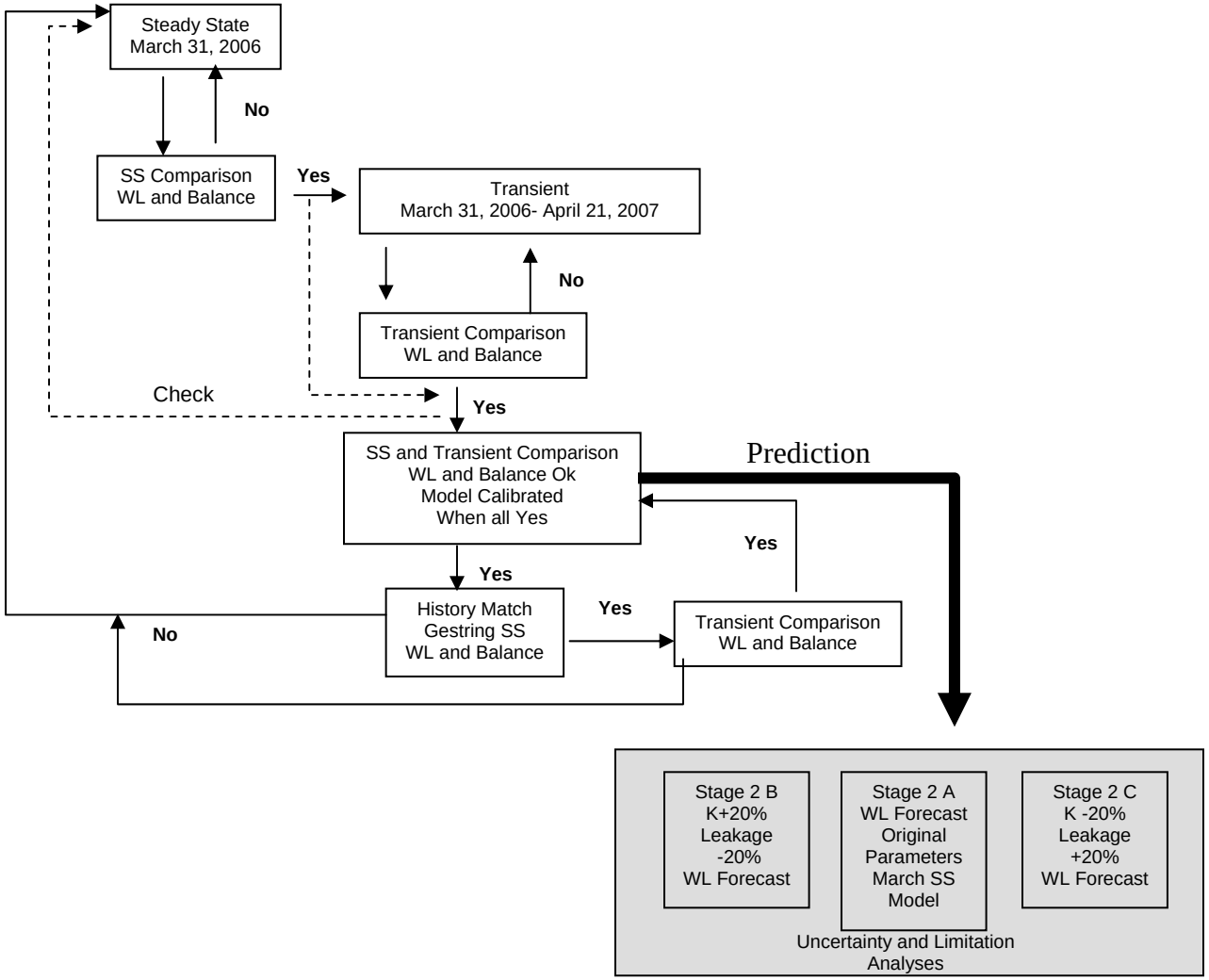

Figure 29 A representation of the process followed to generate a calibrated three-dimensional numerical groundwater model. For the prediction phase three scenarios were generated: A) The post Stage 2 drawdown river levels were represented in the steady state (SS) calibrated model and the new position of the water table was predicted. B) and C) represent the same conditions with parameter increases and decreases within reasonable ranges, a process designed to suggest the possible range of uncertainty in predicted values.

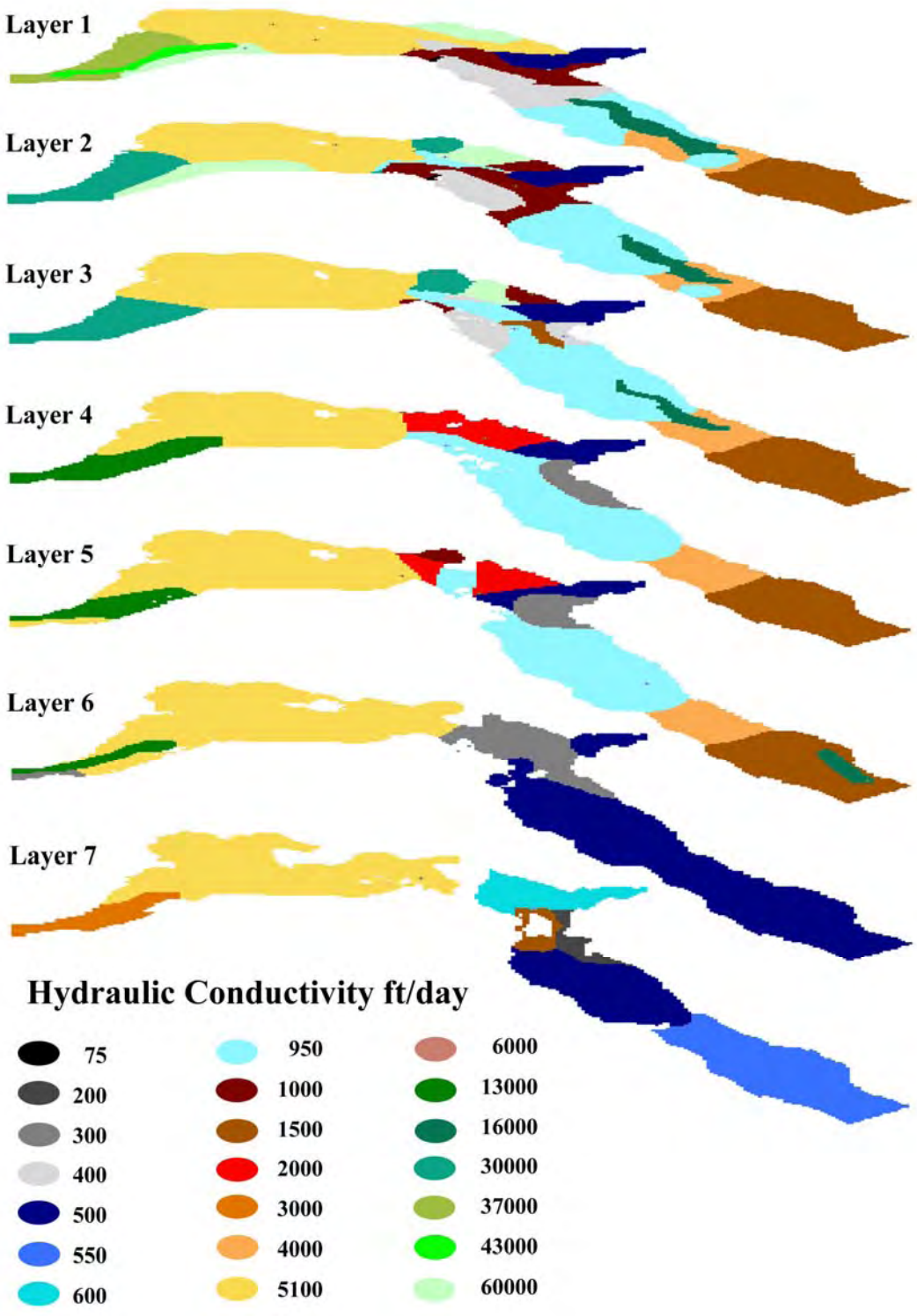

Figure 30 Calibrated hydraulic conductivity distributions for each layer of the numerical model. Hydraulic conductivities less than 500 ft/day are in grayscale with the Milltown Dam (K=75) being black. Conductivities between 500 and 950 ft/day are in bluescale, between 1000 and 10000 ft/day are in redscale, and between 10000 and 60000 ft/day are in greenscale.

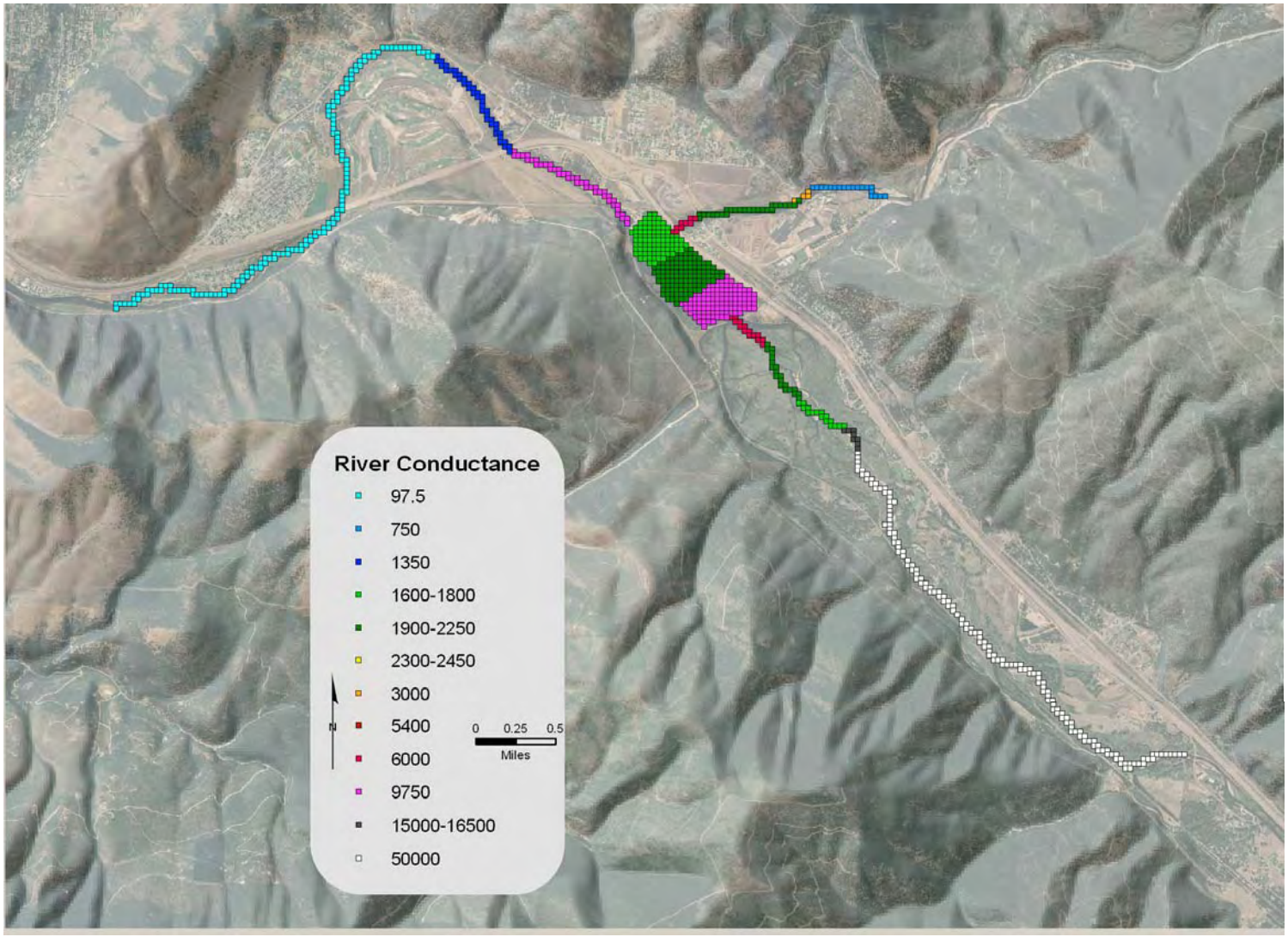

Figure 31 Distribution of riverbed conductance's (ft^2/day) used in the calibrated numerical groundwater model Reach numbers presented in Figure 27.

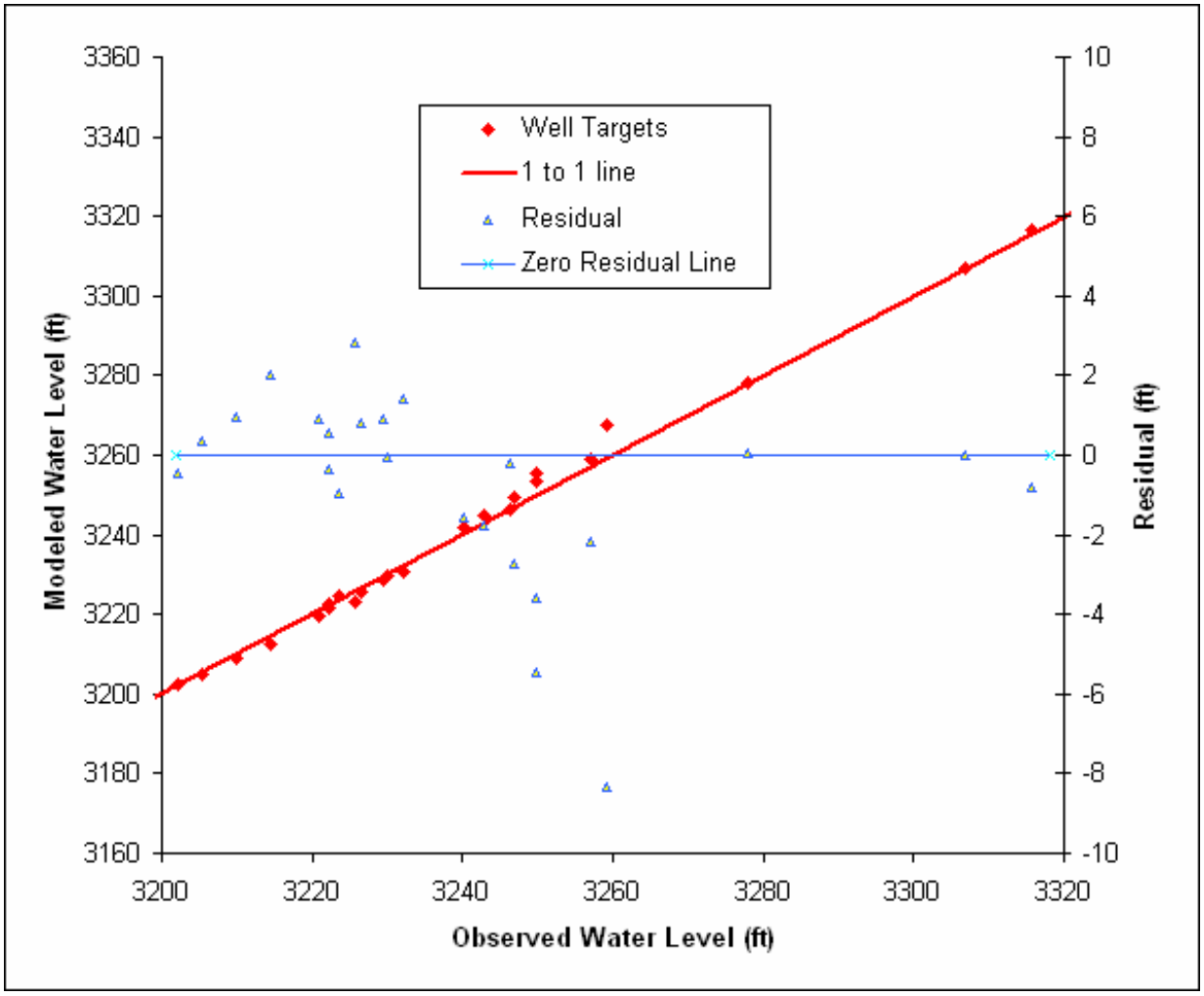

Figure 32 Steady state calibration data. Observed vs. modeled water levels (red) and residual values (blue).

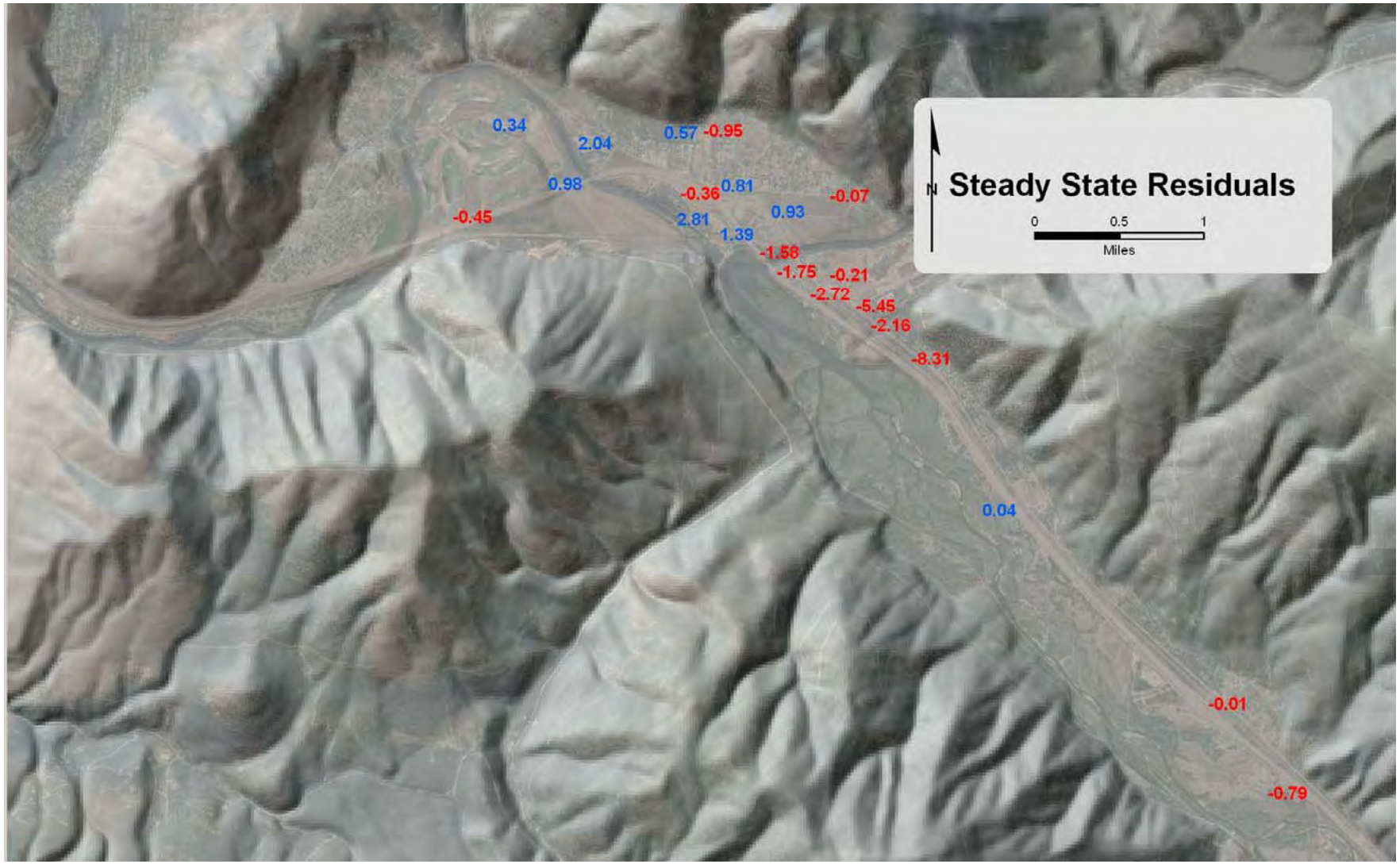

Figure 33 Final distribution of residuals after steady state calibration. The numbers indicate the head difference between the observed water level and the simulated water level. Positive numbers (blue) indicate areas where the simulated water table is lower than observed values. Negative numbers (red) indicate areas where the simulated water table is higher than observed values.

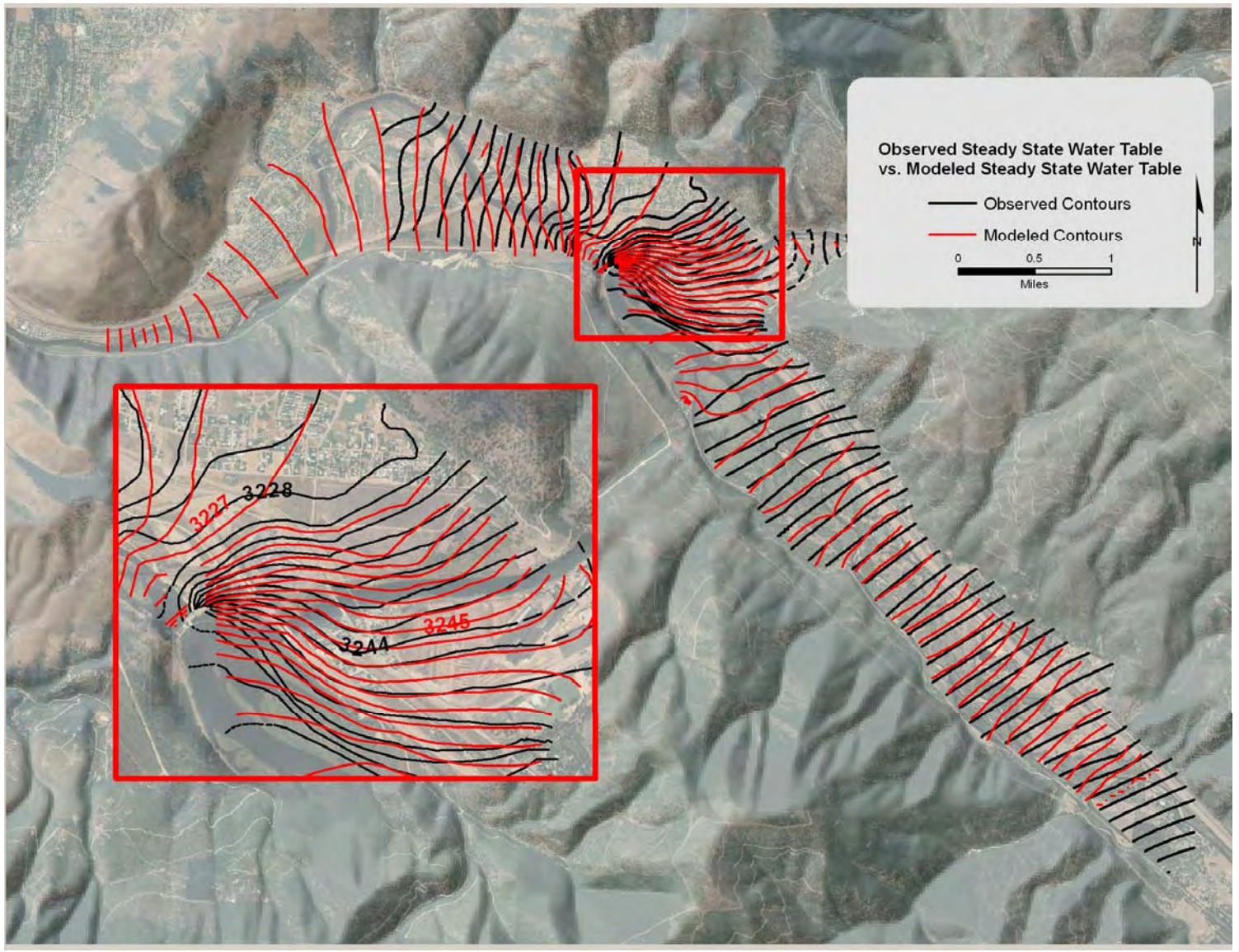

Figure 34 Water table map for the March 31, 2006 head distribution (black lines have 2 ft even contour intervals) and the simulated steady state heads (red lines have 2 ft odd numbered contour intervals).

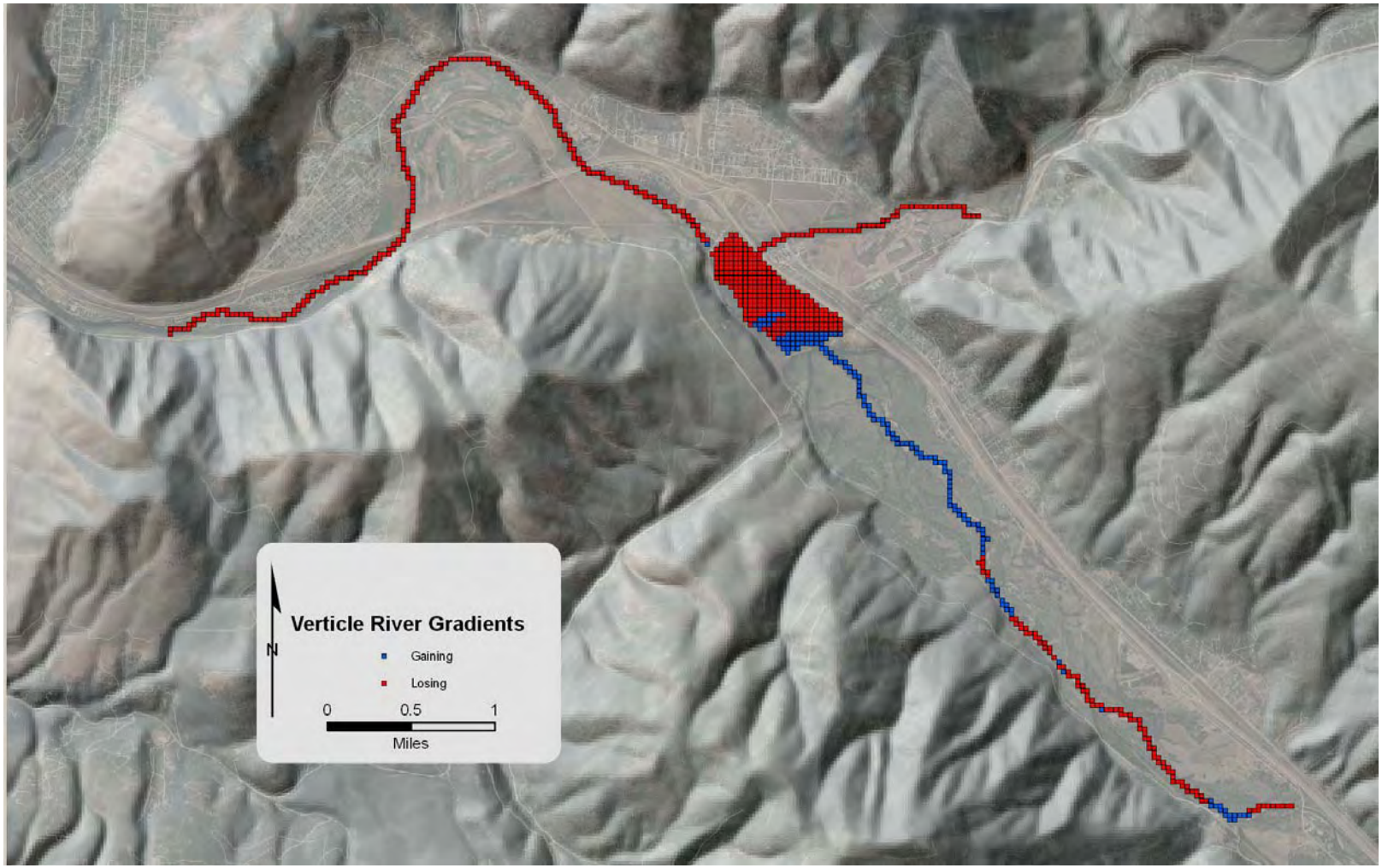

Figure 35 Distribution of simulated gaining and losing river reaches in the calibrated steady state model. This representation illustrates that the calibration target having the simulated gaining and losing reaches be within +/- 0.5 miles of the "observed" location was achieved (Figure 17,18, and 19).

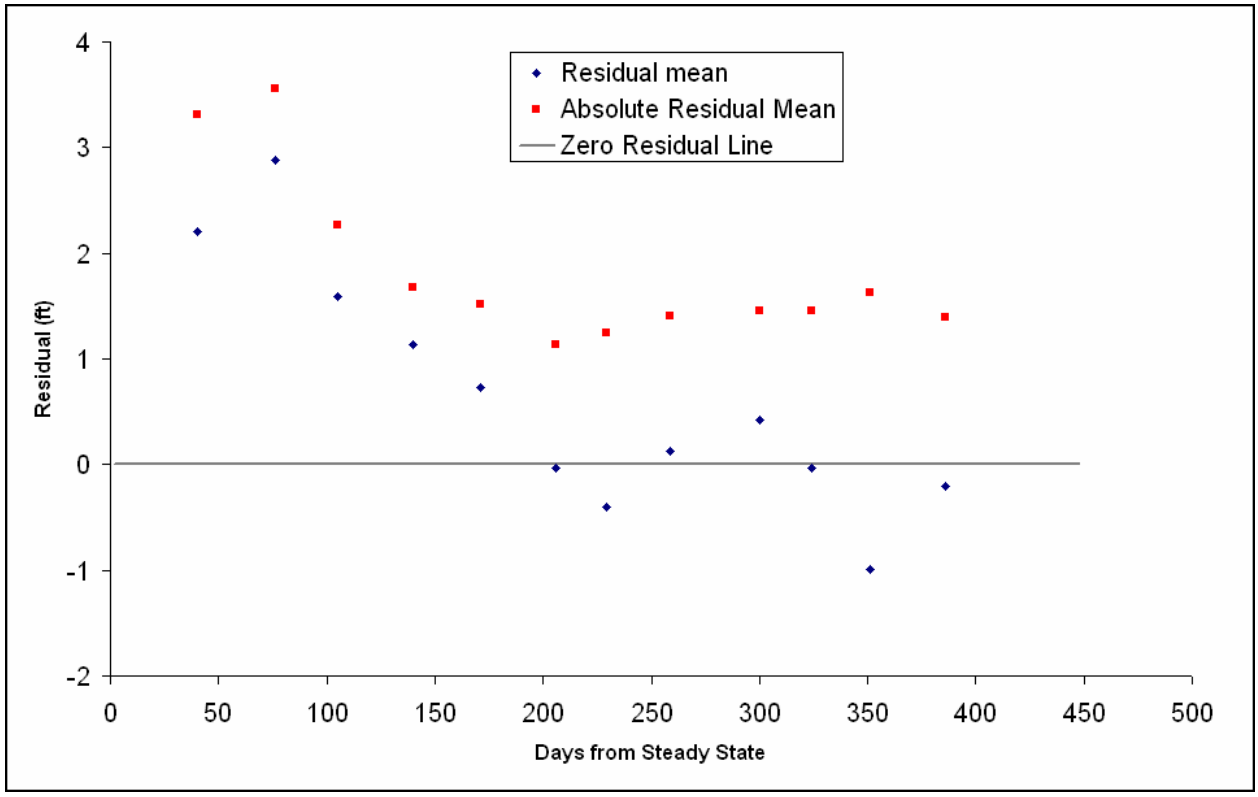

Time	Residual mean	Residual Stdev	Residual Sum of Squares	Absolute Residual Mean	minimum Residual	Maximum Residual	observed range in head
40	2.21	2.98	455	3.31	-7.71	5.59	110.14
76	2.88	2.68	526	3.56	-6.76	6.76	108.57
105	1.59	2.04	294	2.27	-6.25	4.33	118.91
140	1.14	1.66	182	1.68	-5.34	4.28	114.4
171	0.73	1.77	173	1.52	-5.89	4.44	123.18
206	-0.03	1.76	140	1.13	-6.3	4.51	124.83
229	-0.4	1.85	175	1.25	-7.11	4.75	125.26
259	0.13	1.94	182	1.4	-5.78	3.48	126.7
300	0.42	2.03	224	1.46	-5.82	4.32	126.35
324	-0.03	2.03	203	1.46	-6.4	3.93	127.33
351	-0.99	1.98	260	1.63	-6.93	5.06	129.12
386	-0.21	1.88	100	1.39	-5.94	2.99	118.63
Average	0.62	2.05	242.83	1.84	-6.35	4.54	121.12

Figure 36 Plot of the residual mean and absolute residual mean for each modeled stress period. The ending time (days from the initiation of the model) for each stress period is shown in the accompanying table that includes computed statistics).

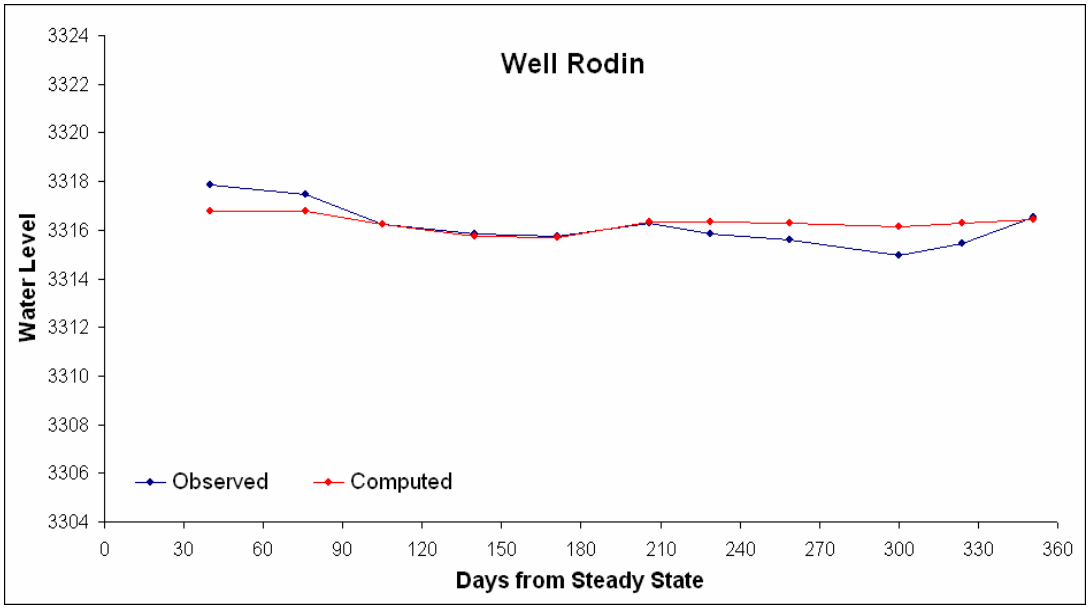

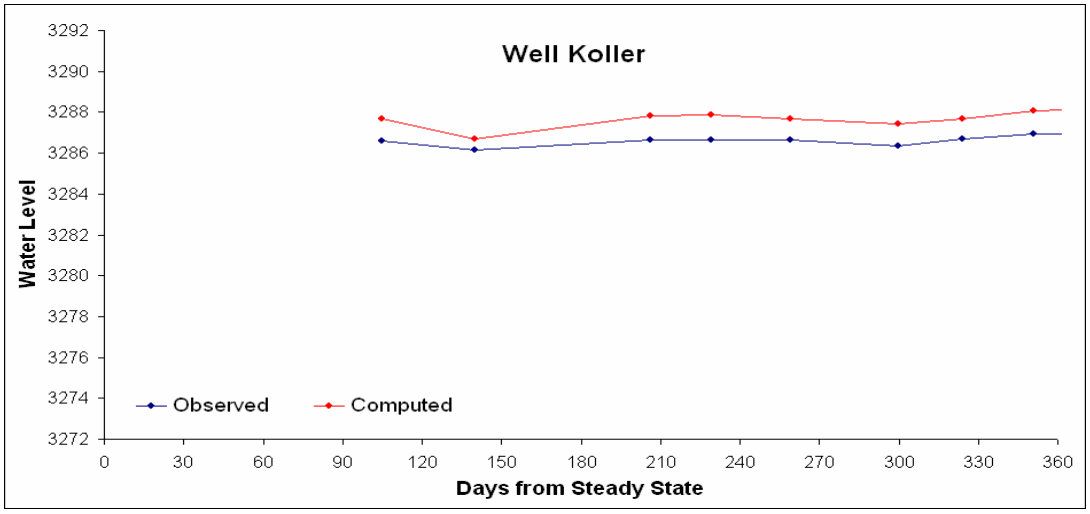

Figure 37a Examples of measured and simulated groundwater hydrographs. Well locations are shown on Figure 10.

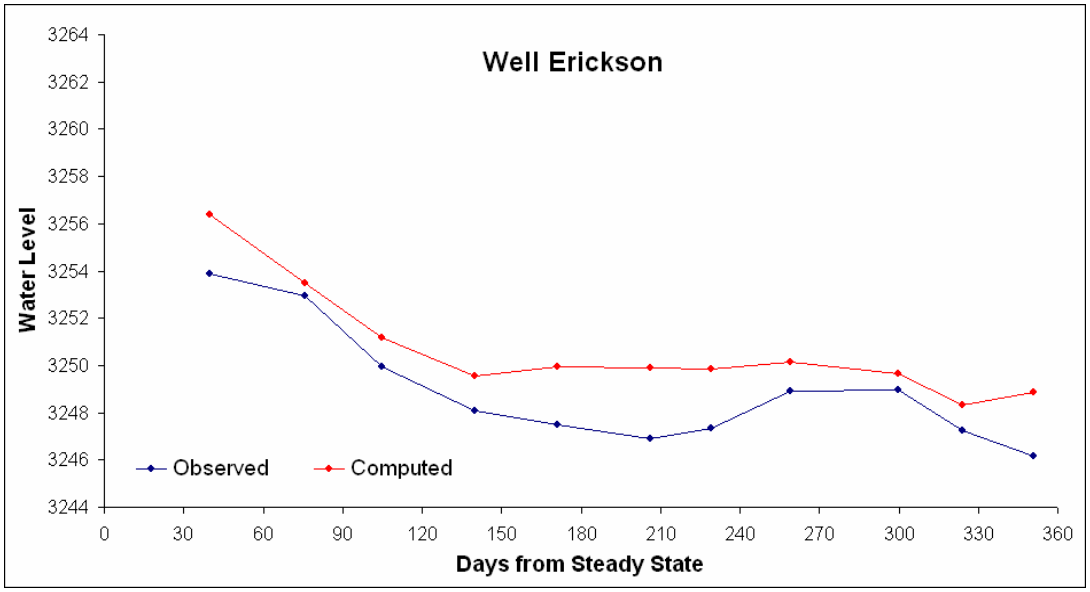

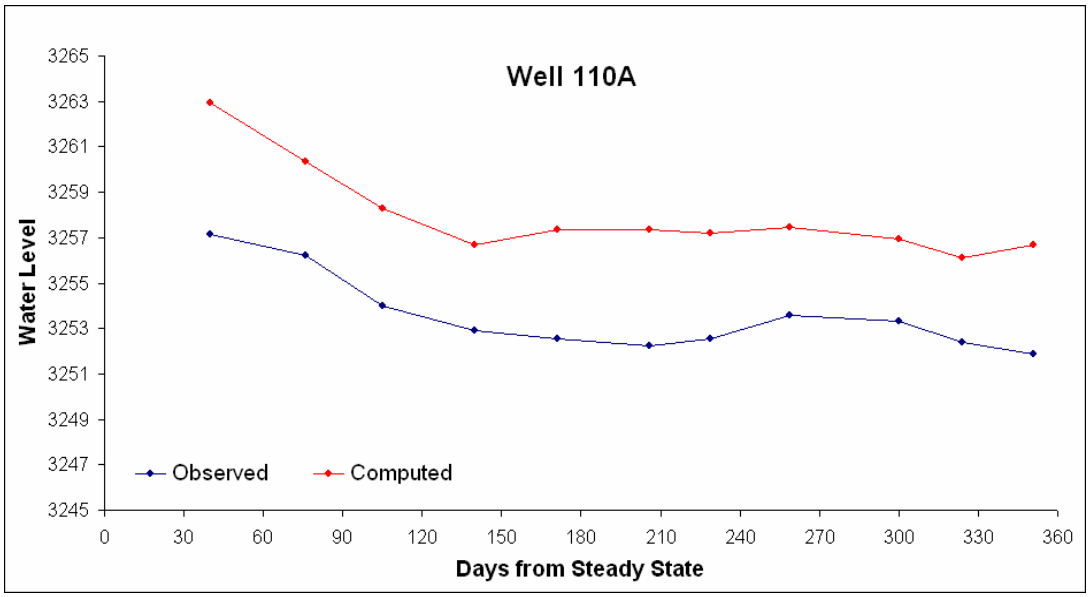

Figure 37b Examples of measured and simulated groundwater hydrographs. Well locations are shown on Figure 10.

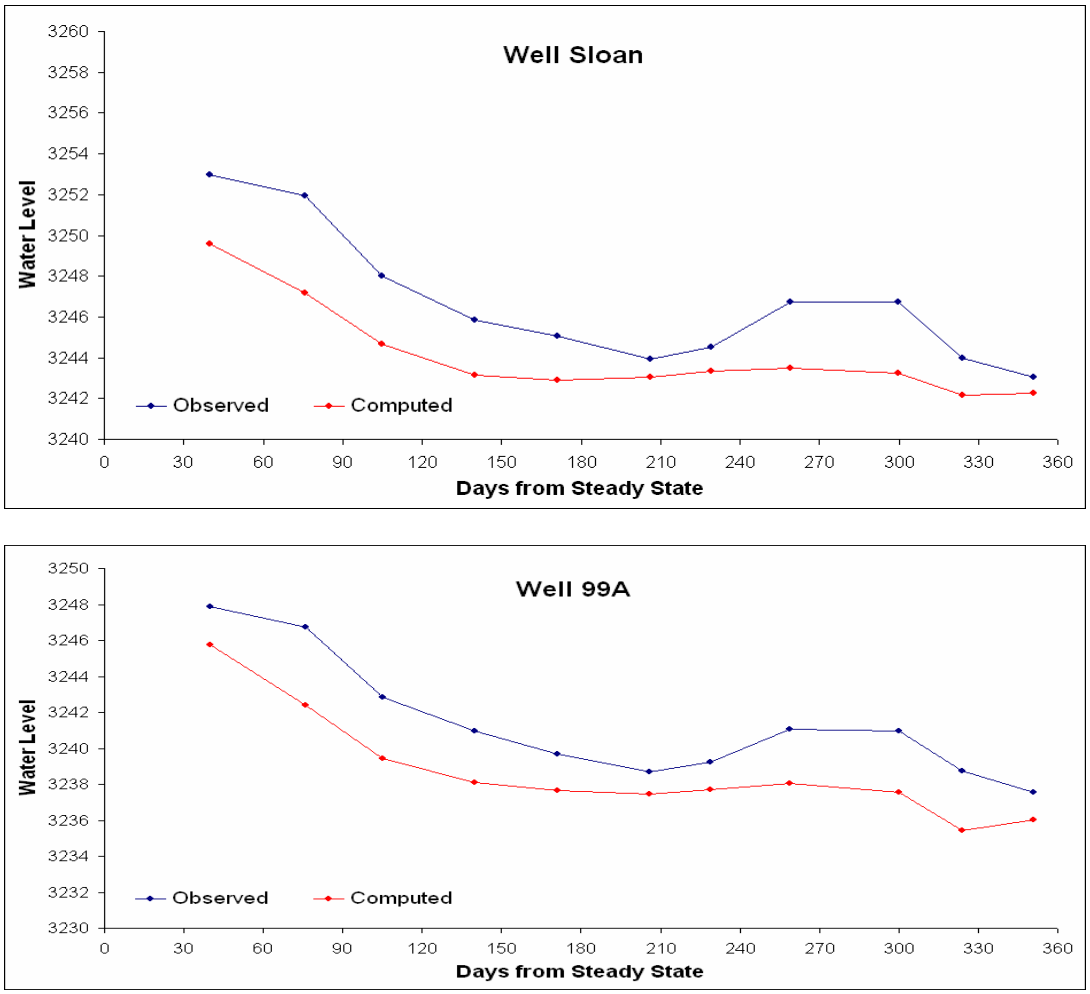

Figure 37c Examples of measured and simulated groundwater hydrographs. Well locations are shown on Figure 10.

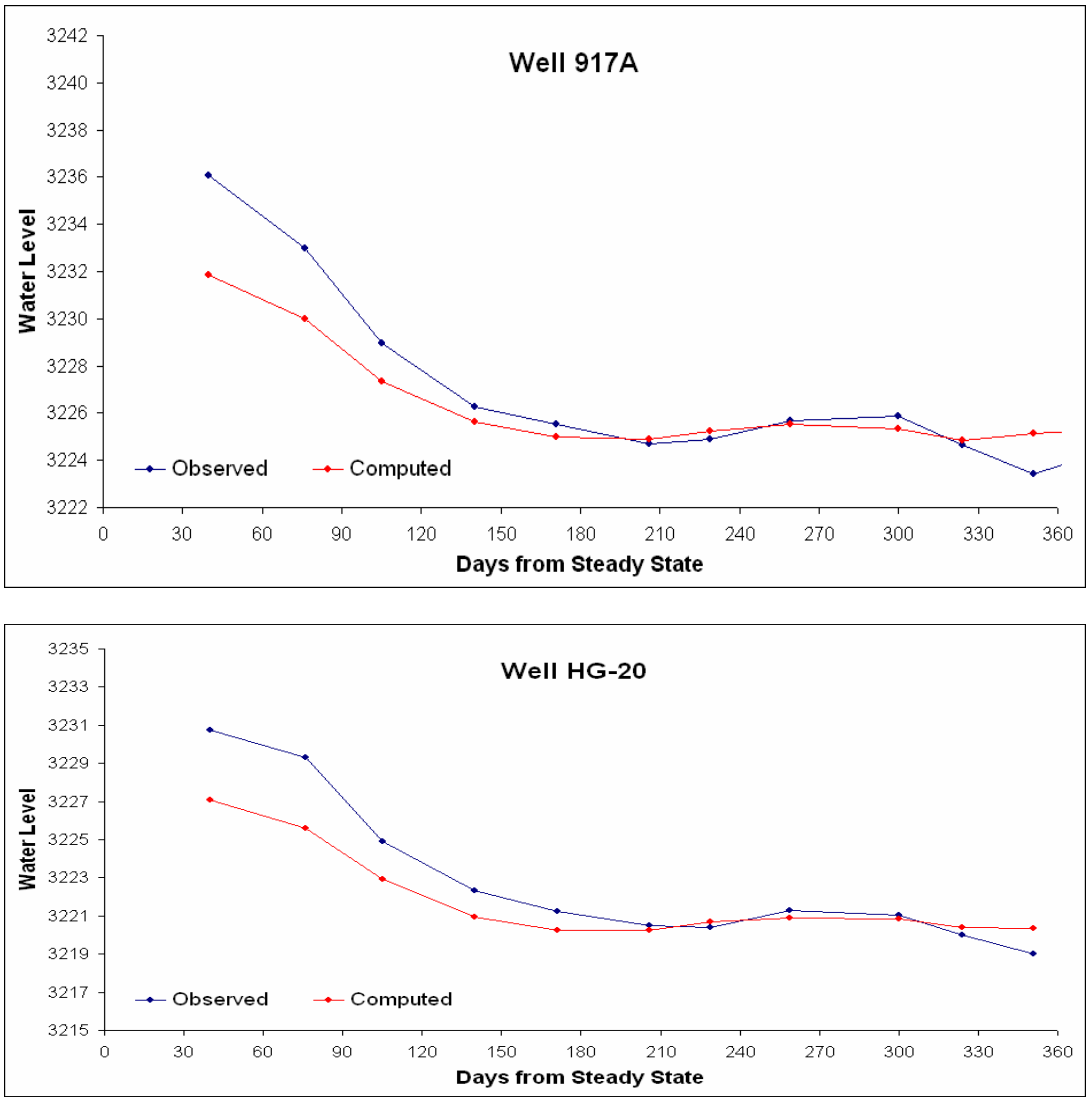

Figure 37d Examples of measured and simulated groundwater hydrographs. Well locations are shown on Figure 10.

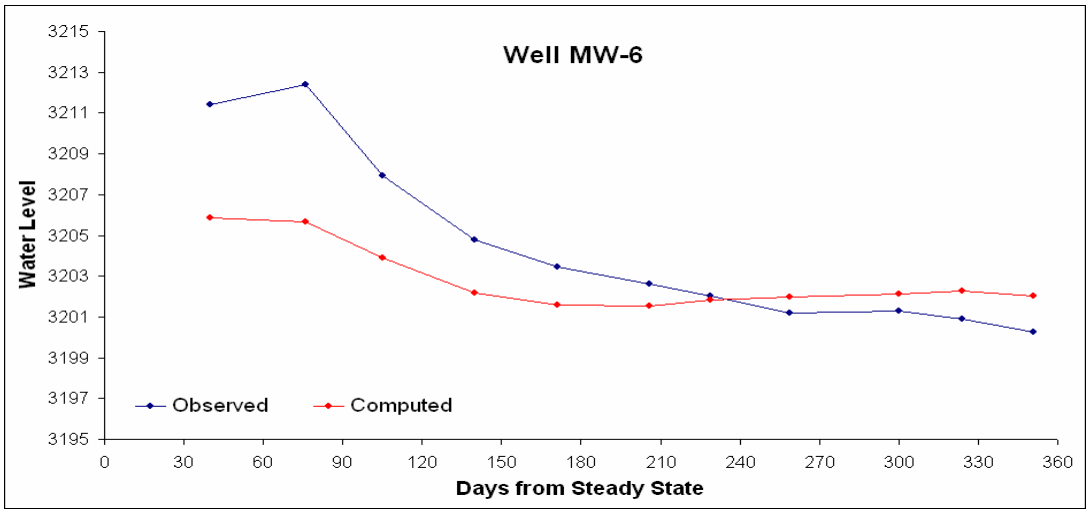

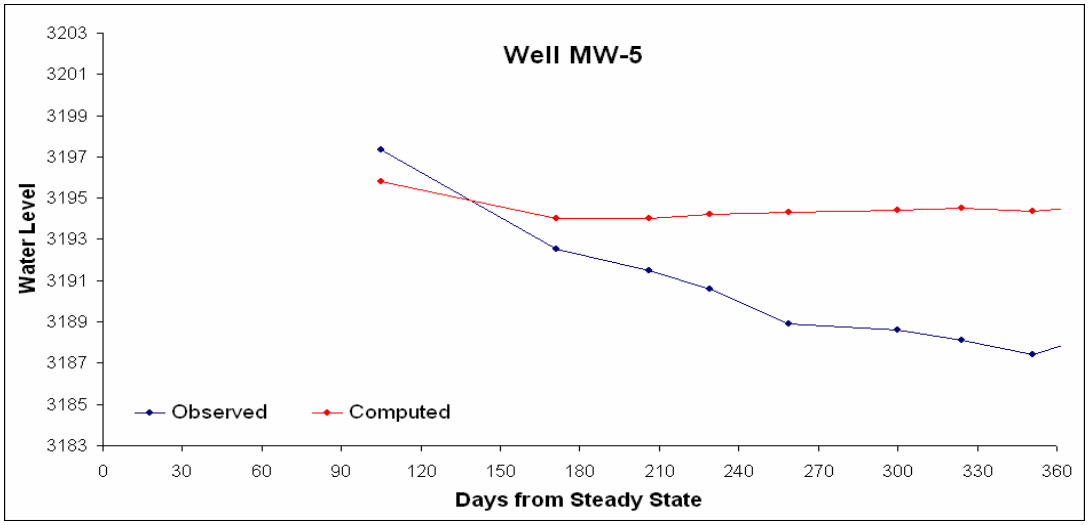

Figure 37e Examples of measured and simulated groundwater hydrographs. Well locations are shown on Figure 10.

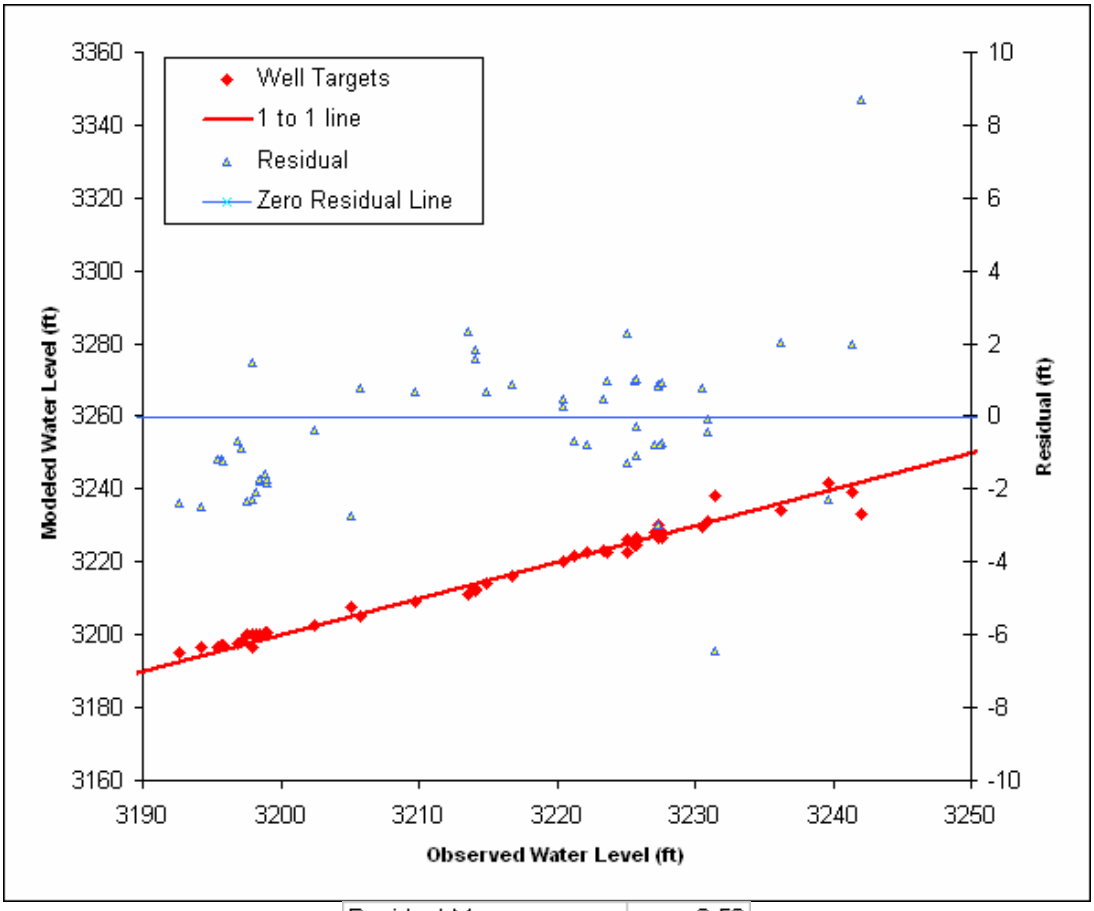

Residual Mean	-0.50
Res. Std. Dev.	2.35
Sum of Squares	310.75
Abs. Res. Mean	1.71
Min. Residual	-7.45
Max. Residual	8.71
Range in Target Values	66.27
Std. Dev./Range	0.04

Figure 38 Calibration data for the steady state history match. Observed vs. modeled water levels (red) and residual values(blue), and a table of head match statistics.

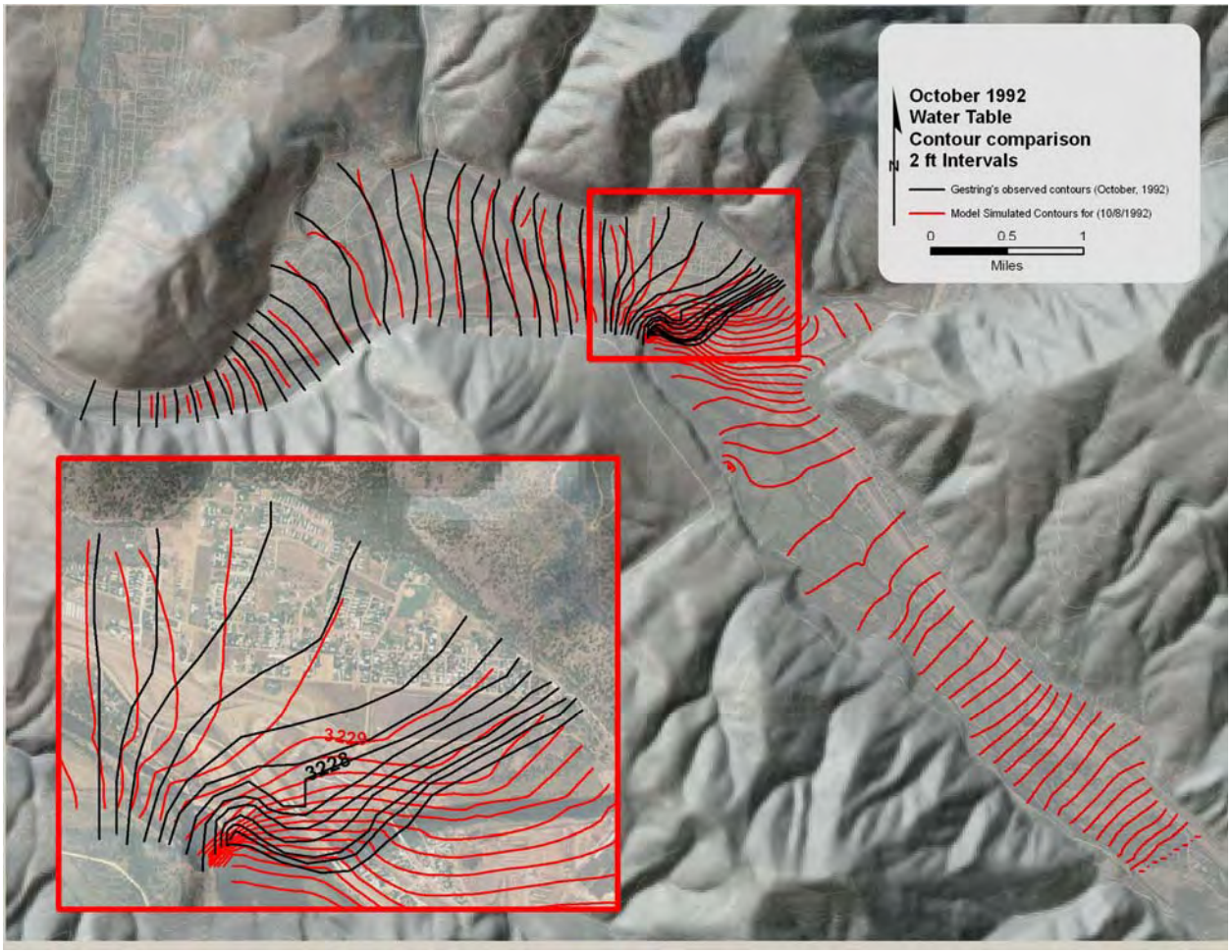

Figure 39 Comparison of modeled historical water table compared to observed historical water table.

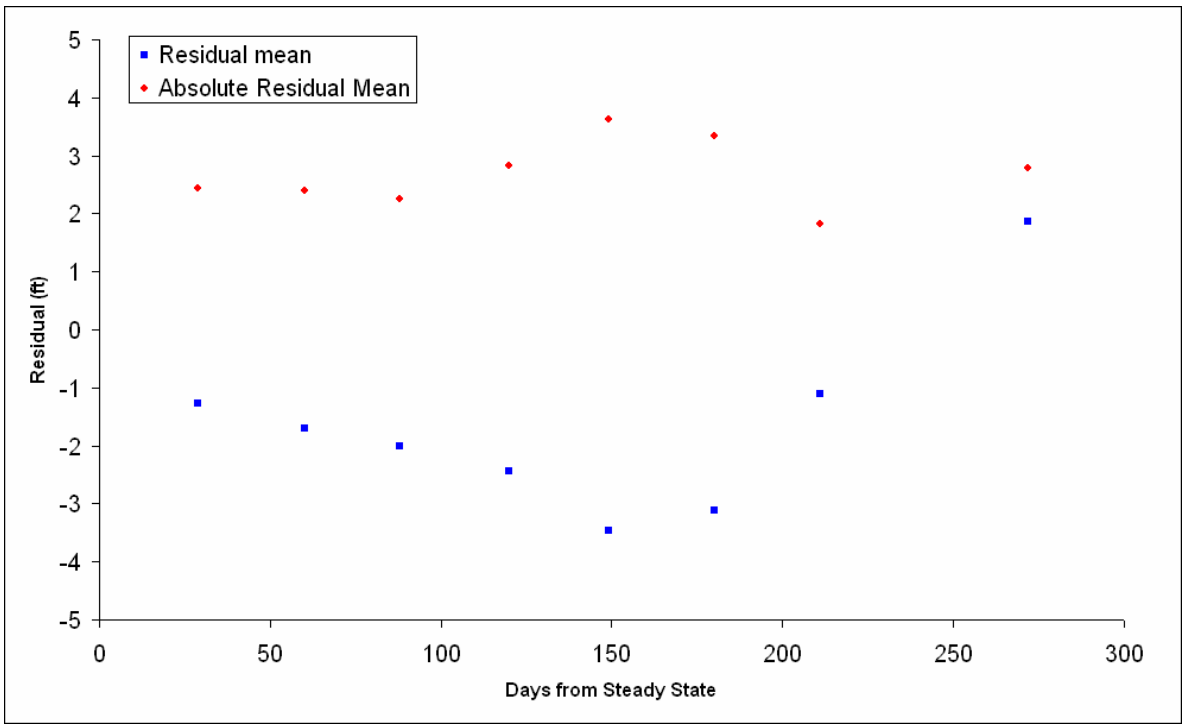

Time	Residual mean	Residual Stdev	Residual Sum of Squares	Absolute Residual Mean	minimum Residual	Maximum Residual
29	-1.28	3.24	474	2.44	-10.53	8.1
60	-1.7	2.82	727	2.4	-10.68	8
88	-2.01	2.2	567	2.25	-8.82	1.62
120	-2.44	2.62	872	2.82	-11.93	6.21
149	-3.47	2.63	131	3.63	-12.7	5.61
180	-3.12	2.36	1150	3.33	-12.43	4.9
211	-1.11	2.42	551	1.83	-10.21	7.4
272	1.86	2.54	755	2.78	-7.09	7.54
Average	-1.66	2.60	653.38	2.69	-10.55	6.17

Figure 40 History matching transient head (ft) residuals, and a table of time step ending time (days from steady state) and head match statistics.

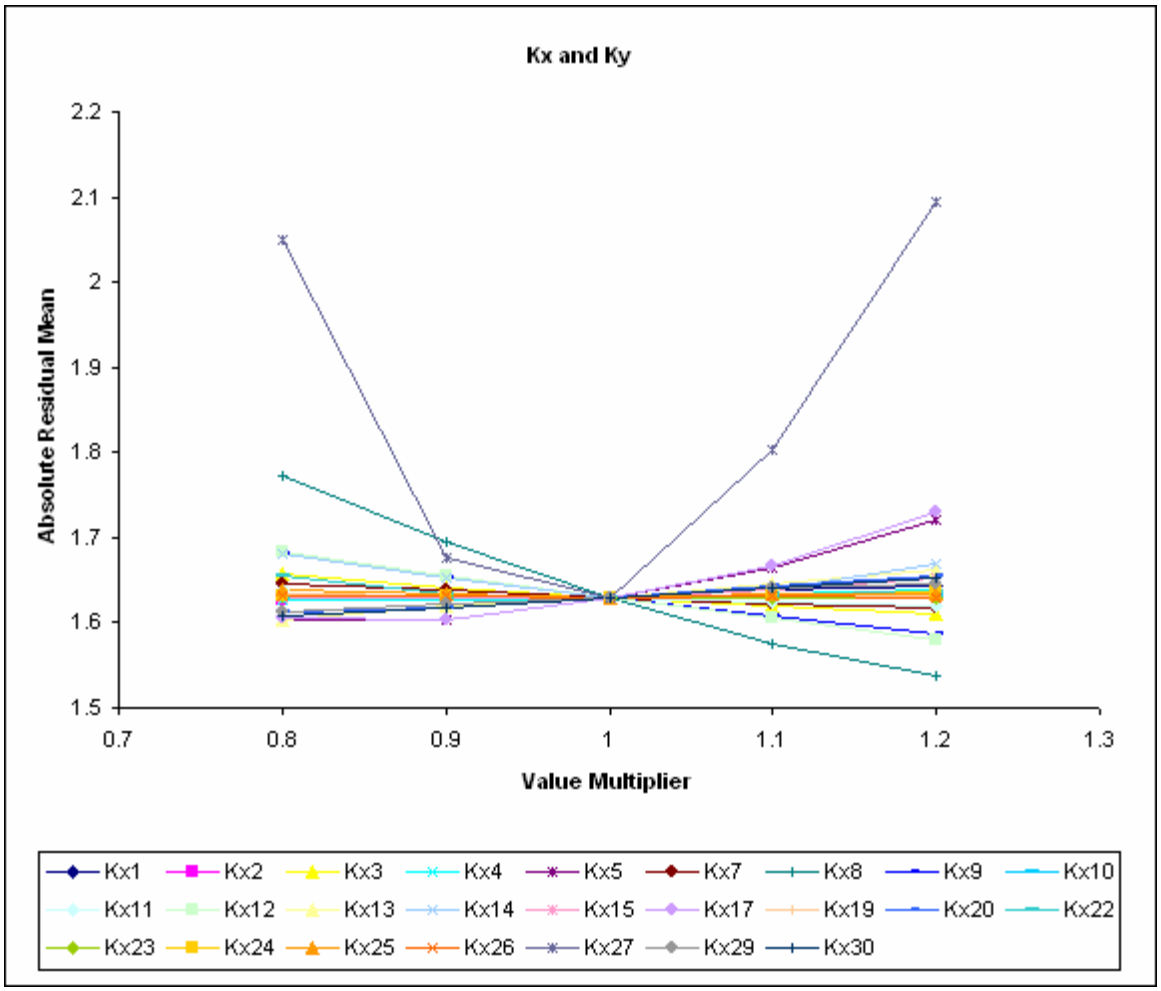

Figure 41 The sensitivity results show how the model is sensitive to different horizontal conductivity zones. The values of Kx and Ky in each zone were equal. The key showing Kx11 represents the 11th horizontal hydraulic conductivity zone.

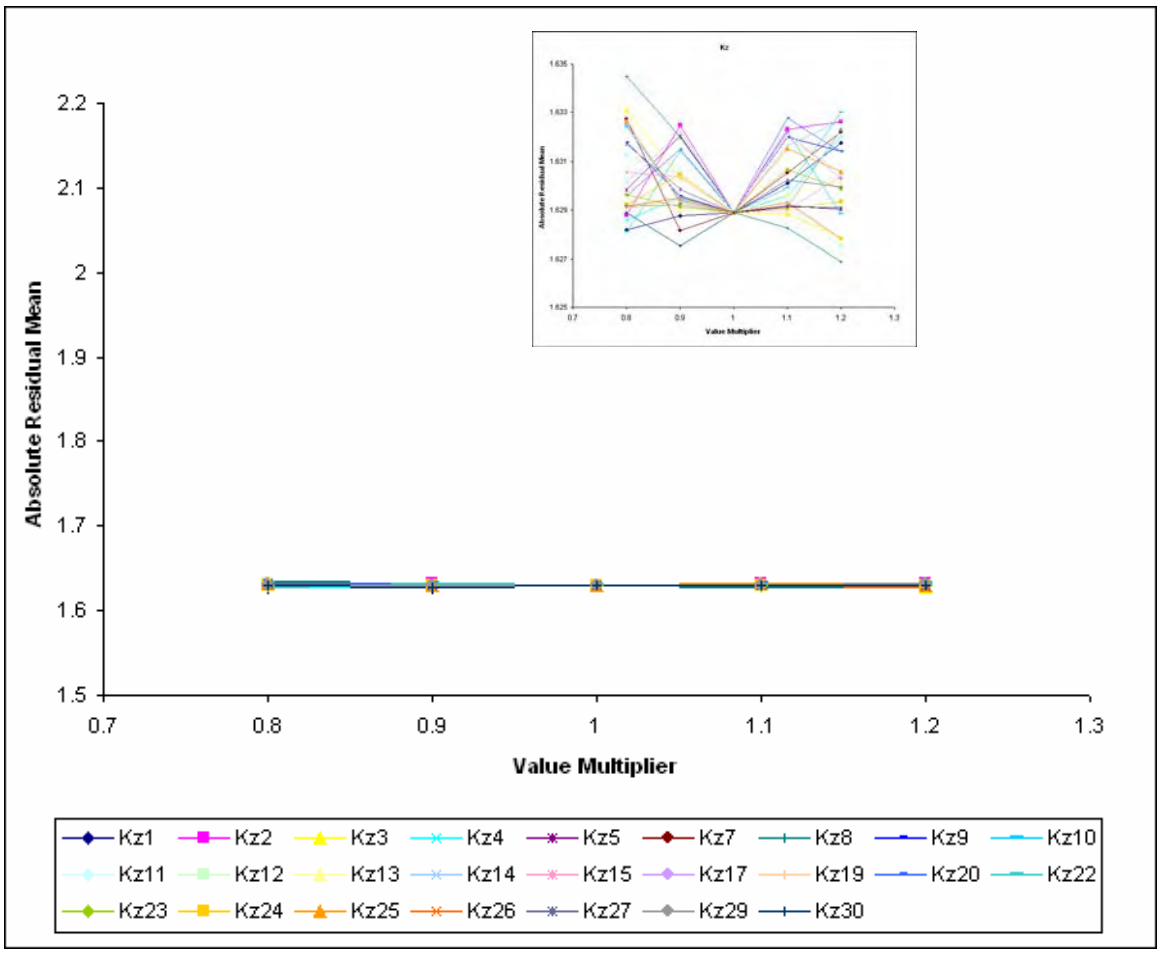

Figure 42 The sensitivity results show the model is not very sensitive to different vertical conductivity zones (e.g. Kz11). Each vertical conductivity zone is 0.10 of the corresponding horizontal conductivity zone (Kx11). The insert is a blow up (change in the vertical scale) that shows variations in the Absolute Residual Mean did occur, however, they were small.

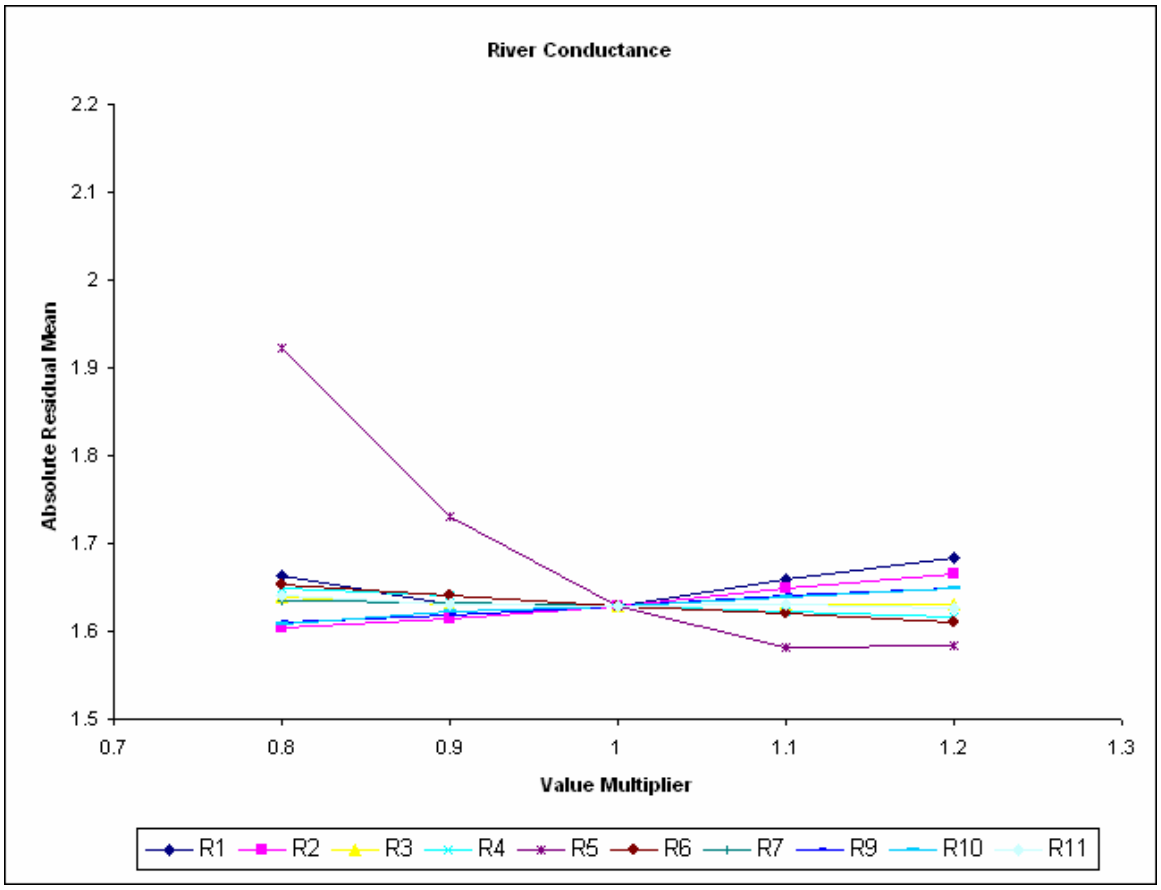

Figure 43 The sensitivity results show how the model is sensitive to variations in values of river bed conductance.. The individual lines represent different river reaches assigned within the model (Figure 27). Within each reach the conductance of the riverbed may vary from cell to cell (Figure 31).

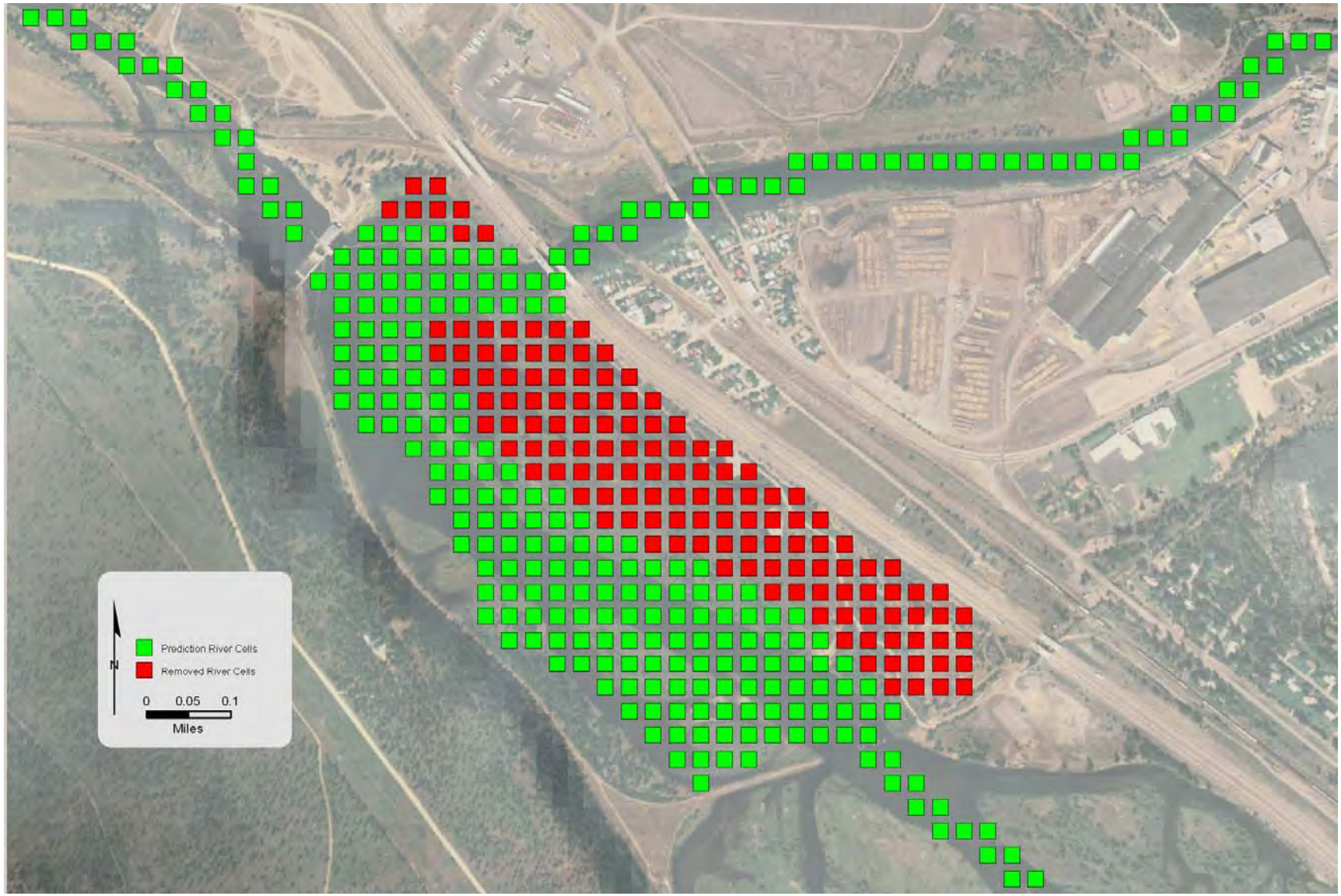

Figure 44 Map of the river cells removed (red) from the reservoir to simulate reduced leakage from dewatering and sediment removal.

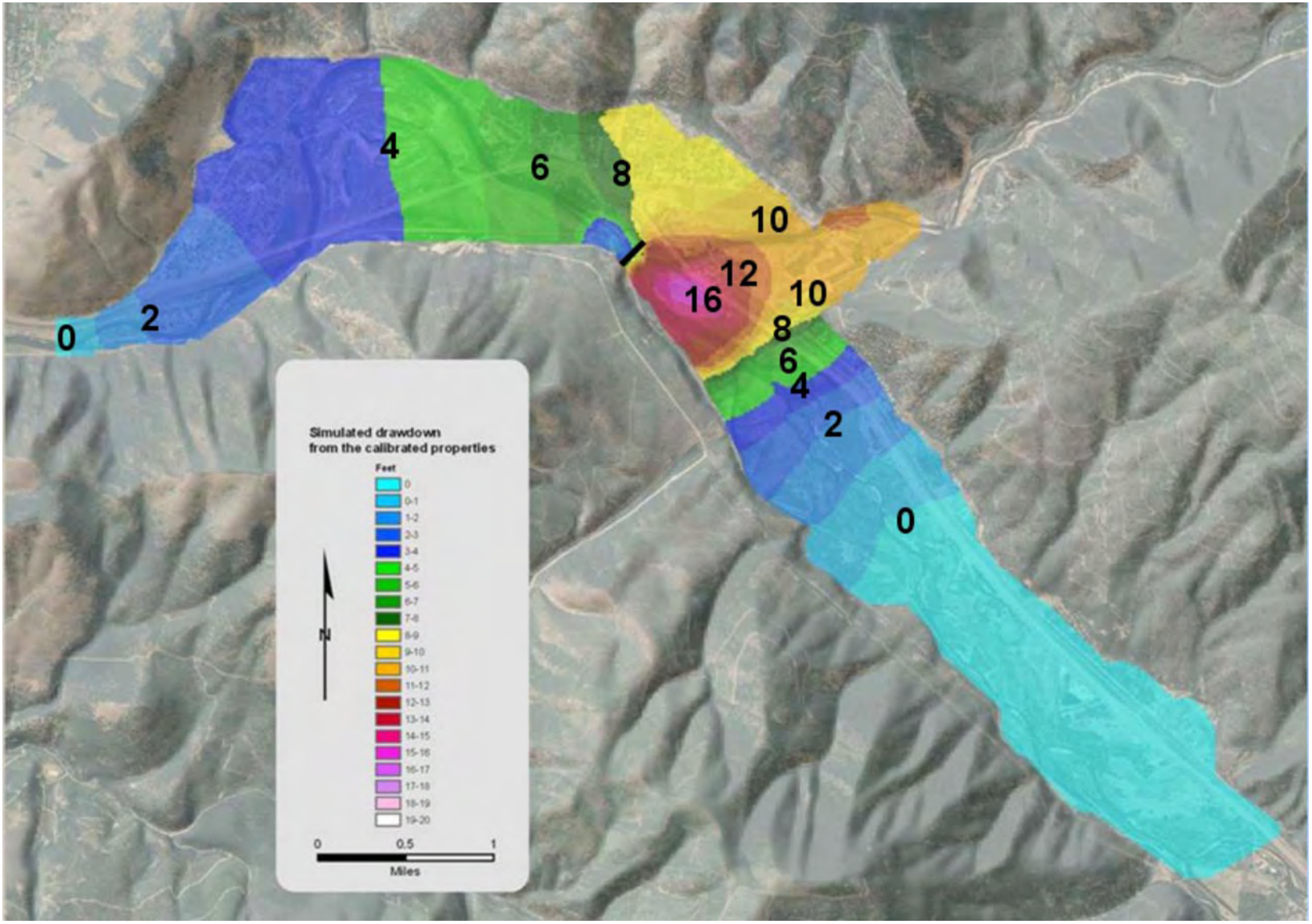

Figure 45 Simulated drawdown. Illustration created by differencing the March 2006 steady state and predicted modeled water tables. Numbers represent midpoint groundwater levels reductions in feet.

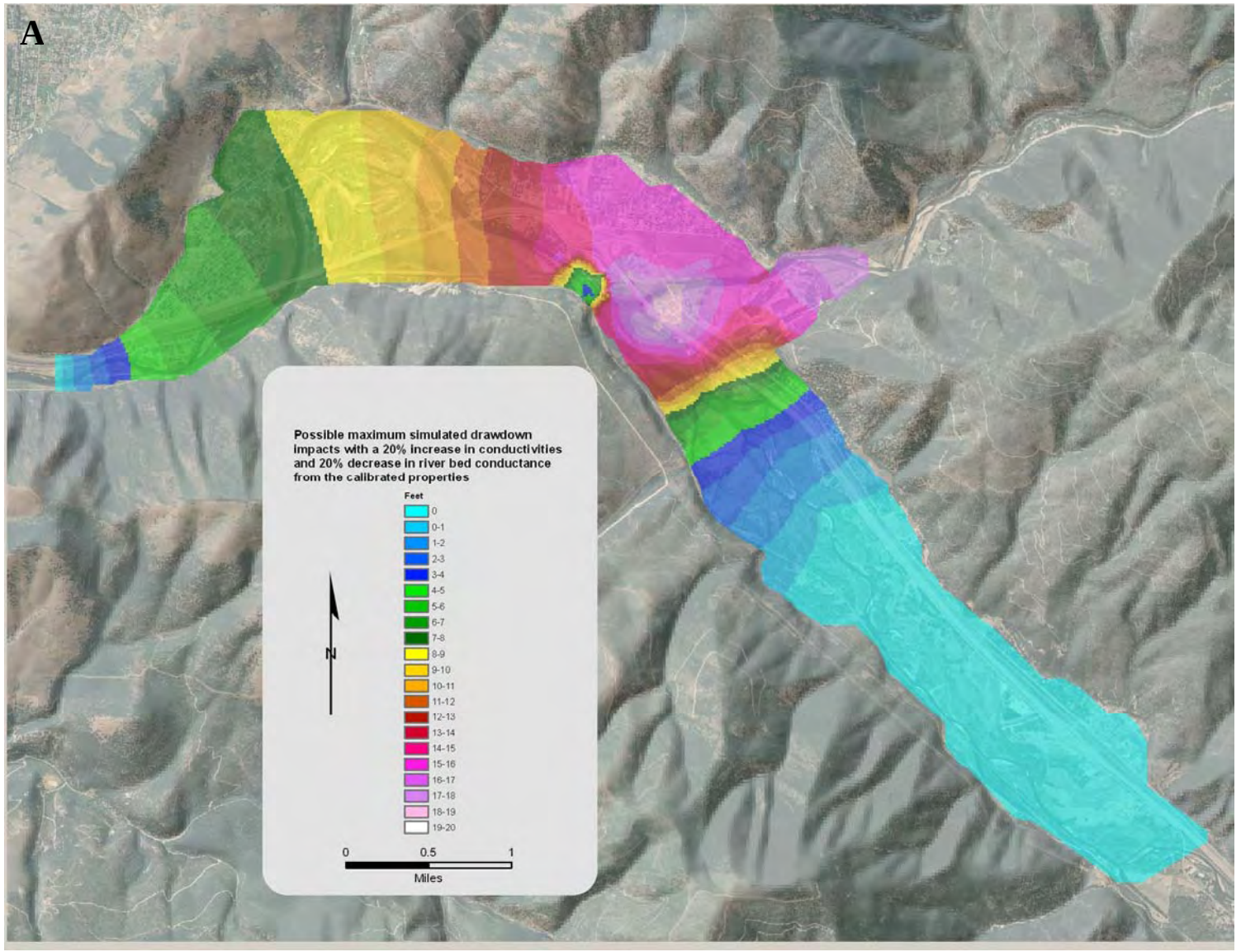

Figure 46a Model predictions based on a 20% increase in conductivities and decrease in river conductance.

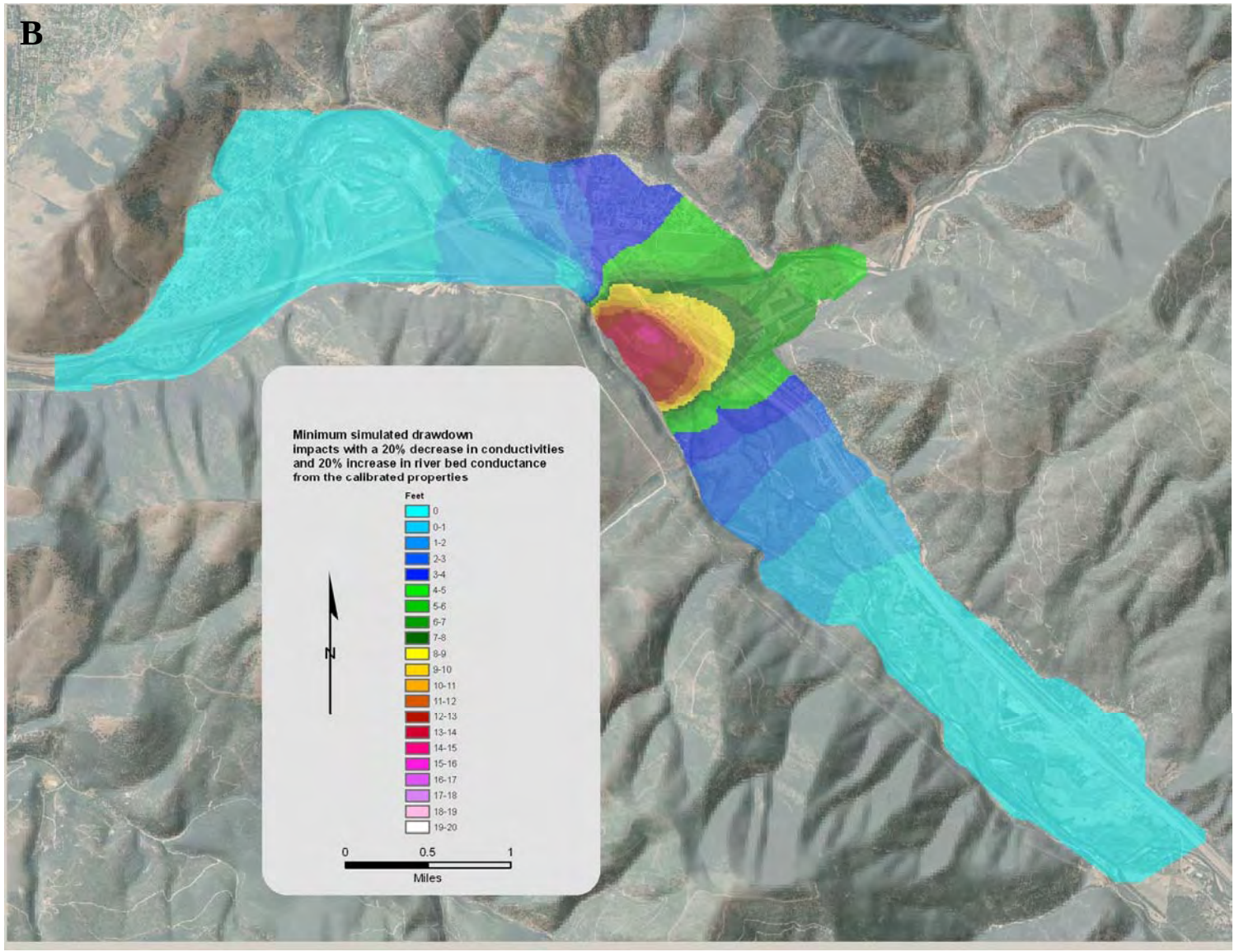

Figure 46b Model predictions based on a 20% decrease in conductivities and increase in river conductance.

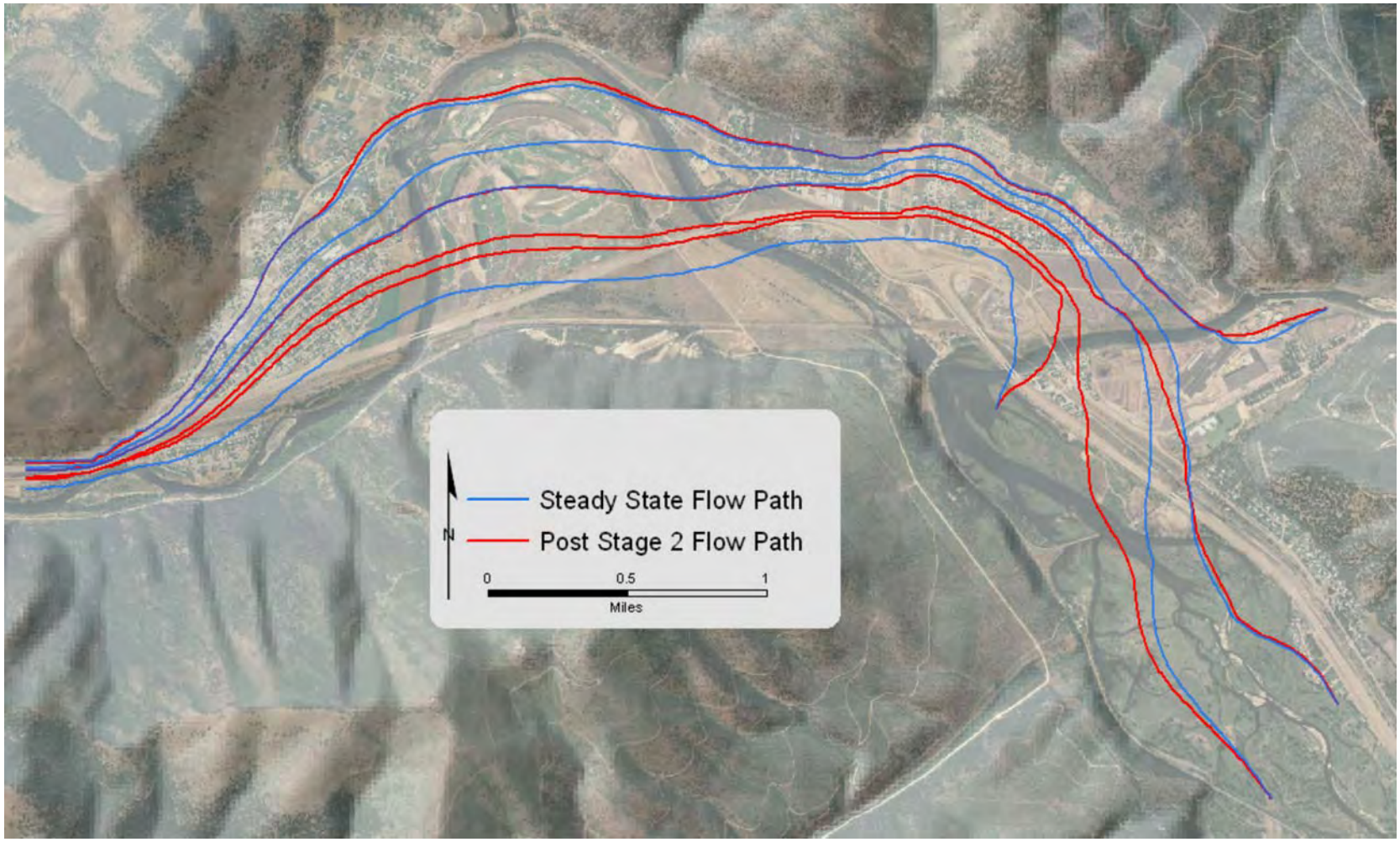

Figure 47 Map of 4 particle traces in level 2, illustrating predicted changes in flow paths following Stage 2 drawdowns.

Appendix B Interpreted well logs from Rockworks. (Excel file available in digital format only)

Appendix C Compiled water level data. (Excel file available in digital format only)

Appendix D Dewatering pump log data (courtesy of Envirocon 2007).

Date	Day	Pump 1	GPM	Pump 2	GPM	Pump 3	GPM	Pump 4	GPM	Pump 5	GPM	Pump 6	GPM	GPM TOTAL
2-Nov	Thursday	start 4 pm	45	start 4 pm	50	start 4 pm	50	start 3 pm	50	start 3 pm	100	start 3 pm	50	345
3-Nov	Friday	on	45	**off 5 pm**	0	on	50	on	50	on	100	on	50	295
4-Nov	Saturday	on	45	**off**	0	on	50	on	50	on	100	**off 10 am**	0	245
5-Nov	Sunday	on	45	**off**	0	**off 6 pm**	50	on	50	on	100	**off**	0	245
6-Nov	Monday	on	45	**off**	0	**off**	0	on	50	on	100	on 5 pm	50	245
7-Nov	Tuesday	on	45	on 9 am	50	**off**	0	on	50	on	100	on	50	295
8-Nov	Wednesday	on	45	on	50	on 3 PM	0	**off 6 AM, on 2 PM**	0	on	100	on	50	245
9-Nov	Thursday	on	45	on	50	on	50	on	50	on	100	on	50	345
10-Nov	Friday	on	45	on	50	**off AM**	0	**off 11 PM**	50	on	100	on	50	295
11-Nov	Saturday	on	45	on	50	**off**	0	**off**	0	on	100	on	50	245
12-Nov	Sunday	on	45	on	50	**off**	0	**off**	0	on	100	on	50	245
13-Nov	Monday	on	45	on	50	**off**	0	**off**	0	on	100	on	50	245

14-Nov	Tuesday	on	45	on	50	on 1 PM	50	on 11 AM	55	on	100	on	50	350	
15-Nov	Wednesday	on	50	on	50	on	50	on	45	on	105	on	55	355	
16-Nov	Thursday	on	50	on	50	on	50	on	60	on	100	on	55	365	
17-Nov	Friday	on	50	on	50	on	50	on	50	on	100	on	55	355	
18-Nov	Saturday	on	50	on	50	on	50	on	50	on	100	on	55	355	
19-Nov	Sunday	on	50	on	50	on	50	on	50	on	100	on	55	355	
20-Nov	Monday	on	50	on	50	on	50	on	50	on	100	on	55	355	
21-Nov	Tuesday	on	50	on	50	on	50	on	50	on	100	on	55	355	
22-Nov	Wednesday	on	50	on	70	on	50	on	50	on	100	on	55	375	
23-Nov	Thursday	on	50	on	70	on	50	on	50	on	100	on	55	375	
24-Nov	Friday	on	50	on	70	on	50	on	50	on	100	on	55	375	
25-Nov	Saturday	on	50	on	70	on	50	on	50	**off 6 pm**	100	on	55	375	
26-Nov	Sunday	on	50	on	70	on	50	on	50	**off**	0	on	55	275	
27-Nov	Monday	on	50	on	70	on	50	on	50	**off**	0	on	55	275	
28-Nov	Tuesday	on	50	on	55	on	50	on	50	**off**	0	on	55	260	
29-Nov	Wednesday	on	50	on	50	on	50	on	50	on 1 pm	100	on	30	330	Eductors off- 3:00
30-Nov	Thursday	on	50	on	50	on	50	on	50	on	130	on	30	360	Eductors off
1-Dec	Friday	on	50	on	50	on	50	on	50	on	130	on	30	360	Eductors off
2-Dec	Saturday	on	50	on	50	on	50	on	50	on	110	on	30	340	Eductors off

3-Dec	Sunday	on	50	on	50	on	50	on	50	on	110	on	30	340	Eductors off
4-Dec	Monday	on	50	on	50	on	50	on	50	on	110	on	30	340	Eductors off
5-Dec	Tuesday	on	50	on	50	on	50	on	50	on	110	on	30	340	Eductors off
6-Dec	Wednesday	on	50	on	70	on	50	on	50	on	110	on	30	360	Eductors off
7-Dec	Thursday	on	50	on	70	on	50	on	50	on	110	on	30	360	Eductors off forever
8-Dec	Friday	on	50	on	70	on	50	on	50	on	110	on	30	360	
9-Dec	Saturday	on	50	on	70	on	50	on	50	on	110	on	30	360	
10-Dec	Sunday	on	50	on	70	on	50	on	50	on	110	on	30	360	
11-Dec	Monday	on	50	on	70	on	50	on	50	on	110	on	30	360	
12-Dec	Tuesday	on	50	on	70	on	50	on	50	on	110	on	30	360	
13-Dec	Wednesday	on	50	on	70	on	50	on	50	on	110	on	30	360	
14-Dec	Thursday	on	50	on	70	on	50	on	60	on	110	on	30	370	
15-Dec	Friday	on	50	on	70	on	50	on	60	on	110	on	30	370	
16-Dec	Saturday	on	50	on	70	on	50	on	60	on	110	on	30	370	
17-Dec	Sunday	on	50	on	70	on	50	**off**	0	**off**	0	**off**	0	170	
18-Dec	Monday	on	50	on	70	on	50	**on 5 pm**	0	**off**	0	**on 10 am**	40	210	
19-Dec	Tuesday	on	50	on	70	on	50	on	70	**on 1 pm**	110	on	40	390	
20-Dec	Wednesday	on	50	on	70	on	50	on	70	on	110	on	40	390	
21-Dec	Thursday	on	50	on	70	on	50	on	70	on	110	on	40	390	

22-Dec	Friday	on	50	on	70	on	50	on	70	on	110	on	40	390
23-Dec	Saturday	on	50	on	70	on	50	on	70	on	110	on	40	390
24-Dec	Sunday	on	50	on	70	on	50	on	70	on	110	on	40	390
25-Dec	Monday	on	50	on	70	on	50	on	70	on	110	on	40	390
26-Dec	Tuesday	on	50	on	70	on	50	on	70	on	110	on	40	390
27-Dec	Wednesday	on	50	on	70	on	40	on	70	on	110	on	40	380
28-Dec	Thursday	on	50	on	70	on	40	on	70	on	110	on	40	380
29-Dec	Friday	on	50	on	70	on	40	on	70	on	110	on	40	380
30-Dec	Saturday	on	50	on	70	on	40	on	40	on	110	on	80	390
31-Dec	Sunday	on	50	on	70	on	40	on	40	on	110	on	80	390
1-Jan	Monday	on	50	on	70	on	40	on	40	on	110	on	80	390
2-Jan	Tuesday	on	50	on	70	on	40	on	40	on	110	on	80	390
3-Jan	Wednesday	on	50	on	70	on	40	on	40	on	110	on	80	390
4-Jan	Thursday	on	50	on	70	on	40	on	40	on	110	on	80	390
5-Jan	Friday	on	50	on	70	on	40	on	40	on	110	on	80	390
6-Jan	Saturday	on	50	on	70	on	40	on	40	on	110	on	80	390
7-Jan	Sunday	on	50	on	70	on	40	on	40	on	110	on	80	390
8-Jan	Monday	on	50	on	70	on	40	on	40	on	110	on	80	390
9-Jan	Tuesday	on	50	on	70	on	40	on	40	on	110	on	80	390
10-Jan	Wednesday	on	50	on	70	on	40	on	40	on	110	on	80	390

11-Jan	Thursday	on	50	on	70	on	40	on	40	on	110	on	80	390
12-Jan	Friday	on	50	on	70	on	40	on	40	on	110	on	80	390
13-Jan	Saturday	on	50	on	70	on	40	on	40	on	110	on	80	390
14-Jan	Sunday	on	50	on	70	on	40	on	40	on	110	on	80	390
15-Jan	Monday	on	50	on	70	on	40	on	40	on	110	on	80	390
16-Jan	Tuesday	on	50	on	80	on	40	on	40	on	110	on	80	400
17-Jan	Wednesday	on	50	on	80	on	40	on	40	on	110	on	80	400
18-Jan	Thursday	on	50	on	80	on	40	on	40	on	110	on	80	400
19-Jan	Friday	on	40	on	70	on	50	on	40	on	110	on	90	400
20-Jan	Saturday	on	40	on	70	on	50	on	40	on	110	on	90	400
21-Jan	Sunday	on	40	on	70	on	50	on	40	on	110	on	90	400
22-Jan	Monday	on	40	on	80	on	50	on	40	on	120	on	90	420
23-Jan	Tuesday	on	40	on	80	on	50	on	40	on	120	on	100	430
24-Jan	Wednesday	on	40	on	80	on	50	on	40	on	120	on	100	430
25-Jan	Thursday	on	40	on	80	on	50	on	40	on	120	on	100	430
26-Jan	Friday	on	40	on	80	on	50	on	40	on	120	on	100	430
27-Jan	Saturday	on	40	on	80	on	50	on	40	on	120	on	100	430
28-Jan	Sunday	on	40	on	80	on	50	on	40	on	120	on	100	430
29-Jan	Monday	on	40	on	80	on	50	on	40	on	120	on	100	430
30-Jan	Tuesday	on	40	on	80	on	50	on	40	on	120	on	100	430

31-Jan	Wednesday	on	40	on	80	on	50	on	40	on	120	on	100	430
1-Feb	Thursday	on	40	on	80	on	50	on	40	on	120	on	100	430
2-Feb	Friday	on	40	on	80	on	50	on	40	on	120	on	100	430
3-Feb	Saturday	on	40	on	80	on	50	on	40	on	120	on	100	430
4-Feb	Sunday	on	40	on	80	on	50	on	40	on	120	on	100	430
5-Feb	Monday	on	40	on	80	on	50	on	40	on	120	on	100	430
6-Feb	Tuesday	on	40	on	80	on	50	on	40	on	120	on	100	430
7-Feb	Wednesday	on	40	on	80	on	50	on	40	on	130	on	100	440
8-Feb	Thursday	on	40	on	80	on	50	on	40	on	130	on	100	440
9-Feb	Friday	on	40	on	80	on	50	on	40	on	130	on	100	440
10-Feb	Saturday	on	40	on	80	on	50	on	40	on	130	on	100	440
11-Feb	Sunday	on	40	on	80	on	50	on	40	on	130	on	100	440
12-Feb	Monday	on	40	on	80	on	50	on	40	on	130	on	100	440
13-Feb	Tuesday	on	40	on	80	on	50	on	40	on	130	on	100	440
14-Feb	Wednesday	on	40	on	70	on	50	on	40	on	130	on	100	430
15-Feb	Thursday	on	40	on	70	on	50	on	40	on	130	on	100	430
16-Feb	Friday	on	40	on	70	on	50	on	40	on	130	on	100	430
17-Feb	Saturday	on	40	on	70	on	50	on	40	on	130	on	100	430
18-Feb	Sunday	on	40	on	70	on	50	on	40	on	130	on	100	430
19-Feb	Monday	on	40	on	70	on	50	on	40	on	130	on	100	430

20-Feb	Tuesday	on	40	on	70	on	50	on	40	on	130	on	100	430
21-Feb	Wednesday	on	40	on	70	on	50	on	40	on	130	on	100	430
22-Feb	Thursday	on	40	on	70	on	50	on	40	on	130	on	100	430
23-Feb	Friday	on	40	on	65	on	45	on	45	on	140	on	100	435
24-Feb	Saturday	on	40	on	65	on	45	on	45	on	140	on	100	435
25-Feb	Sunday	on	40	on	65	on	45	on	45	on	140	on	100	435
26-Feb	Monday	on	40	on	65	on	45	on	45	on	140	on	100	435
27-Feb	Tuesday	on	40	on	65	on	45	on	45	on	140	on	100	435
28-Feb	Wednesday	on	40	on	65	on	45	on	45	on	140	on	100	435
1-Mar	Thursday	on	40	on	65	on	45	on	45	on	140	on	100	435
2-Mar	Friday	on	40	on	65	on	45	on	45	on	140	on	100	435
3-Mar	Saturday	on	40	on	65	on	45	on	45	on	140	on	100	435
4-Mar	Sunday	on	40	on	65	on	45	on	45	on	140	on	100	435
5-Mar	Monday	**off 3 PM**	40	on	65	**off 3 PM**	45	on	45	**off 3 PM**	140	on	100	435
6-Mar	Tuesday	**off**	0	**off 9 AM**	0	**off**	0	**off 9 AM**	0	**off**	0	**off 9 AM**	0	0
7-Mar	Wednesday	**off**	0	**off**	0	**off**	0	**off**	0	**off**	0	**off**	0	0
8-Mar	Thursday	**off**	0	**off**	0	**off**	0	**on 1 PM**	45	**on 1 PM**		**on 1 PM**	10	55
9-Mar	Friday	**on 2 PM**	40	**on 2 PM**	65	**on 2 PM**	45	on	45	on	140	on	10	345
10-Mar	Saturday	on	40	on	70	on	60	on	60	on	130	on	10	370
11-	Sunday	on	40	on	70	on	60	on	60	on	130	on	10	370

Mar														
12-Mar	Monday	on	40	on	70	on	60	**off 10 AM**	0	**off 10 AM**	0	**off 10 AM**	0	170
13-Mar	Tuesday	on	40	on	70	on	60	**on 2 PM**	60	**on 2 PM**	130	**on 2 PM**	70	430
14-Mar	Wednesday	on	40	on	70	on	60	on	60	on	130	on	70	430
15-Mar	Thursday	on	40	on	70	on	60	on	60	on	130	on	70	430
16-Mar	Friday	on	40	on	70	on	60	on	60	on	130	on	70	430
17-Mar	Saturday	on	40	on	70	on	60	on	60	on	130	on	70	430
18-Mar	Sunday	on	40	on	70	on	60	on	60	on	130	on	70	430
19-Mar	Monday	on	40	on	70	on	60	on	60	on	130	on	70	430
20-Mar	Tuesday	on	40	on	70	on	60	on	60	on	130	on	70	430
21-Mar	Wednesday	on	40	on	70	on	60	on	60	on	130	on	70	430
22-Mar	Thursday	on	40	on	70	on	60	on	60	on	130	on	70	430
23-Mar	Friday	**off**	0	**off**	0	**off**	0	on	60	on	130	on	70	260
24-Mar	Saturday	**off**	0	**off**	0	**off**	0	on	60	on	130	on	70	260
25-Mar	Sunday	**off**	0	**off**	0	**off**	0	on	60	on	130	on	70	260
26-Mar	Monday	**off**	0	**off**	0	**off**	0	on	60	on	130	on	70	260
27-Mar	Tuesday	**on 1 PM**	0	**on 1 PM**	0	**on 1 PM**	0	on	60	on	130	on	70	260
28-Mar	Wednesday	on	40	on	70	on	60	on	60	on	130	on	70	430
29-Mar	Thursday	on	40	on	70	on	60	on	60	on	130	on	70	430
30-Mar	Friday	on	40	on	70	on	60	on	60	on	130	on	70	430

31-Mar	Saturday	on	40	on	70	on	60	on	60	on	130	on	70	430
1-Apr	Sunday	on	40	on	70	on	60	on	60	on	130	on	70	430
2-Apr	Monday	on	40	on	70	on	60	on	60	on	130	on	70	430
3-Apr	Tuesday	**off**	0	**off**	0	**off**	0	**off**	0	**off**	0	**off**	0	0
4-Apr	Wednesday	**off**	0	**off**	0	**off**	0	**off**	0	**off**	0	**off**	0	0
5-Apr	Thursday	**off**	0	**off**	0	**off**	0	**off**	0	**off**	0	**off**	0	0
6-Apr	Friday	on	40	on	60	on	60	on	70	on	130	on	90	450
7-Apr	Saturday	on	40	on	60	on	60	on	70	on	130	on	90	450
8-Apr	Sunday	on	40	on	60	on	60	on	70	on	130	on	90	450
9-Apr	Monday	on	40	on	60	on	60	on	70	on	130	on	90	450
10-Apr	Tuesday	on	40	on	60	on	60	on	70	on	130	on	90	450
11-Apr	Wednesday	on	40	on	60	on	60	on	70	on	130	on	90	450
12-Apr	Thursday	on	40	on	60	on	60	on	70	on	130	on	90	450
13-Apr	Friday	on	40	on	60	on	60	on	70	on	130	on	90	450
14-Apr	Saturday	on	40	on	60	on	60	on	70	on	130	on	90	450
15-Apr	Sunday	on	40	on	60	on	60	on	70	on	130	on	90	450
16-Apr	Monday	on	40	on	60	on	60	on	70	on	130	on	90	450
17-Apr	Tuesday	on	40	on	60	on	60	**off**	**0**	**off**	**0**	**off**	**0**	160
18-Apr	Wednesday	on	40	on	60	on	60	**off**	**0**	**off**	**0**	**off**	**0**	160
19-Apr	Thursday	on	40	on	60	on	60	on	70	on	130	on	90	450

20-Apr	Friday	on	40	on	60	on	60	on	70	on	130	on	90	450
21-Apr	Saturday	on	40	on	60	on	60	on	70	on	130	on	90	450
22-Apr	Sunday	on	40	on	60	on	60	on	70	on	130	on	90	450
23-Apr	Monday	on	40	on	60	on	60	on	70	on	130	on	90	450
24-Apr	Tuesday	on	40	on	60	on	60	on	70	on	130	on	90	450
25-Apr	Wednesday	on	40	on	60	on	60	on	70	on	130	on	90	450
26-Apr	Thursday	on	40	on	60	on	60	on	70	on	130	on	90	450
27-Apr	Friday	on	40	on	60	on	60	on	70	on	130	on	90	450
28-Apr	Saturday	on	40	on	60	on	60	on	70	on	130	on	90	450
29-Apr	Sunday	on	40	on	60	on	60	on	70	on	130	on	90	450
30-Apr	Monday	on	40	on	60	on	60	on	70	on	130	on	90	450
1-May	Tuesday	on	40	on	60	on	60	on	70	on	130	on	90	450
2-May	Wednesday	on	40	on	60	on	60	on	70	on	130	on	90	450
3-May	Thursday	on	40	on	60	on	60	on	70	on	130	on	90	450
4-May	Friday	on	40	on	60	on	60	on	70	on	130	on	90	450
5-May	Saturday	on	40	on	60	on	60	on	70	on	130	on	90	450
6-May	Sunday	on	40	on	60	on	60	on	70	on	130	on	90	450
7-May	Monday	on	40	on	60	on	60	on	70	on	130	on	90	450
8-May	Tuesday	on	40	on	60	on	60	on	70	on	130	on	90	450
9-May	Wednesday	on	40	on	60	on	60	on	70	on	130	on	90	450

10-May	Thursday	on	40	on	60	on	60	on	70	on	130	on	90	450
11-May	Friday	on	40	on	60	on	60	on	70	on	130	on	90	450
12-May	Saturday	on	40	on	60	on	60	on	70	on	130	on	90	450
13-May	Sunday	on	40	on	60	on	60	on	70	on	130	on	90	450
14-May	Monday	on	40	on	60	on	60	on	70	on	130	on	90	450
15-May	Tuesday	on	90	on	60	on	80	on	80	on	170	on	70	550
16-May	Wednesday		90		60		80		80		170		70	550
17-May	Thursday		90		60		80		80		170		70	550

Appendix E Steady state model calibration results

Residual Mean			-0.7315			
Res. Std. Dev.			2.380619			
Sum of Squares			148.8586			
Abs. Res. Mean			1.634093			
Min. Residual			-8.30975			
Max. Residual			2.80712			
Range in Target Values			113.393			
Std. Dev./Range			0.020994			
Name	X	Y	Layer	Observed	Computed	Residual
DB-007	877569.6	983518.7	4	3259.12	3267.43	-8.30975
DA-41	875840.8	985010.16	4	3249.877	3255.33	-5.45286
103a	874288.3	985272.33	3	3249.794	3253.368	-3.57413
104b	874414.8	985715.84	2	3246.754	3249.476	-2.72186
DB-001	876321.6	984560.65	3	3256.969	3259.13	-2.16147
99A	873379.3	986325.75	6	3242.86	3244.607	-1.74678
108a	872834	986877.54	5	3240.153	3241.73	-1.57679
DB-079	871081.1	990661.9	3	3223.66	3224.609	-0.94945
Rodin(turah)	888694.2	969959.16	5	3315.6	3316.391	-0.79115
MW#3	863279.9	987980.96	1	3202.207	3202.66	-0.45277
922A	870386.6	988719.77	7	3222.333	3222.694	-0.36113
111a	875039.9	986161.78	7	3246.374	3246.589	-0.21453
HG-23	875034	988635.09	3	3229.88	3229.946	-0.06644
Ubben	886822.2	972736.33	4	3306.78	3306.788	-0.00806
DA-29A	879682	978781.29	5	3278.031	3277.99	0.041069
MW#6	864424.2	990845.92	1	3205.233	3204.898	0.335198
HG-27	869757.1	990604.34	4	3222.22	3221.652	0.567569
HG-20	871534.1	988941.57	2	3226.593	3225.788	0.80541
923A	869699.8	988454.75	5	3220.777	3219.846	0.931273
C-4	873090.7	988131.88	4	3229.407	3228.475	0.932052
MW#7	866158.4	989001.98	1	3209.917	3208.941	0.976308
917A	871500.1	987425.29	4	3232.05	3230.659	1.390892
HG-17	867085.2	990264.88	2	3214.497	3212.453	2.044208
920	870151.7	987907.65	1	3225.72	3222.913	2.80712